Transition pathways for the Belgian Industry: application to the case of the lime sector

Auteur : Mitraki, Rafailia
Promoteur(s) : Léonard, Grégoire
Faculté : Faculté des Sciences appliquées
Diplôme : Master : ingénieur civil en chimie et science des matériaux, à finalité spécialisée en Chemical Engineering
Année académique : 2023-2024
URI/URL : http://hdl.handle.net/2268.2/20254

University of Liège
Faculty of Applied Sciences

Transition pathways for the Belgian Industry: application to the case of the lime sector

Written by:
Rafailia MITRAKI

Thesis presented for obtaining the Master's degree in
Chemical and Materials engineering

Academic Supervisor:
Grégoire LÉONARD

Academic Year: 2023-2024

Acknowledgment

First and foremost, I want to express my sincere gratitude to Prof. Grégoire Léonard for welcoming me into his team and allowing me to work on such an interesting research topic. His invaluable advice and comments played a decisive role in the completion and improvement of my work. I also want to thank him for proofreading this report.

My heartfelt thanks to Muhammad Salman, who consistently made himself available to answer my questions and offer guidance. I would also like to thank him for his meticulous proofreading of this report. I am truly grateful for the support provided.

I would like to thank So-Mang Kim for his invaluable help with CO_2 capture. I also want to acknowledge Alex Aubert for generously sharing his insights and patiently answering my questions throughout this thesis.

I would also like to thank the IPESE group of EPFL for providing the necessary Blueprint models for completion of the superstructure and for their throughout support and guidance.

Finally, I would like to thank my closest friends, with whom I've laughed a lot –and cried a few times– during these five years of study. And, above all, a sincere thank you to my mom, whose unwavering belief in me and encouragement have been my driving force. Without her, I would not be where I am today.

Abstract

Faced with the climate emergency, it is crucial to reduce CO_2 emissions, which can be a complex task for hard-to-abate industries such as lime production. This thesis therefore, under the framework of the TRI-LATE project, aims to evaluate different energy transition pathways for the lime sector in Belgium. Lime is an essential product, used in a wide variety of applications: construction, steelmaking, effluent treatment, production of chemicals, etc. However, this sector is a major emitter of CO_2, accounting for 1% of global anthropogenic emissions. The calcination reaction in lime kilns ($CaCO_3 + heat \rightleftharpoons CaO + CO_2$) alone generates 0.786 t_{CO_2}/t_{lime} and takes place at very high temperatures (typically 900–1100 °C), currently achieved by burning fossil fuels. Overall, between 1 and 1.8 t_{CO_2}/t_{lime} are emitted depending on the considered kiln technology. The obtained quicklime can then be milled or hydrated ($CaO + H_2O \rightleftharpoons Ca(OH)_2 + heat$) to produce hydrated lime or milk of lime, depending on the amount of water added. As the sector's emissions are almost entirely linked to kiln operation, the use of carbon-neutral fuels, the possible kiln electrification and the implementation of CO_2 capture or alternative "cold" production routes are being studied and proposed by industrial experts.

The objective of this study is to analyze various energy transition pathways for CO_2 emissions reduction in the lime sector. For this purpose, the Blueprint (BP) model of lime sector is developed, consisting of detailed mass and energy balances, as well as economic considerations (i.e., annualized CAPEX and OPEX). Moreover, all the possible emission-reduction pathways for lime production (i.e., fuel switching towards hydrogen, biogas, biomethane or solid biomass; electrification of kilns using plasma torches; CO_2 capture by chemical absorption with MEA or by oxycombustion) are included and a superstructure of pathways is developed. Furthermore, the OSMOSE Lua tool, developed at EPFL, is utilized for the evaluation of the superstructure of various alternatives for three different years (2030, 2040, 2050) and three different EnergyVille's scenarios (electrification, clean molecules, central). Finally, a comparison between all alternative lime production routes and the base case 'NG' (natural gas-fired lime kiln without CC) is performed on the basis of three key performance indicators: specific energy consumption (kWh/t_{lime}), specific CO_2 emissions (kg_{CO_2}/t_{lime}) and specific total cost (€/t_{lime}).

In 2030, the specific total cost of the base case is €269–270/t. The results indicate that the optimum energy transition pathways are 'Biomass-CC' and 'NGOxy-CC', resulting in a reduction in specific total cost (STC) of 27–28% and 16–18% compared to the base case, respectively, depending on the scenario considered. The CO_2 emissions reduction potential compared to the base case amounts to 115% for 'Biomass-CC' and 90% for 'NGOxy-CC'. 'Plasma-CC' comes 3rd, with a cost reduction of 12–18% and an emission reduction of 93% compared to a natural gas-fired kiln without CC. In 2040, firing a lime kiln with natural gas requires a specific total cost of €370/t. The economically optimal solution remains 'Biomass-CC' (49% lower STC than 'NG'), followed by 'Plasma-CC' (40–45% lower STC than 'NG', depending on the scenario). 'NGOxy-CC' and 'Biogas-CC' both achieve a STC reduction of 40–41%. Compared to the base case, 'Biogas-CC' configuration enables 124% lower CO_2 emissions. In 2050, the STC of 'NG' reaches €476/t. By implementing 'Biomass-CC', 'Biogas-CC', 'Plasma-CC' or 'NGOxy-CC', the specific total cost can be reduced by 60–61%, 53–54%, 51–62%, and 51–54% respectively, compared to 'NG'. The use of hydrogen in lime kilns, on the other hand, represents one of the most expensive transition pathways for the sector. Despite relatively low costs, the problems associated with biomass availability and the low TRL of plasma technology should not be overlooked.

This study provides a comprehensive analysis of a wide variety of energy transition pathways for the lime sector, however, there is still room for improvement. Future researches should focus on investigation of other CO_2 capture processes, use of more accurate economic data, consideration of acid gas removal prior to CO_2 capture, and inclusion of scope 2 CO_2 emissions.

Résumé

Face à l'urgence climatique, il est crucial de réduire les émissions de CO_2, ce qui peut s'avérer complexe pour des industries difficiles à décarboner comme la production de chaux. Cette thèse, dans le cadre du projet TRILATE, vise donc à évaluer différentes voies de transition énergétique pour le secteur de la chaux en Belgique. La chaux est un produit essentiel, utilisé dans une grande variété d'applications : construction, sidérurgie, traitement des effluents, production de substances chimiques. Ce secteur est cependant un important émetteur de CO_2, représentant 1% des émissions anthropiques mondiales. La réaction de calcination ($CaCO_3 + chaleur \rightleftharpoons CaO + CO_2$) génère à elle seule 0,786 t_{CO_2}/t_{chaux}. De plus, elle se déroule à de très hautes températures (900–1100℃), actuellement atteintes par combustion de combustibles fossiles. Globalement, entre 1 et 1,8 t_{CO_2}/t_{chaux} sont émises en fonction du type de four considéré. La chaux vive obtenue peut ensuite être broyée ou hydratée ($CaO + H_2O \rightleftharpoons Ca(OH)_2 + chaleur$) en chaux hydratée ou lait de chaux, en fonction de la quantité d'eau ajoutée. Les émissions du secteur étant presque entièrement liées au fonctionnement des fours, l'utilisation de combustibles bas carbone, l'électrification des fours et la mise en place de captage du CO_2 ou de voies de production « à froid » sont étudiées par des experts.

L'objectif de cette étude est d'analyser différentes voies de transition énergétique permettant la réduction des émissions de CO_2 dans l'industrie de la chaux. Pour ce faire, le Blueprint (BP) du secteur de la chaux a été développé, comprenant des bilans de masse et d'énergie détaillés, ainsi que des considérations économiques (CAPEX et OPEX annualisés). En outre, toutes les voies possibles de réduction des émissions pour la production de chaux (c'est-à-dire l'utilisation d'hydrogène, de biogaz, de biométhane ou de biomasse solide ; l'électrification des fours à l'aide de torches à plasma ; la capture du CO_2 par absorption chimique avec la MEA ou par oxycombustion) sont incluses et une superstructure de diverses voies de transition énergétique a été développée. Ensuite, l'outil OSMOSE Lua, développé à l'EPFL, est utilisé pour l'évaluation de la superstructure pour trois années différentes (2030, 2040, 2050) et trois scénarios différents d'EnergyVille (électrification, molécules propres, central). Enfin, une comparaison entre toutes les voies alternatives de production de chaux et le cas de base 'NG' (four à chaux alimenté au gaz naturel sans CC) est effectuée sur la base de trois indicateurs de performance clés : consommation d'énergie spécifique (kWh/t_{chaux}), émissions spécifiques de CO_2 (kg_{CO_2}/t_{chaux}) et coût total spécifique (€/t_{chaux}).

En 2030, le coût spécifique total du cas de base est de 269–270 €/t. Les résultats indiquent que les voies de transition optimales sont 'Biomass-CC' et 'NGOxy-CC', ce qui se traduit par une réduction du coût total spécifique (CTS) de respectivement 27–28% et 16–18% par rapport au cas de base, en fonction du scénario considéré. Le potentiel de réduction des émissions de CO_2 par rapport au cas de base s'élève à 115% pour 'Biomass-CC' et à 90% pour 'NGOxy-CC'. La configuration 'Plasma-CC' arrive en troisième position, avec une réduction des coûts de 12–18% et une réduction des émissions de 93% par rapport à un four alimenté au gaz naturel sans CC. En 2040, un four à chaux alimenté au gaz naturel nécessite un coût total spécifique de 370 €/t. La solution optimale d'un point de vue économique reste 'Biomass-CC' (CTS 49% plus bas que pour 'NG'), qui est cette fois suivie par 'Plasma-CC' (CTS 40 à 45% inférieur à 'NG', selon le scénario). Les configurations 'NGOxy-CC' et 'Biogas-CC' atteignent toutes deux une réduction du CTS de 40 à 41%. Par rapport au cas de base, la configuration 'Biogas-CC' permet de réduire les émissions de CO_2 de 124%. En 2050, le CTS de la configuration 'NG' atteint 476 €/t. En mettant en oeuvre les configurations 'Biomass-CC', 'Biogas-CC', 'Plasma-CC' ou 'NGOxy-CC', le coût total spécifique peut être réduit de, respectivement, 60–61%, 53–54%, 51–62% et 51–54%, par rapport à 'NG'. L'utilisation d'hydrogène dans les fours à chaux, en revanche, représente l'une des voies les plus coûteuses pour le secteur. Malgré des coûts relativement bas, les problèmes liés à la disponibilité de la biomasse et le faible TRL de la technologie plasma ne doivent pas être négligés.

Cette étude fournit une analyse d'une grande variété de voies de transition énergétique pour le secteur de la chaux, mais elle peut encore être améliorée. Les futures recherches devraient se concentrer sur l'étude d'autres processus de capture du CO_2, l'utilisation de données économiques plus précises, la prise en compte de l'élimination des gaz acides avant la capture du CO_2, et l'inclusion des émissions de CO_2 de scope 2.

List of abbreviations

Abbreviation	Meaning
ASK	Annular Shaft Kiln
ASU	Air Separation Unit
BECCUS	Bioenergy with carbon capture, utilization and storage
BioCH4	Biomethane
BP	Blueprint
CAPEX	Capital Expenditure
CC	Carbon Capture
CCS	Carbon Capture and Storage
CEPCI	Chemical Engineering Plant Cost Index
EPFL	École Polytechnique Fédérale de Lausanne
EU	European Union
EU ETS	European Emissions Trading System
KPI	Key Performance Indicator
LKD	Lime Kiln Dust
LRK	Long Rotary Kiln
MCFC	Molten Carbonate Fuel Cell
MEA	Monoethanolamine
MFSK	Mixed Feed Shaft Kiln
MILP	Mixed-Integer Linear Programming
NG	Natural Gas
OPEX	Operational Expenditure
ORC	Organic Rankine Cycle
PFRK	Parallel Flow Regenerative Kiln
PRK	Rotary Kiln with Preheater
TRL	Technology Readiness Level
UN	United Nations

Contents

1 Introduction

Climate change is undoubtedly caused by the relentless increase in greenhouse gases emissions from human activities. A considerable increase in atmospheric CO_2 concentration has been observed, rising from 278 ppm in 1750 [1] to 421 ppm in 2023 [2]. The mitigation of global warming has become a priority for many countries including Belgium.

As stated in the Paris Agreement, it is crucial to limit the global average temperature increase by the end of the century below 1.5℃ compared to pre-industrial levels. In fact, according to the UN's Intergovernmental Panel on Climate Change, this value represents a threshold which once crossed will induce much more severe and frequent droughts, heatwaves and rainfalls than currently experienced. To reach the Paris Agreement climate objectives, around 12 Gt CO_2 and more than 100 Gt CO_2 should be captured and stored during the 2015-2030 and 2030-2050 periods respectively [3]. Moreover, net-zero CO_2 emissions must be reached by 2050.

In 2022, the global carbon dioxide emissions related to power generation and industry amounted to respectively 38.1% and 25.4%, as can be seen in Figure 1.

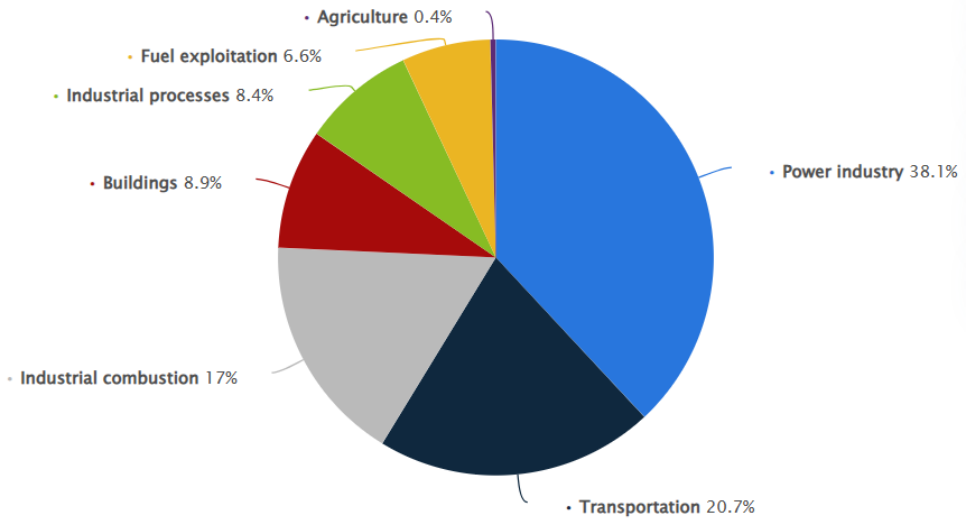

Figure 1: Worldwide CO_2 emissions by sector in 2022 (From [4])

The decarbonization of the power sector is progressing thanks to a higher share of solar panels and wind turbines each year. In Belgium, the share of electricity production from renewable sources increased from 3.6% in 2007 to 25.1% in 2020, as can be seen in Figure 2. In 2023, renewable sources represented 33% of the total electricity generation in Belgium, catching up with nuclear power (41%) and outstripping fossil-based electricity (26%) [5], as can be seen in Figure 3.

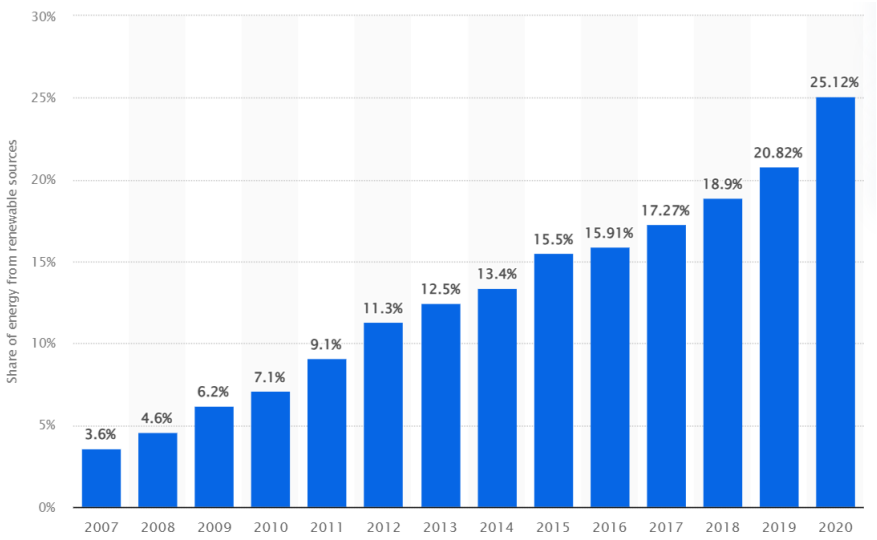

Figure 2: Share of electricity from renewable sources in Belgium from 2007 to 2020 (From [6])

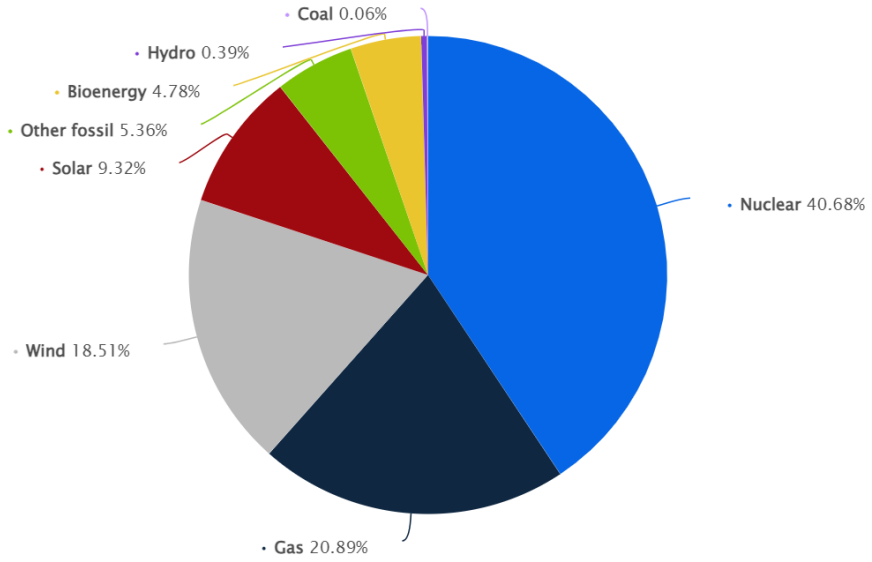

Figure 3: Electricity generation in Belgium in 2023 (From [5])

The Belgian industry is facing more challenges in terms of CO_2 emissions reduction due to hard-to-abate sectors –such as glass, steel, cement or lime– representing approximately 20% of the global CO_2 emissions [7]. The economical or technical difficulty for emissions reduction in these sectors stems from high-temperature heat requirements and process-related emissions. However, addressing CO_2 emissions in hard-to-abate industries is key for reaching Paris Agreement targets.

The lime sector represents alone around 1% of the global anthropogenic CO_2 emissions [8], coming from the implemented reaction and the heat supply. In fact, the energy-intensive calcination process requires temperatures between 900 and 1100℃. The heat requirements –typically between 3200 and 4200 MJ/t of lime [9]– are fulfilled by fossil fuel combustion, contributing for about one third of the sector's emissions [10]. The fuel-related CO_2 emissions are addressed by investing in best available kiln technologies (reducing energy requirements and, thus, the related emissions) [11], electrification and fuel switching towards biomass, waste or green hydrogen [12]. However, such efforts are not sufficient since roughly two thirds of the CO_2 emissions are intrinsic to the calcination reaction taking place within the lime kiln. Thus, to reach carbon

neutrality by 2050, integration of carbon capture units in lime plants is inevitable [13].

The present Master's thesis focuses on the evaluation of possible energy transition pathways for the lime sector. This work is done under the framework of the TRILATE project. This project studies the potential of energy transition and the necessary infrastructure required for it in the Belgian industrial clusters identified by the ECM group at UGent. EnergyVille (KU Leuven, VITO), Fluxys Belgium, Elia Transmission Belgium, UGent and ULiège join forces to develop scientific models for processes, industrial plants and energy systems, necessary for an integrated energy infrastructure analysis. The objective of the TRILATE project is to determine the investments and planning needed for a reliable and profitable energy transition for the Belgian industry.

The ULiège's role in the TRILATE project consists in modeling process Blueprints (BPs) related to the industrial sectors present in the aforementioned clusters, such as chemicals, glass, cement, steel or lime industries, as well as H_2 and CO_2-related technologies. The OSMOSE tool, developed at École Polytechnique Fédérale de Lausanne (EPFL), is used for modeling these BPs which consist of mass and heat balances as well as economics in steady-state. Moreover, the identification of integration opportunities and optimal production routes by an exergo-economic methodology will enable project partners planning the future energy infrastructure in Belgium and neighboring countries by assessing sustainability scenarios, taking into account possible symbiosis among urban and industrial clusters.

2 Objectives of the work

The objective of the present work is to develop the superstructure of various energy transition pathways for the lime sector and to evaluate them based on technical, economical and environmental aspects. To achieve that goal, a thorough literature review is performed first for gathering data about the production of lime and derivatives as well about CO_2 reduction possibilities applicable to the sector, namely fuel switching, carbon capture and alternative "cold" production routes.

Then, a detailed Blueprint (BP) for the lime sector is developed with the OSMOSE tool, consisting of detailed steady-state mass and energy balances, as well as annualized investment and operating costs. The BP includes the production of quicklime –by calcination of limestone in a natural gas-fired kiln– and lime derivatives, such as hydrated lime, milk of lime and lime putty. The data used in the models are sourced from scientific literature and validated by an industrial. Moreover, three main energy transition routes are considered:

- **Fuel switching**: shift from natural gas to alternative fuels with net-zero CO_2 emissions –such as biogas, biomethane or solid biomass–, hydrogen and electrification options;
- **Carbon capture** via chemical absorption with monoethanolamine or oxycombustion of natural gas;
- **Alternative "cold" production routes**: production of hydrated lime at room temperature is also investigated. The first possibility is an electrochemical simultaneous production of hydrated lime $Ca(OH)_2$, H_2, O_2 and CO_2. The second possibility is a chemical decarbonation of limestone by reaction with $NaOH$.

Finally, the aforementioned transition routes are evaluated for different future scenarios ("central" scenario, "electrification" scenario and "clean molecules" scenario from EnergyVille) and different years (2030, 2040 and 2050) influencing the cost of natural gas, electricity, hydrogen, biomass and CO_2 emissions. Biogas and biomethane costs are also obtained from IEA's report for conducting simulations.

The optimal energy transition pathways for each scenario are determined, thanks to the OSMOSE Lua optimization framework, considering the specific total cost (€/t_{lime}), the specific energy requirements (kWh/t_{lime}) and the related specific CO_2 emissions (t_{CO_2}/t_{lime}). However, one must note that the prices of energy resources and CO_2 emissions are not predicted prices for future but are extracted from TIMES-BE model. This model provides costs of resources based on marginal production for each future scenario and considers several assumptions or simplifications, which will be detailed later on.

3 Literature review

3.1 General information: products, properties, markets

Lime manufacturing is based on limestone, a natural mineral mainly consisting of calcium carbonate $CaCO_3$ and a low concentration of $MgCO_3$ (between 0 and 5% [14]), found widely around the world. Dolomite or dolomitic limestone, a sedimentary rock of chemical formula $CaCO_3.MgCO_3$, with a typical $MgCO_3$ concentration between 35 and 46% [14], can also be used as raw material for lime production. In the lime industry, several products are offered [15] [16]:

- Quicklime CaO: produced by thermal dissociation of limestone;
- Dolime $CaO.MgO$: produced by thermal dissociation of dolomitic limestone;
- Calcium hydroxide $Ca(OH)_2$: produced by reaction between quicklime and water. Depending on the water excess, the obtained lime product is designated as hydrated lime, milk of lime or lime putty.
  - Hydrated lime: dry calcium hydroxide powder;
  - Milk of lime: suspension of calcium hydroxide in water, typically containing between 18 wt% and 40 wt% $Ca(OH)_2$ [17];
  - Lime putty: dispersion of calcium hydroxide with a solid content between 55 and 70% [15];
- Lime kiln dust: fine powder of CaO (and MgO), that is a co-product of the lime calcination process [18]

A visual representation of the lime cycle is depicted in Figure 5.

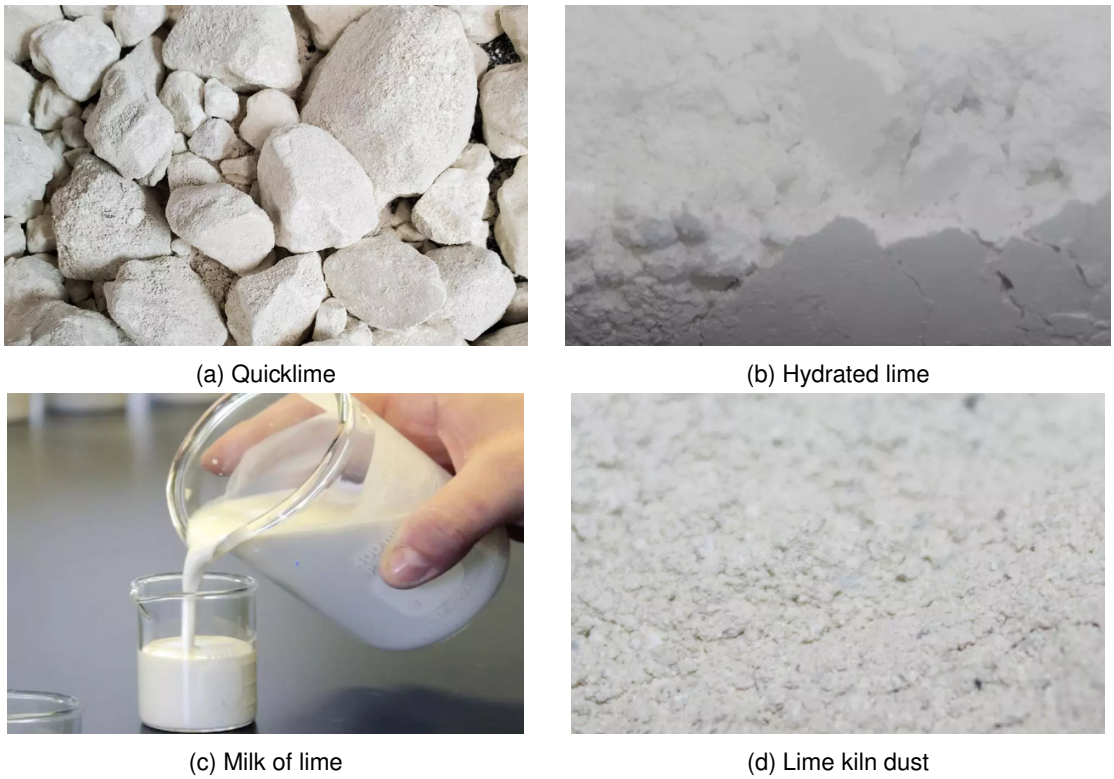

(a) Quicklime (b) Hydrated lime

(c) Milk of lime (d) Lime kiln dust

Figure 4: Product offering in the lime industry (From Carmeuse [19])

Calcium oxide and magnesium oxide have a relatively high melting temperature, respectively 2580℃ and 2800℃. The melting point of calcined dolomite is about 2400℃ and it forms a eutectic mixture (67% CaO,

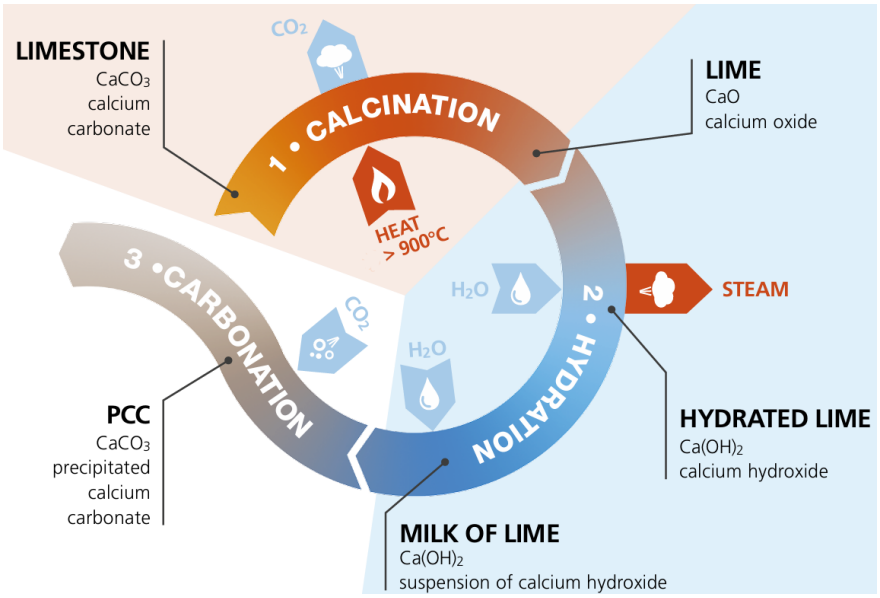

Figure 5: Lime cycle (From [3])

33% MgO) at 2370 ℃. The boiling point of CaO and MgO is respectively 2850 ℃ and 3600 ℃. The specific heat of CaO and $CaO.MgO$ is respectively 0.182 cal/g.℃ and 0.198 cal/g.℃ at 20 ℃ [15].

Hydrated lime is usually white but a grayish or brownish color may be observed in case of high impurity levels. The specific heat of $Ca(OH)_2$ varies between 0.27 cal/g.℃ at 0 ℃ and 0.37 cal/g.℃ at 400 ℃. The specific heat of dolomitic hydrated lime $Ca(OH)_2.Mg(OH)_2$ is 5% higher than the one of $Ca(OH)_2$. Hydrated lime is not stable at high temperatures (547 ℃ at 1 atm). In fact, $Ca(OH)_2$ decomposes to CaO and H_2O. On the other hand, magnesium hydroxide $Mg(OH)_2$ decomposes at much lower temperatures (190 ℃ at 1 atm) [15].

According to Eurostat data, in 2016, the total lime production in EU28 was estimated at 23.9 million tons and represented around 2 billion euros [16]. In 2022, the market size of the lime sector was of 48 million tons and is estimated to grow up to 78 million tons by 2032. The major actors in the lime industry include Carmeuse S.A, Schäfer Kalk GmbH & Co KG, Al Jazeera Industrial Group, Golden Lime Public Company Limited, Lhoist and Nordkalk [20].

According to Statista [21], in 2022, the five largest lime producers across the world were China (310 000 Mton), USA (17 000 Mton), India (16 000 Mton), Russia (11 000 Mton) and Brazil (8400 Mton). The lime production by type and country in EU28, in 2016, is depicted in Figure 6. From the 23.9 million tons of lime produced in 2016, the majority was coming from Germany (29%), France (13%) and Italy (11%). Belgium represented 6% of the total lime production and ranked 6th on the podium. Quicklime production in 2016 represented 17.4 million tons, i.e. 73% of the total production. The largest quicklime producers were Germany (29%), France (14%) and Italy (8%). In 2016, 4.8 million tons of slaked lime were produced, mainly in Germany (29%), Italy (13%) and France (9%). Finally, 37% of the 1.7 million tons of hydraulic lime were produced in Italy, while 36% were coming from Germany.

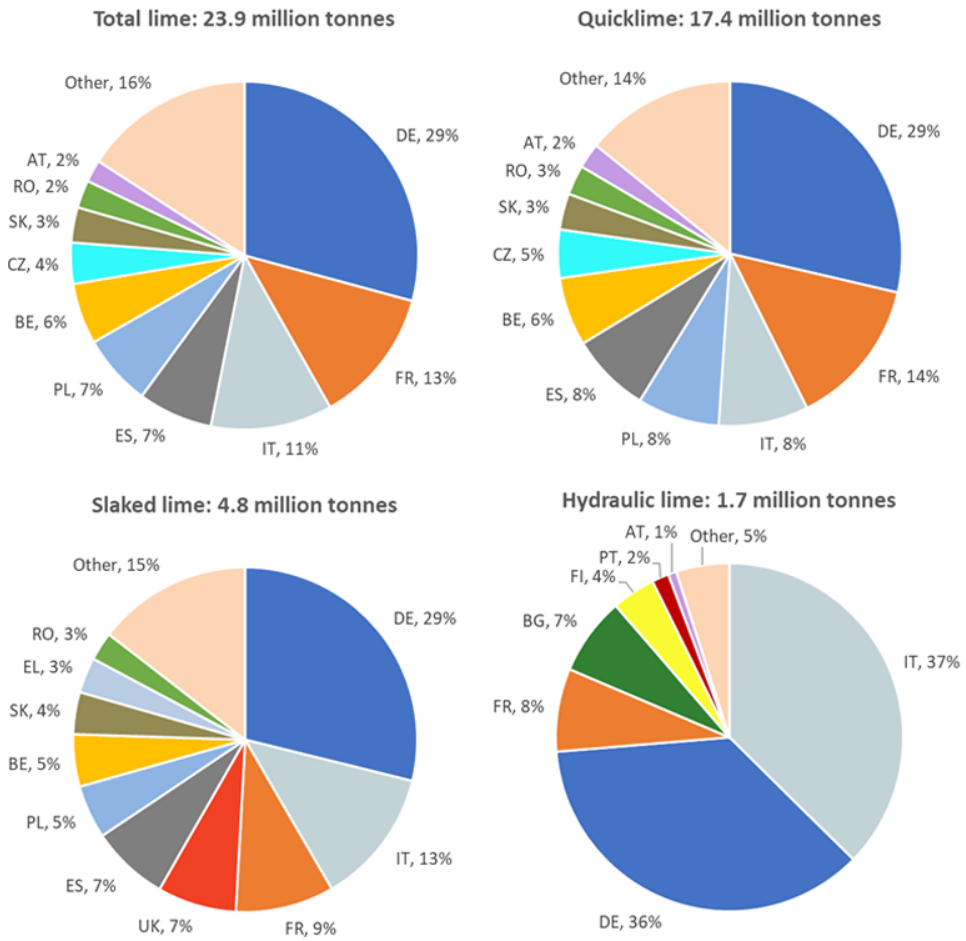

Figure 6: Lime sold production in EU28 by type of product and country in 2016 (From [16])

3.2 Uses of lime

In Europe, around 150 g of lime per person are used every day [3]. Lime is used in a wide variety of applications [15]:

- **Construction & building**:
  - **Treatment of soils**: Drying of soils can be achieved quickly by the exothermic hydration of quicklime, which consumes part of the water and evaporates the rest with the reaction heat. Modification of soils is achieved by reactions between minerals and quicklime or slaked lime which, after several hours, lead to changes in the soil plasticity, workability and compaction characteristics. Soil stabilization consists in a pH increase due to the formation of calcium silicates and aluminates by reaction between lime and siliceous or aluminous components contained in the soil.
  - **Hot mix asphalt**: Hot mix asphalt consists of mainly stone, sand or gravel, mixed with a heated binder, i.e. asphalt cement [22]. Hydrated lime can be used in hot mix asphalt as anti-stripping agent. In fact, a loss in strength can be observed in asphalt-aggregate mixtures in presence of water which is caused by a loss of the aggregate–binder bond. Typically, between 1 and 1.5 wt% of hydrated lime is sufficient. Hydrated lime can also be used as mineral filler leading to an increased binder viscosity, an increased tensile and compressive strength, and an increased resistance to water stripping. Finally, hydrated lime can be used as an antioxidant, i.e. it reduces the binder oxidation which may lead to a premature failure of the hot mix asphalt.

  - **Masonry mortars**: Mortars consist of sand, a binder (which can be calcium lime, dolomitic lime, hydraulic lime, or a lime-cement mixture), a void-filling material, and water providing cohesion to the mixture. Lime can also be used as void filler if mixed with sand to produce sand-lime mortars.
  - **Exterior rendering and interior plasters**: The use of lime in external renderings allows an improved durability of the rendering as well as a good grip between the rendering and the background material. The same advantages are observed for internal plasters. Moreover, the growth of mold and the iron or steel corrosion are inhibited by the high alkalinity of the obtained mixture.
  - **Calcium silicate products**: Lime can be used as binder for calcium silicate products such as sandlime bricks, fire-resistant boards or concrete.

- **Iron and steel-making**:
  - **Impurity removal during steelmaking process**: Impurities, such as silica and iron oxide, contained in the metal are removed by fluxing agents, such as quicklime and dolomite, to form a molten slag.
  - **Sinter strand process**: During the sinter strand process, the finely divided iron oxide are sintered. Smaller ore particles, between 0.5 and 2 mm, are agglomerated into larger ones by adding around 1 kg of quicklime per ton of sinter.
  - **Desulfurization of pig iron**: Sulfur removal from the molten iron into the slag in the blast furnace can be achieved thanks to several elements which are, from the most to the least effective, cerium (Ce), calcium (Ca), strontium (Sr), barium (Ba), magnesium (Mg) and sodium (Na). Usually, around 7 kg/t pig iron of a powdered mixture of lime and calcium carbide CaC_2 is used, leading to a decrease of the sulfur level of 20%. Powdered mixtures of lime with magnesium or aluminum can also be used as desulfurizing agents.

- **Water treatment**:
  - **pH adjustment**: For water treatment, high-calcium slaked lime is notably used for pH adjustment to reach the optimum conditions for coagulation, flocculation, and precipitation of metals, sulfates, fluoride, phosphates, etc. Slaked lime can also be used to neutralize acids contained in water, or to adjust the water pH and thus minimize corrosion and leaching of metals.
  - **Hard water softening**: There exist two types of water hardness: “carbonate” hardness, also called "temporary” hardness, which is due to the presence of calcium and magnesium bicarbonates; and “non-carbonate” hardness, also called “permanent” hardness, which is caused by other calcium and magnesium salts. Carbonate hardness is reduced by reaction of the aforementioned bicarbonates with slaked lime, leading to the precipitation of calcium carbonate and magnesium hydroxide. Non-carbonate hardness is treated with slaked lime and soda ash Na_2CO_3, i.e. the lime-soda process.
  - **Disinfection**: Sewage sludge can be disinfected by the use of ground quicklime which leads to a pH increase up to 12.4 as well as a temperature rise above 50 ℃ due to the exothermic hydration reaction of quicklime, which also causes water removal from the sludge.

- **Gaseous effluent treatment**: Lime can be used for the removal of some heavy metals, furans and dioxins. Moreover, since lime is the cheapest alkali, it is widely used for the removal of acidic gases such as SO_x, NO_x, HCl and HF. Acidic gases can be removed by five types of techniques:
  - **wet scrubbing:** milk of lime neutralizes the acidic gases, mainly SO_2, and the reaction products are removed as a suspension;

  - **semi-dry scrubbing:** gases are treated with a spray of milk of lime (reacting mainly with SO_2) and a dust collector allows the removal of reaction products;
  - **high temperature dry injection of hydrated lime:** hydrated lime over 850 ℃ calcines and the acidic gases (principally SO_2) react with the obtained calcium oxide while the reaction products are removed in a dust collector;
  - **low temperature dry injection of hydrated lime:** hydrated lime, below 300 ℃, is used to remove mainly HCl, HF and SO_2, while the reaction products are removed in a dust collector;
  - **low temperature absorption by hydrated lime:** hydrated lime, in a fixed bed below 300 ℃, allows mainly the removal of HF from ceramic products calciners.

- **Agriculture, food**: adjustment of soil-pH; refining of sugar beet and sugar cane; preparation of gelatin, calcium phosphates, insecticides and fungicides, ...
- **Chemicals**: Quicklime and hydrated lime are used in the production of various chemicals such as precipitated calcium carbonate, calcium hypochlorite bleaches, diacetone alcohol, anthraquinone dyes, trichloroethylene, etc. They serve as source of calcium, desiccant, causticizing agent, flocculant and precipitant, lubricant, or hydrolyzing agent.
- **Other uses**: leather production, stabilization of waste, refining non-ferrous metals, flotation of metal ores, production of petrochemical additives, glass and refractories, etc.

The breakdown of the lime market in 2018 according to different uses is depicted in Figure 7. A majority (∼39%) of the produced lime is used in the iron and steel industry. The next most important uses of lime are the environmental protection (∼15%), i.e. water and effluent treatment, and the construction materials (∼12%).

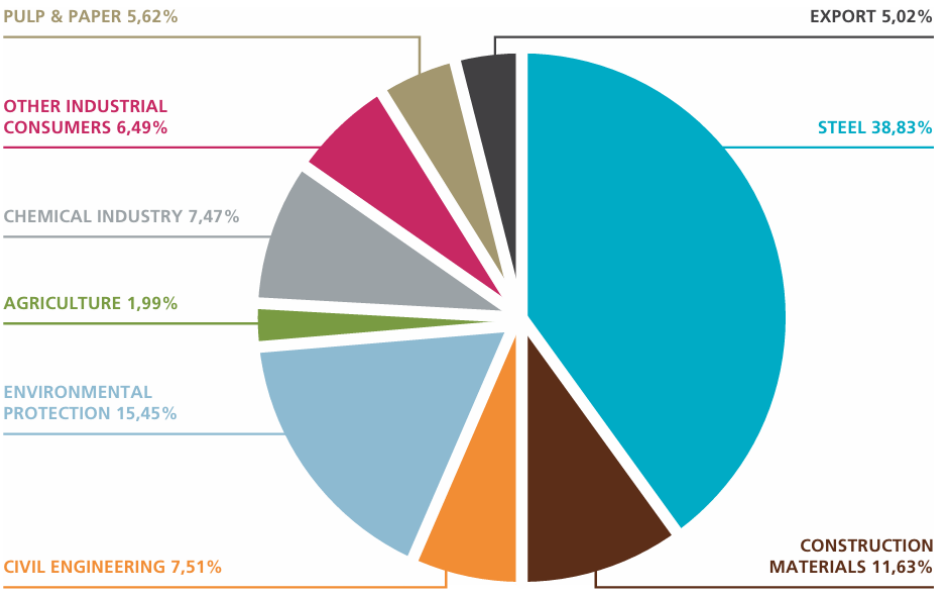

Figure 7: Lime applications by sector in 2018 (From [3])

3.3 Structure of the lime industry

An overview of the lime industry is depicted in Figure 8.

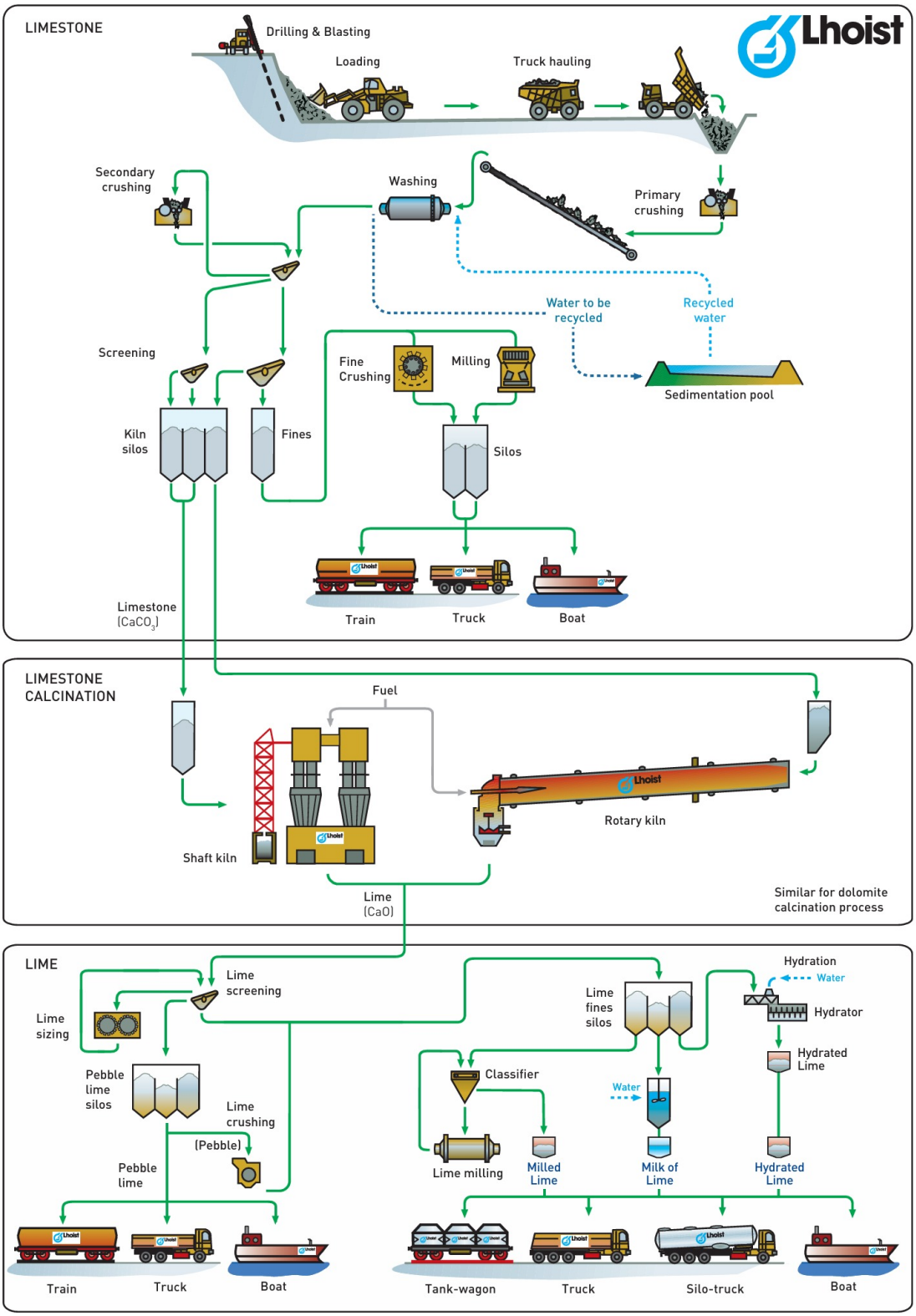

Figure 8: Overview of the lime production process (From Lhoist)

The lime industry consists of four stages: limestone extraction and processing; quicklime production; lime milling; lime derivatives production. After being extracted and purified, limestone, i.e. mainly calcium carbon-

ate, is fed in a calciner, in which its thermal decomposition takes place at very high temperatures, typically between 900 and 1200℃. The produced quicklime undergoes crushing, milling and/or screening steps prior to its storage within silos. After being stored, the lime can be delivered directly to end users. Stored quicklime can also be sent in a hydrating plant to react with water and produce hydrated lime, i.e. dry powdered product, or slaked lime, i.e. a suspension of calcium hydroxide in water [9].

3.3.1 Limestone extraction and processing

Nowadays, limestone is almost exclusively extracted by open-pit quarrying, consisting of five operations: overburden removal, drilling, blasting, loading and hauling. The first step carried out for limestone extraction is the **overburden removal**, i.e. the removal of the material overlying the ore body, namely the top-soil, the sub-soil and possibly other rocks. Then, a primary fragmentation of the rock is performed by **drilling**, before **blasting** operations using TNT-based dynamites or ANFO (Ammonium Nitrate/Fuel Oil). The rock can then be **loaded** and **hauled** by truck to the processing plant [15].

The limestone processing consists of five main operations: crushing and grinding, sizing, beneficiation, storage, and transport. **Crushing** consists of size reduction operations, using for example jaw crushers, gyratory crushers or impact crushers. Limestone fines are produced by a **grinding** step requiring hammer mills, beater mills, tube mills, and roller presses. Limestone **sizing** is necessary to produce accurately-sized products, or to reduce impurities levels which frequently concentrate in the fines. Sizing is performed by screening, or classification for smaller particle sizes. The next step is the limestone **beneficiation** improving the limestone quality. Scalping allows the removal of unwanted clay, while screening allows the removal of heavy metals in the finer fractions. A washing step is performed to increase the product's purity, especially for chemical quality limestones. The obtained products are **stored** in silos or in stockpiles [15].

The energy requirement for limestone mining and processing is estimated at 32 013 Btu/t [23], i.e. 33.8 MJ/t, which is negligible compared to the energy consumption of the calcination step (see sections 3.3.2.1 – 3.3.2.5). Mining accounts for 71% of this energy consumption, while the rest is associated to the limestone processing.

3.3.2 Limestone calcination for quicklime production

Quicklime is produced by calcination, i.e. thermal decomposition, of limestone or, to a smaller extent, dolomite or dolomitic limestone [15]. Limestone is characterized by a very high calcium carbonate content, typically more than 90% $CaCO_3$, and a few percent of $MgCO_3$. Dolomite usually contains about 40–44% $MgCO_3$ and 54–58% $CaCO_3$. Dolomitic limestone is characterized by an intermediate $MgCO_3$ content [9].

When limestone enters the kiln, there is first a preheating step during which limestone is heated from the ambient temperature up to 800℃ by direct contact with kiln gases, i.e. the products of combustion and excess of air. At 800℃, the decomposition of the surface layer of limestone particles begins and the temperature rises. Once the temperature exceeds the decomposition temperature of 900℃, thermal dissociation of limestone particles proceeds beyond the surface [15]. Lime calcination usually takes place between 900℃ and 1200℃ [9]. For high calcium limestones, the calcination step occurs according to the reaction equation 1. The heat necessary for this decomposition is of 760 kcal/kg CaO at 25℃ and 723 kcal/kg CaO at 900℃ [15]. For dolomites and dolomitic limestones, the decomposition mechanism is more complex, generalized by the overall reaction equation 2, and requires 723 kcal/kg $CaO.MgO$ at 25℃ [15].

$$CaCO_3 + heat \rightleftharpoons CaO + CO_2 \tag{1}$$

$$CaCO_3.MgCO_3 + heat \rightleftharpoons CaO.MgO + 2CO_2 \tag{2}$$

Remark: Depending on the calcination temperature, three types of calcined dolomite can be obtained: light burnt, dead burnt and half burnt dolomite. Light burnt dolomite $CaO.MgO$ is produced similarly to high calcium quicklime, with lower energy requirements since the dissociation of $MgCO_3$ requires less heat and occurs at a lower temperature. Dead burnt, or sintered, dolomite is produced at higher temperatures, between 1400 ℃ and 1800 ℃, leading to exhaust gases leaving the kiln at around 420 ℃. Half burnt dolomite $CaCO_3.MgO$ is produced at 650 ℃ and in small quantities [9].

Lime sintering can occur if the $CaCO_3$ is completely dissociated before the particle leaves the kiln. However, this step is negligible. Before leaving the kiln, the particles are cooled down with air below 100 ℃ [15], to avoid damaging the conveyor belt [24].

The calcination step is highly energy intensive. The required energy is provided by various fuels such as natural gas, coke oven gas, coal, lignite, heavy and/or light oils. Waste, such as used oil, plastics or paper, can also be used as fuel. Most kilns are able to operate on several fuels, the choice of which is highly impacting for the overall process due to many aspects [9]:

- Cost of fuels, which may represent between 30 and 60% of the production cost per ton of lime;
- Quality of the lime: impurities, whiteness, reactivity, and sulfur content of the produced lime are affected by the used fuel;
- Emissions, such as CO_2, CO, dust, SO_2 and NO_x.

There are different types of kilns for lime manufacture, with a typical lifetime of 30 to 45 years [9]. The choice of the most suitable kiln depends on several considerations [15] [9]:

- Characteristics of the limestone: particle size, strength of the limestone and the lime;
- Quality of the quicklime: percentage of $CaCO_3$, sulfur, reactivity, particle size;
- Availability and cost of suitable fuels;
- Constraints in terms of height and area;
- Investment and operational costs of the kiln;
- Environmental impact.

The energy consumption for limestone calcining depends on various parameters, such as the grain size of the limestone feed, the feed humidity, the considered fuel, or the use of dolime. Typical energy consumption values are reported for different types of kilns, in the following sections [9].

In EU-27, 90% of the kilns used in Europe are shaft kilns (551 kilns) according to a 2013 report of the European Commission [9]. There exist different types of shaft kilns. Mixed feed shaft kilns account for 21% of this total (116 kilns), Parallel Flow Regenerative Kilns for 29% (158 kilns), Annular Shaft Kilns for 13% (74 kilns), and "other" kilns for 37% (203 kilns) [8] [9]. The major characteristics of different kilns used for quicklime production are described in the following sections.

3.3.2.1 Parallel Flow Regenerative Kilns

The Parallel Flow Regenerative Kiln (PFRK) is the most common type of kiln in the EU. In 2013, 158 PFRK have been recorded in the EU. The PFRK design consists of two shaft kilns connected by a crossover channel. Each shaft kiln consists of three zones, namely, from the top to the bottom, the preheating zone, the burning zone and the cooling zone [10]. A schematic representation of the PFRK is depicted in Figure 9.

Limestone is fed at the top of both shafts and exits the kiln as CaO. Fuel is injected in the first shaft through lances at the top of the burning zone. The combustion of the injected fuel takes place in a counter-current fashion with the cooling air being blown at the bottom of the shaft. The cooling air is thus progressively heated and serves for the preheating of limestone [10].

The operation of PFRK takes place in two stages of 8 to 15 minutes. During the first stage, fuel –which can be gaseous (natural gas, coke oven gas, ...), liquid (heavy or light oil) or solid (lignite, hard coal) [25], as well as waste fuels or biomass [9] – is injected into shaft 1 and is burned thanks to the cooling air which is blown at the bottom of it [15]. The limestone calcination occurs between 950 °C and 1050 °C. A mixture of off-gases and cooling air at around 1050 °C is transferred towards the shaft 2 through the crossover channel before being mixed with the cooling air from the bottom of this shaft and allowing the heating of the limestone in the preheating zone [10]. The second stage begins after 8 to 15 minutes. The fuel is injected into shaft 2 while flue gases are now vented at the top of shaft 1 [15].

A PFRK operation requires about 20–40 kWh/t_{CaO} of electricity, while the heat use is between 3200 and 4200 MJ/t_{CaO}. Moreover, the grain size of the limestone feed is between 10 and 200 mm [9]. The residence time of limestone within the kiln is of about 8h [10]. Due to the high excess of air, the CO_2 concentration in the fumes is low, typically around 20% by volume [15]. The efficiency, based on the theoretical energy requirement for the thermal dissociation of $CaCO_3$, i.e. 1819.4 kJ/kg_{CaCO_3}, of a PFRK ranges from 75 to 99%. Furthermore, between 1 and 1.2 t_{CO_2}/t_{CaO} are emitted [10]. The PFRK configuration is thus the most efficient and the less emitting alternative.

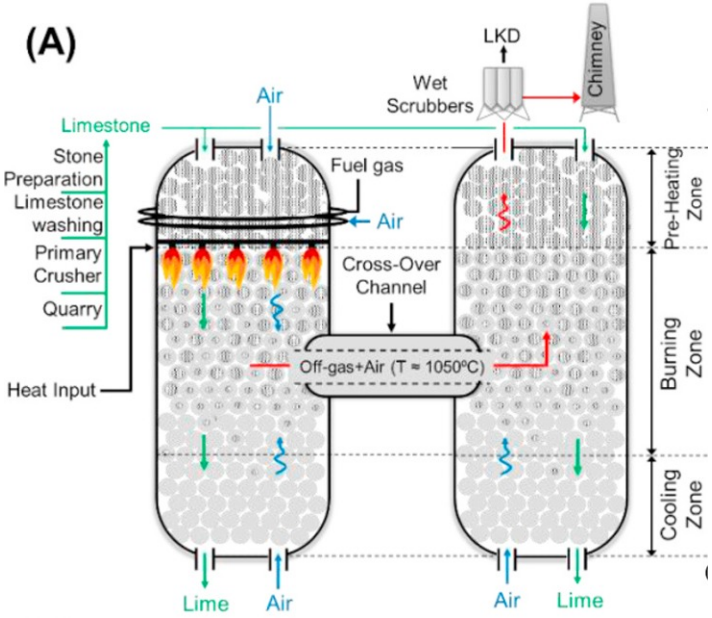

Figure 9: Schematic representation of a PFRK (From [10])

3.3.2.2 Annular Shaft Kilns

The Annular Shaft Kilns (ASK) consist of a central cylinder, separated from the external shell by the annular zone, within which the limestone goes from the top to the bottom of the shaft, passing once again through three zones: preheating, calcination, and cooling zones [10]. A good heat distribution is achieved by the presence of the aforementioned central cylinder [15]. As for the PFRK, gaseous, liquid and solid fuels can be used [24].

In an ASK, there are two burners, i.e. the upper burner and the lower burner, in which fuel is injected. In the upper burner is combusted the majority of the fuel with a sub-stoichiometric amount of air. The lower burner, operated with an excess of oxygen, provides the remaining oxygen necessary to the upper burner through part of its exhaust gases. A mixture of the exhaust gases from the lower burner and cooling air at about 900 °C is recirculated to moderate the lower zone flame temperature [15]. A schematic overview of the ASK is depicted in Figure 10.

Even though this design leads to lower thermal losses compared to the PRK (see section 3.3.2.5) and LRK (see section 3.3.2.4) configurations, it requires longer residence times, typically between 8 and 20h, as well as higher construction costs [10]. The ASK configuration yields off-gases characterized by a relatively high CO_2 concentration, around 29 and 34 vol%. The ASK design has an electric consumption between 18 and 50 kWh/t_{CaO} [10] and the heat use is between 3300 and 4900 MJ/t_{CaO}. Moreover, the grain size of the limestone feed is between 10 and 150 mm [9]. The efficiency of an ASK ranges between 65 and 69%. Furthermore, between 1 and 1.3 t_{CO_2}/t_{CaO} are emitted [10].

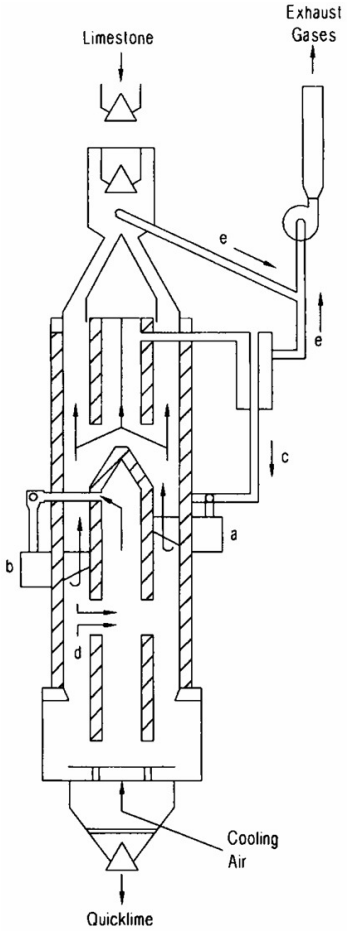

Figure 10: Schematic representation of an ASK (a) upper burners; (b) lower burners; (c) combustion air to upper burners; (d) combustion air to lower burners; (e) kiln exhaust gases (From [15])

3.3.2.3 Mixed Feed Shaft Kilns

In a Mixed Feed Shaft Kiln (MFSK), the limestone and the fuel, generally coke or anthracite, are mixed and fed at the top of the kiln [24]. The MFSK consists of three zones: preheating, burning and cooling zones. The preheating zone allows to reach a temperature of around 800-850 ℃ for both the limestone and the flue gases. The next zone is the burning zone, which can be divided into a reduction section and an oxidation section, within which the flue gas temperature and the bed temperature range respectively from 1000 ℃ to 1400 ℃, and from 800 ℃ to 1000 ℃ [10]. In the reduction section, carbon dioxide is reduced according to $C + CO_2 \longrightarrow 2CO$ [24]. The cooling zone allows the decrease of the final product temperature below 200 ℃ [10]. A schematic of the MFSK design is depicted in Figure 11.

MFSKs accept a feed size between 20 and 200 mm. The heat and electricity use range respectively from 3400 to 4700 MJ/t_{CaO}, and between 5 and 15 kWh/t_{CaO} [9]. The efficiency of a MFSK varies between 68 and 93%. Furthermore, between 1 and 1.5 t_{CO_2}/t_{CaO} are emitted [10].

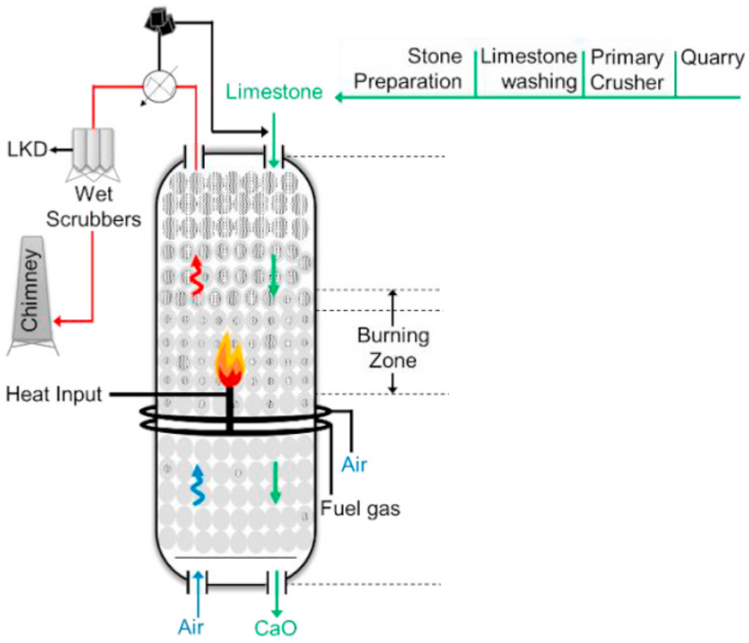

Figure 11: Schematic representation of a MFSK (From [10])

3.3.2.4 Long Rotary Kilns

The Long Rotary Kiln (LRK) is schematically depicted in Figure 13. It is typically between 50 and 225 m long, has a diameter between 2 and 6 m, and an inclination between 1 and 4° to the horizontal allows the feed to move along the kiln [10].

Limestone is fed at the upper end of the kiln, in counter-current of the fuel and air mixture fed at the lower end [10]. Heat from the off-gases is used for limestone preheating. This heat recovery can be achieved with various internals, such as internal refractory dams –increasing limestone's residence time–, lifters –causing limestone to cascade through the gases–, metal dividers and refractory trefoils –dividing the lime kiln into smaller tubes, or chains [15]. In kilns fed with lime mud or sludge, chains (see Figure 12) are heated by the combustion gases, allowing a better heat transfer and water evaporation from the feed, thus increasing the overall process efficiency [26].

This configuration is characterized by strong heat losses by convection and radiation, leading to a poorly efficient process. The residence time within the kiln is around 80-100 min [10]. The heat use for the operation of a LRK varies between 6000 and 9200 MJ/t_{CaO} while the electricity use is relatively low, between 18 and 25 kWh/t_{CaO}. The acceptable particle size of the feed ranges from 2 to 60 mm. LRKs accept various types of fuel: gas, liquid or pulverized solid fuels, waste and biomass [9]. The efficiency of a LRK ranges from 35 to 53%. Furthermore, between 1.2 and 1.8 t_{CO_2}/t_{CaO} are emitted [10]. The LRK is thus the least efficient and the most polluting configuration.

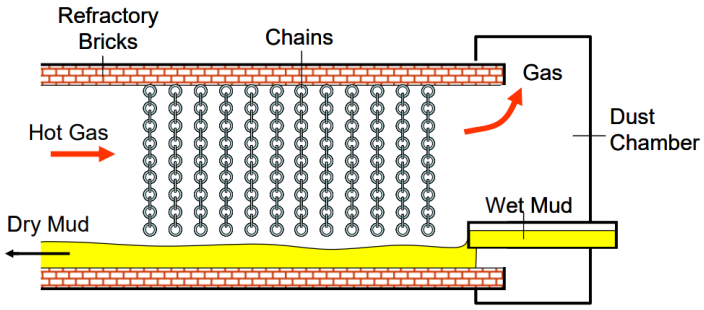

Figure 12: Chain section (From [26])

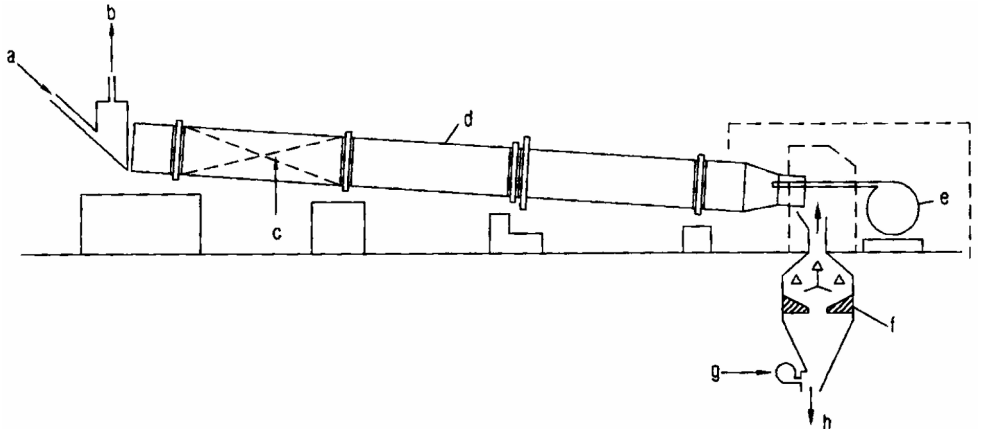

Figure 13: Schematic overview of a LRK (a) limestone; (b) exhaust gases; (c) refractory trefoils; (d) kiln shell; (e) fuel plus secondary air; (f) lime cooler; (g) cooling air; (h) quicklime (From [15])

3.3.2.5 Rotary Kilns with Preheater

A Rotary Kiln with Preheater (PRK) design is depicted in Figure 14. It consists of a calciner preceded by preheaters such as cyclones taking advantage of the possible heat recovery from off-gases through turbulent mixing [10]. The limestone is finally heated up to around 900℃ in the calciner by heat exchange with the off-gases, and is totally calcined during its residence time of about 30 min. A counter-current air flow allows the cooling of the lime exiting the calcination zone at around 1200℃ [10].

A higher process efficiency than for the LRK is observed. Moreover, the improved heat recovery in the preheaters induce a significant length decrease of the rotating unit compared to the LRK configuration. In fact, the kiln length is typically between 40 and 90 m long. However, higher maintenance costs are associated with the PRK configuration [10].

The operation of a PRK requires 5100 to 7800 MJ/t_{CaO} of heat, and between 17 and 45 kWh/t_{CaO} of electricity. This type of kiln operates with grain sizes of limestone between 10 and 60 mm [9]. The efficiency of a PRK varies between 41 and 62%. Furthermore, between 1.1 and 1.4 t_{CO_2}/t_{CaO} are emitted [10].

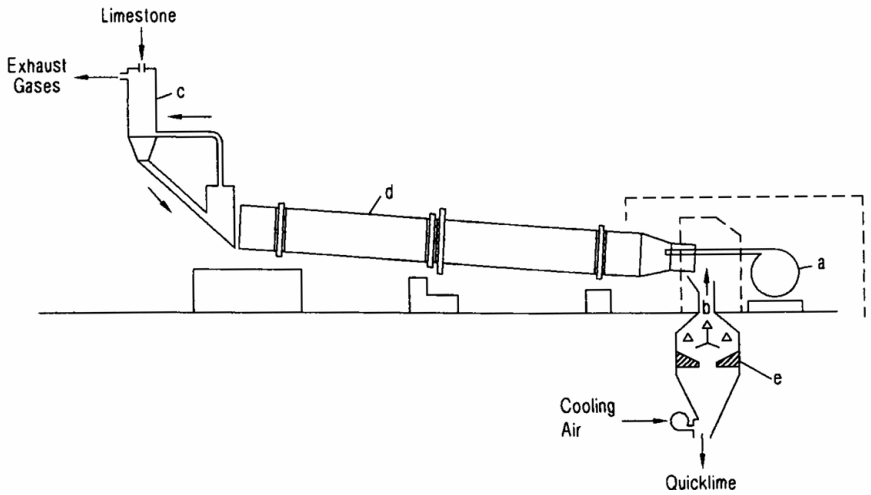

Figure 14: Schematic overview of a PRK (a) fuel; (b) preheated combustion air; (c) preheater; (d) rotary kiln; (e) cooler (From [15])

3.3.2.6 Other Kilns

Other types of kilns exist, even though they are much less frequent. These include double-inclined shaft kilns, central burner shaft kilns, external chamber shaft kilns, multi-chamber shaft kilns, beam burner shaft kilns, flash calciner kilns, internal arch shaft kilns, rotating hearth kilns, 'topshaped' kilns [9].

3.3.2.7 Waste heat recovery from kiln flue gases

The exhaust gases consist typically of CO_2 ($\sim$ 20 vol%), O_2 ($\sim$ 8 vol%), N_2 ($\sim$ 64 vol%) and H_2O ($\sim$ 7 vol%). Moreover, 1.4–2 mg/Nm^3 of lime kiln dust (LKD), 100—2000 mg/Nm^3 of NO_x, and 50—400 mg/Nm^3 of SO_x are typically found in the exhaust gases of a lime kiln [10].

The LKD can be removed by wet scrubbers and sold as drying, modifying, or stabilizing agent for soils, sediments, sludges and wastes [18]. The NO_x emissions can be limited by the implementation of Selective Non-Catalytic Reduction or Selective Catalytic Reduction, transforming NO_x into N_2 and H_2O. The SO_x emissions can be limited by sulfur scrubbing, or adsorbent injection in the flue gases for example [10].

Depending on the type of fuel considered, the air excess and the type of kiln, different flue gas temperatures are reached. For a shaft kiln with a lime exit temperature of 80 °C and an air excess number varying between 1 and 1.5, the flue gas temperature ranges from 50 to 300 °C for high-calorific gas, and from 150 to 400 °C for other fuels such as anthracite or lignite [24]. For rotary kilns, the flue-gas temperature at the stack is much higher. In PRKs, a temperature of 250 °C may be reached while in LRKs, temperatures up to 700 °C are observed [13]. This waste heat could be recovered for electricity production in an Organic Rankine Cycle (ORC).

A schematic representation of an ORC is depicted in Figure 15. An ORC consists of an organic fluid which cycles between four components: a turbine coupled to a generator, a condenser, a pump and a boiler [27]. A high-temperature and pressure vapor (state 1) is sent into a turbine. The coupled generator converts the mechanical energy into electricity. A pressure and temperature decrease occurs within the turbine. The obtained vapor (state 2) is condensed (state 3) and pressurized back to the high pressure of the cycle (state 4). The initial state (state 1) is reestablished by the boiler.

Between 2012 and 2013, Lhoist, Steetley and HeatCatcher worked on waste heat recovery from lime kilns with an ORC, during the WHEATREC4PG project. A thermal power recovery of 4 MW from the exhaust gases of a rotary kiln has been converted into 0.5 MW$_e$ of electric power thanks to 4 x 125 kWh ORCs. It has

been proven that 3000 MWh/year of low-carbon electricity can be generated, leading to a 25% improvement of the plant's electrical efficiency and the reduction of 1600 t CO_2/year. An investment of £1.3 million is necessary. However, savings are expected compared to purchasing 3000 MWh/year of electricity [3].

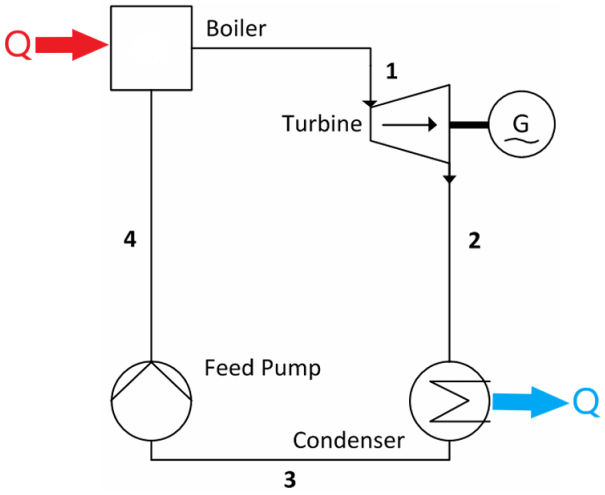

Figure 15: Scheme of an ORC (Adapted from [27])

3.3.3 Lime milling and grounding

Quicklime exiting the kiln is screened to remove the fines fraction (usually below 5 mm). In some plants, there is a picking conveyor belt removing partially calcinated lumps. Jaw crushers and roll crushers are used to reduce the size of too big particles. The crushed lime is sent towards a multi-deck screen, producing pebble lime (typically between 15 and 45 mm), granular lime (typically between 5 and 15 mm) and secondary fines fractions (typically less than 5 mm). Bigger particles may be sent towards a secondary crusher before being recycled to the multi-deck screen [15] as depicted in Figure 16.

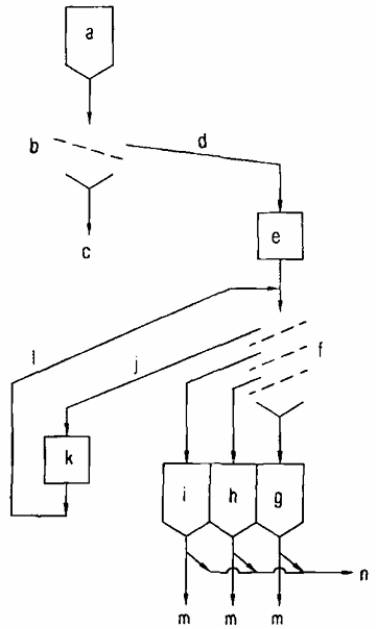

Figure 16: Basic lime processing plant (a) shaft kiln; (b) fines screen; (c) primary fines; (d) picking belt; (e) primary crusher; (f) multi-deck screen; (g) secondary fines bunker; (h) granular lime bunker; (i) pebble lime bunker; (j) oversize lime; (k) secondary crusher; (l) recycle of crushed oversize; (m) loading-out points; (n) internal feed to ground lime and/or hydrating plants (From [15])

The obtained fractions can be sent towards hydration plants, or be stored. The storage conditions are very important. In fact, quicklime should be stored in dry conditions to avoid the exothermic hydration reaction (see section 3.3.4). Moreover, quicklime should also be stored in conditions free from draughts to avoid air slaking. Air slaking consists of the reaction of quicklime with water and carbon dioxide from the atmosphere according to the following equations:

$$CaO + H_2O \rightleftharpoons Ca(OH)_2 \tag{3}$$

$$Ca(OH)_2 + CO_2 \rightleftharpoons CaCO_3 + H_2O \tag{4}$$

Finally, due to the exothermic nature of the reaction between quicklime and water, the storage should not be near flammable materials.

Lime grinding of coarser grades, using impact mills, requires between 4 and 10 kWh per ton of quicklime, while between 10 and 40 kWh per ton of quicklime are required finer grades, produced by ball mills, ring-roll mills and high-pressure mills with de-agglomerators [9].

The obtained milled product is denominated 'lump lime' if its average particle size is below 20 cm, 'pebble lime' for sizes between 0.6 and 2.5 cm, 'ground lime' for sizes below 0.25 cm, and 'pulverised lime' for particles with a size below 10^{-4} cm [10].

3.3.4 Quicklime hydration and slaking

3.3.4.1 Hydrated lime

Hydrated lime refers to the dry calcium hydroxide powder obtained by the hydration process, i.e., reaction between quicklime and a controlled excess of water moderating the process temperature. Hydrated lime contains less than 1% of unreacted water [15].

For high calcium quicklimes, the chemical reaction involved in the process is equation 5:

$$CaO + H_2O \rightleftharpoons Ca(OH)_2 + heat \tag{5}$$

This reaction releases 276 kcal/kg CaO and is typically carried out at around 100 ℃ since above 350 ℃ the inverse reaction takes place. Moreover, the higher the temperature, the finer the obtained particles. To produce hydrated lime, twice the stoichiometric amount of water is added while the excess of water is removed as steam [15].

The magnesium oxide is not very reactive, and typically, under normal hydration conditions, less than 25% of MgO reacts according to the equation 6. Thus, highly hydrated dolomitic lime $Ca(OH)_2.Mg(OH)_2$ is produced in an autoclave under steam pressure at temperatures above 100 ℃, i.e. hydrothermal conditions, according to reaction 7 where 211 kcal/kg $CaO.MgO$ are released [15].

$$CaO.MgO + H_2O \rightleftharpoons Ca(OH)_2.MgO + heat \tag{6}$$

$$CaO.MgO + 2H_2O \rightleftharpoons Ca(OH)_2.Mg(OH)_2 + heat \tag{7}$$

The hydration of quicklime is affected by the quicklime characteristics such as its reactivity, its mean apparent density, the particle size distribution, the percentage of carbonate, sulfur and magnesium oxide, or other impurities [15].

Hydrating plants generally consist of four stages illustrated in Figure 17. The first stage is the quicklime **handling and crushing**. The buffer storage of quicklime between the kiln and the hydrating plant allows more

flexibility. The crushing step allows a size reduction of the quicklime particles thanks to impact breakers, rolls, jaw crushers or cone mills.
The second stage is the **hydration**. A basic hydrator consists of three stages as depicted in Figure 18. Firstly, water and quicklime are strongly mixed in the pre-hydrator. Then, the exothermic hydration reaction 5 occurs and leads to the boiling of the excess water. Finally, there is a finishing stage to remove the coarse grit, $CaCO_3$, unslaked quicklime and water-burnt hydrate. The hydrator operates under slight suction to avoid any dust emission [15].
The third stage is the **classification**. This stage depends on the quality of the feed as well as the required quality of the products. The raw hydrate is sent towards a primary air classifier. The oversized particles, i.e. the primary tailings, consist of unburnt limestone, hydrated quicklime and gritty hydrate. The primary tailings are milled and fed towards a secondary air classifier. If too high amounts of CaO are observed in the secondary fines, they may be sent back to the hydrator. If it is necessary to isolate a $CaCO_3$-rich fraction, one may feed the primary tailings to a beater mill, which preferentially reduces the particle size of soft quicklime and gritty hydrate, while the one of the harder limestone remains unchanged. Then, an air classification allows the separation of the lime-enriched secondary fines from the carbonate-enriched secondary tailings.
The fourth and last stage is the **storage and dispatch** of the hydrated lime [15].

The operation of the hydrators, the air classifiers and the conveyors requires approximately between 5 and 30 kWh/ton of quicklime [9].

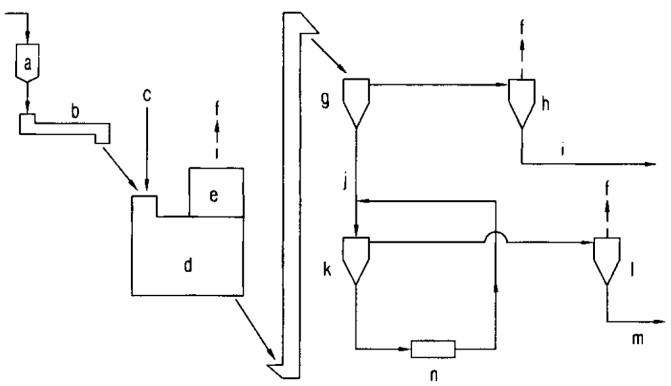

Figure 17: Basic hydrating plant (a) quicklime bunker; (b) weigh feeder; (c) water; (d) hydrator; (e) dust collector; (f) discharges to atmosphere; (g) primary classifier; (h) cyclone; (i) primary fines; (j) primary tailings; (k) secondary classifier; (l) cyclone; (m) secondary fines; (n) mill (From [15])

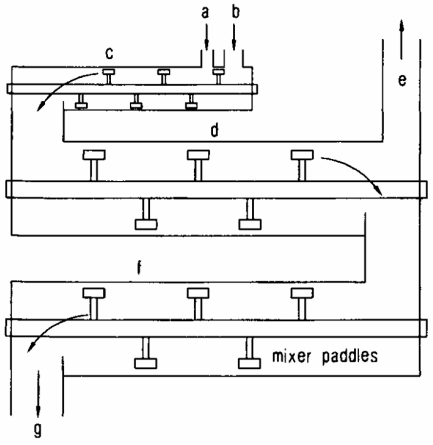

Figure 18: Representation of a 3-stage hydrator (a) water; (b) quicklime; (c) pre-hydrator; (d) hydrator; (e) steam and air to dust collector; (f) finishing stage; (g) raw hydrate (From [15])

3.3.4.2 Milk of lime

Milk of lime refers to a suspension of hydrated lime in water, with a solid content up to 40 wt%. Higher solid content leads to a so-called lime slurry. If the solid content is between 55 and 70%, the obtained dispersion is called lime putty [15] (see section 3.3.4.3). Milk of lime is produced by slaking, implementing the same reactions as in the case of hydration (see equations 5 and 7). The water-to-lime ratio is although different, typically between 3:1 and 4:1. The quality of the final product obtained by slaking is affected by different factors, including the particle size distribution of quicklime, the reaction temperature or the agitation during slaking [15].

Grit produced during slaking is typically removed since it leads, among other things, to abrasion of pumps and pipelines, or shut-downs to remove the settled grit which do not redisperse. Grit production can be avoided by slaking in a mill grinding the grit. Another possibility is to perform the slaking of finely ground quicklime. The last possibility for avoiding grit is to produce milk of lime from hydrated lime [15].

Lime slaking can be performed in one of the four following slakers: detention, paste, ball mill, and batch. The first three configurations are operated in continuous mode.

- **Detention slaker**: Detention slakers, also called slurry slakers, consisting of a tank agitated with an impeller [15] which can be either horizontally or vertically mounted, are the most common design due to their relatively low CAPEX [28]. Detention slakers are temperature-controlled. In fact, quicklime is fed to the slaker while the water flowrate is adapted to maintain the slaking temperature around the desired value, typically between 70 °C and 85 °C [28]. Usually, for high-calcium quicklimes the water-to-lime weight ratio varies between 3.5:1 and 4:1, while this ratio is lower for dolomitic quicklimes [15]. The average residence time in such slakers is between 6 and 12 minutes. A degritting step is performed after slaking, generally using a vibratory screen. Degritting may also be performed with an inclined rake or screw [28].
- **Paste slaker**: Paste slakers consist of a horizontal tank and two horizontally-mounted counter-rotating paddle shafts [15]. Slaking is performed typically between 85 °C and 90 °C, with a water-to-lime weight ratio between 2.5:1 and 3:1. The residence time in such slakers is 4-5 minutes [28]. The consistency of the produced paste is controlled by the paddles torque and the water flowrate [15]. After slaking, the obtained paste is diluted with water to a water-to-lime ratio of 4:1, and degritted usually with inclined rakes or screws, even if vibratory screens may also be used [28].
- **Ball mill slaker**: The ball mill slaker is the most expensive configuration but avoids the need for degritting. Process temperature and residence time are similar to the ones observed in detention slakers. The particularity of the ball mill slaker is a grinding step –usually using steel balls– leading to the production of highly-reactive slurry and the pulverization of the grit [28].
- **Batch slaker**: Batch slakers consist of a tank in which water and quicklime are mixed thanks to a vertical impeller. Once slaked between 85 °C and 95 °C [15], the milk of lime is pumped out of the tank, and degritted by a vibrating screen when necessary. Batch slakers offer a high flexibility in terms of residence time, which is unlimited [28].

Milk of lime can also be produced directly from hydrated lime which is fed to a mixer with a given amount of water [15].

3.3.4.3 Lime putty

By settling of milk of lime and withdrawal of the supernatant, it is possible to produce lime putty. Lime putty can also be produced by mixing hydrated lime with water according to a water-to-lime weight ratio between 0.7:3 and 1:3 depending on the desired texture.

Since its properties improve over time, lime putty is usually not directly used after production. Its storage is much less demanding than for quicklime. In fact, lime putty can be stored in a moist environment. Moreover, if left uncovered, the carbonation of lime putty leads to the formation of a protective crust [15].

3.4 Energy transition pathways

Lime manufacturing is an energy-intensive process, with more than 90% of the energy consumption associated with the limestone calcination [29]. The calcination step generating between 1 and 1.8 tons of CO_2 per ton of CaO [10], the lime sector represents about 1% of the global anthropogenic CO_2 emissions [8]. In 2019, direct CO_2 emissions for the European lime sector amounted to 19.5 million tons of CO_2 [12].

The lime industry is qualified as "hard to abate" sector. In fact, roughly two thirds (68%) of the CO_2 emissions are intrinsic to the thermal degradation of limestone and are, thus, considered unavoidable. The rest of the emissions are related to fuel combustion in the kiln (30%) and electricity requirements (2%) [10].

The objective of the European lime sector by 2030 is to reduce its CO_2 emissions by 20% compared to 2019. According to the European Lime Association (EuLA), 5 million tons of CO_2 per year are expected to be permanently removed from the atmosphere. This objective can be achieved by focusing on three axes: fuel switching towards biomass, waste, and green hydrogen; use of renewable electricity; CO_2 capture, utilization and storage [12]. Kiln upgrade can also reduce CO_2 emissions. The potential of various solutions for CO_2 emissions reduction is depicted in Figure 19.

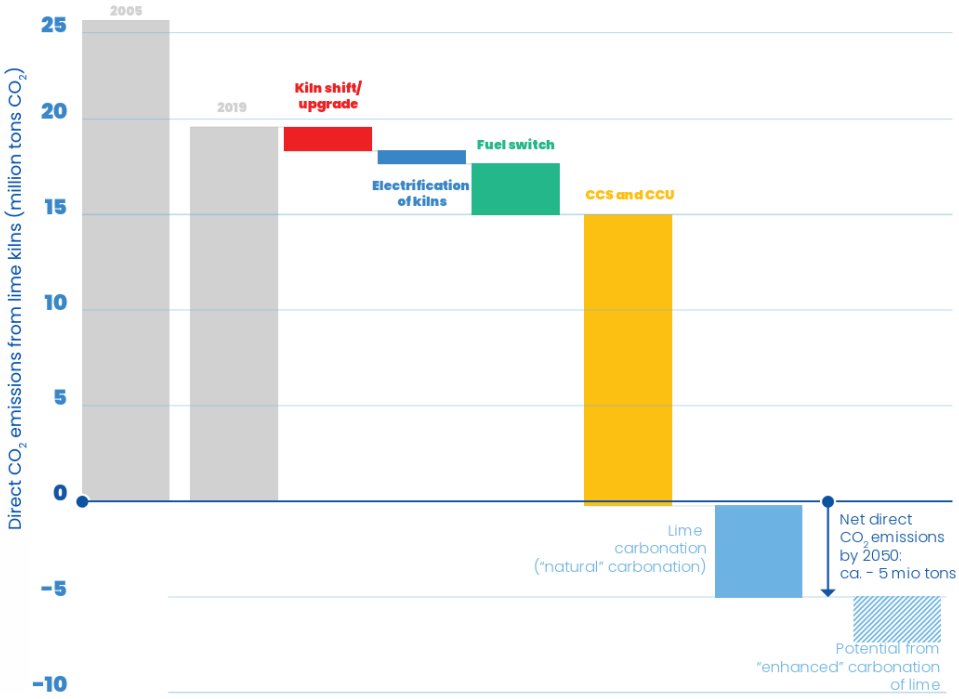

Figure 19: Pathway to negative emissions by 2050 (From [12])

Efforts for decarbonizing the lime sector and even possibilities for reaching net negative emissions are presented in several reports such as *Net Negative 2040 Roadmap* of Mineral Products Association [11], *A pathway to negative CO_2 emissions by 2050* of the European Lime Association (EuLA) [12], and *Carbon Action 2030* of Lhoist [30].

To date, significant efforts have been focused on the improvement of the process efficiency by investing in best available kiln technologies and improving the fuel efficiency [11]. In 2023, the European average

thermal efficiency for the lime production was around 88% [12].

Scope 2 emissions, i.e. indirect emissions related to energy consumption, have also been reduced by sourcing electricity from renewable sources or generating renewable electricity onsite by Anaerobic Digestion and Combined Heat and Power (CHP) systems as in the project of Lhoist [11]. In 2019, 900 GWh of electricity were consumed by the lime sector, contributing to 250 000 tons of scope 2 CO_2 emissions. The implementation of carbon capture technologies and electrified kilns is expected to increase by 80% the total electricity consumption by 2030. A tenfold electricity consumption is expected by 2050 [12].

The different energy transition pathways investigated for the lime sector are described in more detail in the following sections.

3.4.1 Carbon Capture & Storage

Carbon Capture and Storage (CCS) represents one of the most promising transition pathways. CCS can be implemented according to three different configurations: pre-combustion, post-combustion and oxycombustion. The pre-combustion capture consists in the carbon removal from the fuel before its burning. However, this technique is not optimal for the lime sector since the majority of CO_2 emissions are related to the process itself and not to the fuel burning. In the oxycombustion configuration, fuel is burnt in –almost– pure oxygen instead of air, resulting in a substantial increase in the CO_2 concentration in the flue gas. This elevated concentration significantly facilitates the subsequent capture and purification of CO_2. The post-combustion capture consists in the treatment of exhaust fumes [31].

According to Simoni et al. [10], the post-combustion configuration is better adapted to the lime sector than the pre-combustion configuration, since CO_2 released by both the limestone calcination and the fuel combustion can be captured. Different technologies of carbon capture are envisaged [10]. These are listed just below and presented in more details in the following sections:

- physical/chemical absorption;
- membrane separation;
- physical/chemical adsorption;
- direct separation;
- oxy-fuel combustion;
- fuel cells;
- calcium looping;
- cryogenic separation.

3.4.1.1 Absorption

In a gas-liquid contactor, a gaseous effluent is contacted with a liquid solvent, the so-called absorbent. As the gases flow through the column, CO_2 is selectively dissolved in the absorbent, leaving a CO_2-lean stream at the top of the column. The CO_2-rich solvent undergoes a regeneration step to release the captured CO_2. The regenerated solvent is recycled back to the absorption column while the CO_2 is stored or used [32]. A schematic representation of CO_2 capture by absorption is depicted in Figure 20.

Absorption can be either physical, i.e. based on Henry's law for the absorption of CO_2 into solvents (typically Rectisol, propylene carbonate and Selexol), or chemical, i.e. using solvents (mainly amine and carbonate solutions such as monoethanolamine (MEA), diethanolamine (DEA) or methyl diethanolamine (MDEA)) chemically reacting with CO_2. Physical absorption is operated at low temperature and high pressure, while the solvent is regenerated by a temperature increase and/or a pressure decrease. During chemical absorption, a weakly bound intermediate molecule is produced. Thus, the trapped CO_2 is released by applying heat

[32]. While chemical absorption is suitable for both pre-combustion and post-combustion capture, physical absorption is usually applied for pre-combustion capture. In fact, physical solvents are less efficient at low CO_2 concentrations, which make them less suitable for post-combustion capture. Absorption allows the capture of 90–98% of the CO_2 initially present in the effluent to be treated. The recovered CO_2 stream is more than 99% pure [33].

Physical and chemical absorption energy consumption respectively ranges between 4 and 6 MJ/kg CO_2, and between 2 and 4.5 MJ/kg CO_2 [34]. The capture process is hindered by the presence of SO_x and NO_x in the flue gas to be treated [33].

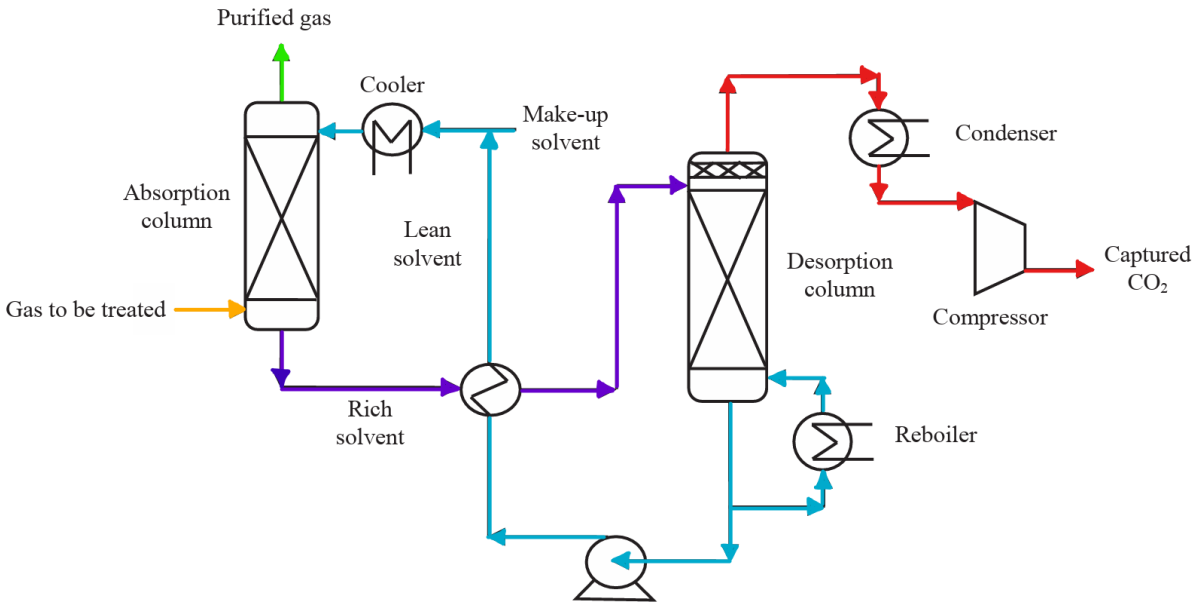

Figure 20: CO_2 capture based on gas-liquid absorption (Adapted from [35])

One advantage of the absorption process is that this configuration can be easily retrofit in existing plants [10]. Despite the high CO_2 selectivity and large capacities of the absorption technology, the high energy requirements, toxicity and high costs of solvents, thermal and oxidative solvent degradation –leading to the formation of corrosive products– are the barriers that impede the widespread implementation of this technique [33].

Amine-based CO_2 capture and storage is studied in the DINAMX project in which Lhoist is participating with Arcelor Mittal, TotalEnergies and IFP Energies Nouvelles. This project is being conducted between 2020 and 2024. It investigates a special "de-mixing amine blend" characterized by lower energy requirements for regeneration. A lab scale pilot has been validated for flue gas exiting a lime kiln [3].

3.4.1.2 Membrane separation

Selective permeable membranes are used for gas-gas separation, to separate CO_2 from flue gases. There exist polymeric membranes (made of organic materials), ceramic membranes (made of inorganic materials), and hybrid membranes (made of organic and inorganic materials). The separation of CO_2 from the gas mixture occurs by CO_2 permeation through the membrane. This phenomenon comprises three steps [32]:

1. CO_2 adsorbs on the high-pressure side of the membrane;
2. CO_2 diffuses through the membrane;
3. CO_2 desorbs once it reaches the lower-pressure side of the membrane.

Two membrane configurations exist: conventional membranes (see Figure 21b) and membrane contactors (see Figure 21a). Membrane contactors act as an interface between the absorption solvent and the gaseous mixture to be treated, avoiding the dispersion of both phases [34]. Conventional membranes separate selectively one or more gaseous components from a gaseous mixture. Membrane technology applied for post-combustion CO_2 capture is still at the research or development stages. It has shown promising results but has not been tested yet in a lime plant [10].

Membrane separation represents an interesting alternative for carbon capture due to its low CAPEX and OPEX, its slow performance decline, and its easy installation and transport. At laboratory scale, around 60-70% recovery has been reached, with a CO_2 stream purity of about 90% [36]. The reduced operational complexity, affordability, and low energy consumption (0.5-0.6 MJ/kg CO_2) compared to absorption processes make the membrane technology attractive for CO_2 capture. However, the membrane life span is shortened when exposed to acid gases such as NO_x and SO_2 [32]. The low thermal stability of commercial membranes requires compression and cooling units upstream of the membrane, which increase the CAPEX and OPEX. Moreover, the low CO_2 concentration in the treated off-gases is an inadequate driving force for the permeation process [34], i.e. the partial pressure difference of CO_2 on both sides of the membrane [36].

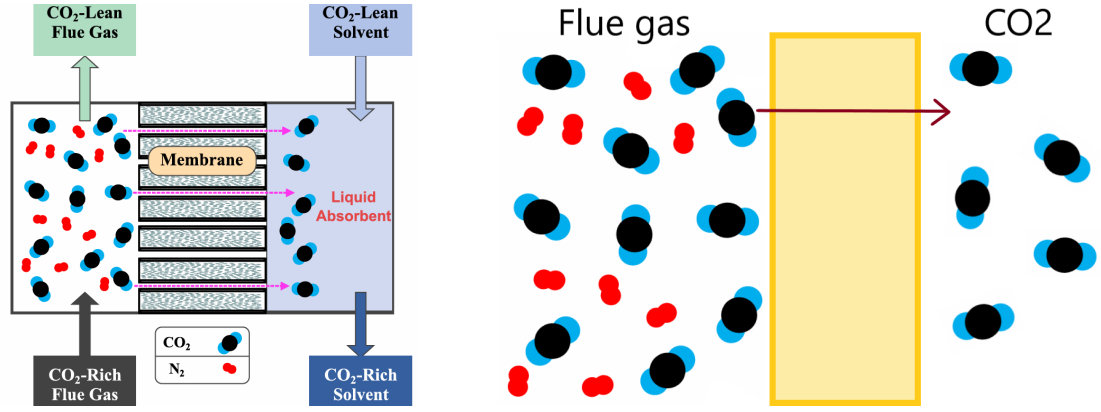

(a) Membrane contactor (From [34])

(b) Conventional membrane (Adapted from [34])

Figure 21: Membrane technology for CO_2 capture

The Norcem CO_2 capture project, conducted between 2013 and 2017, demonstrated the possibility of CO_2 separation by a membrane at pilot scale. This project, operated by the Norwegian University of Science and Technology, took place in Brevik cement plant (Norway) [36]. The polyvinylamine hollow fiber membrane tested captured a 70 mol% pure CO_2 stream. The membrane showed no significant performance decrease after exposure to SO_2 and NO_x [37].

3.4.1.3 Adsorption

For CO_2 capture by adsorption, solid adsorbents, typically activated carbon, zeolites –natural (e.g., ZAPS, ZNT, ZN-19) or synthetic (e.g., X, Y, A, ZSM)–, or metal-organic frameworks –i.e., porous solid networks composed of metal ions and organic ligands– are used [34]. When the gas mixture is contacted with solid adsorbents, the CO_2 molecules are separated from the other gases by preferentially adsorbing to the adsorbent's surface either physically (physisorption) or chemically (chemisorption). Van de Waals forces are involved in physisorption, whereas chemical bond formation is involved in chemisorption [36]. Once saturation is reached, adsorbent regeneration is performed by applying heat, pressure, or a combination of both. The regeneration step induces the release of the previously captured CO_2, which can then be stored or used [32]. A schematic representation of the adsorption process is depicted in Figure 22.

Adsorption processes can be used for pre-combustion and post-combustion capture. The adsorbent should be characterized by a high adsorption capacity and selectivity for CO_2, fast kinetics for adsorption and desorption, good chemical and physical stability, and a regeneration step at moderate conditions [33].

The capture efficiency of the adsorption process ranges from 70 to 95%. Between 1.5 and 4 MJ/kg CO_2 are required to perform the separation [34].

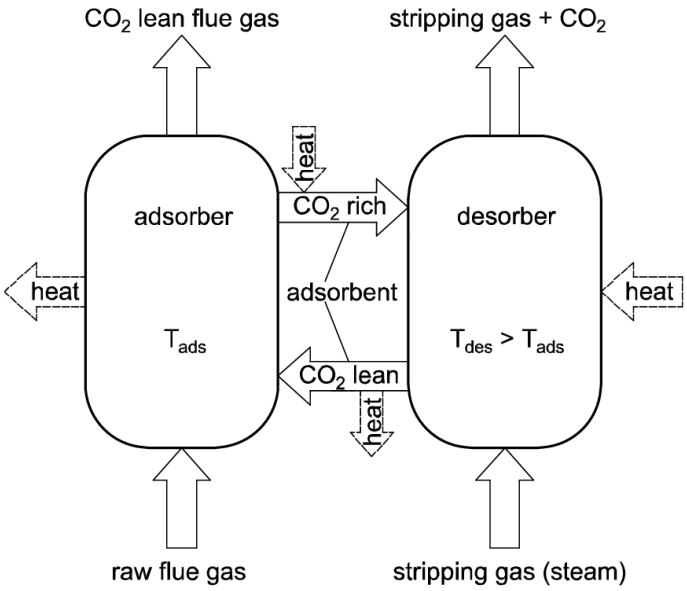

Figure 22: CO_2 capture by adsorption (From [38])

Carbon capture by adsorption was studied at the Brevik cement plant (Norway) in 2016. The Research Triangle Institute investigated the use of polyethyleneimine loaded on silica as solid sorbent, enabling a capture rate of 80–90%. Tests demonstrated the negative impact of SO_2 on the sorbent capacity (-30% for a SO_2 concentration of 100 ppm) [36].

3.4.1.4 Direct separation

Direct Separation has been investigated by Lhoist and Tarmac through the Low Emissions Intensity Lime and Cement (LEILAC1) European-funded project. The LEILAC1 pilot plant (2016 – 2021; TRL 7-8 [3]), built at Heidelberg Cement's plant in Lixhe (Belgium), has a capture capacity of 25 000 t_{CO_2}/y, corresponding to a 100 t_{lime}/d kiln [36].

It consists of Calix's new design of a kiln in which specially designed steel tubes supply indirect heat for the calcination reaction. Limestone is fed at the top of the Direct Separation Reactor (DSR). On its way down to the bottom of the DSR, limestone is heated and calcined by conductive and radiative heat transfer. The required heat is provided by natural gas combustion in the external furnace [36]. By separating the combustion of fuels for heat supply from the calcination of limestone, the CO_2 released by the thermal decomposition of $CaCO_3$ remains pure enough for use or storage [39], leading to a CO_2 emissions reduction of 63%. It has been shown that this configuration has a very low energy penalty of 0.6 GJ/t CO_2 captured [40].

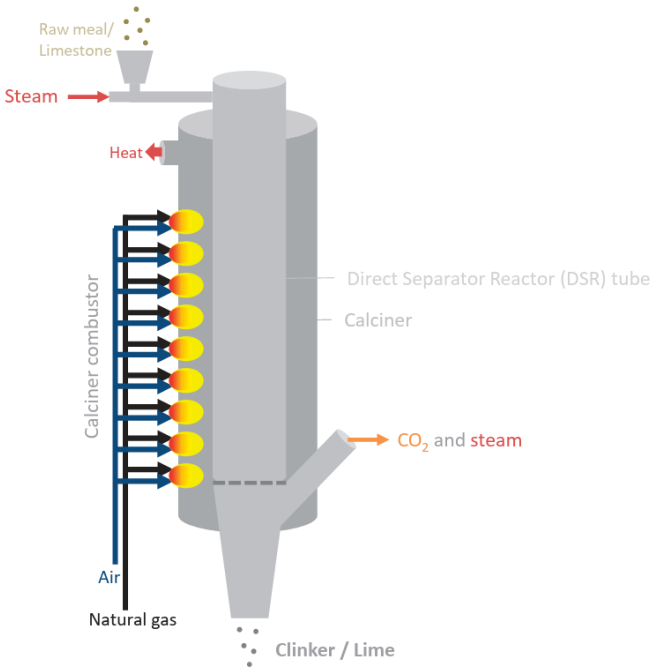

Figure 23: LEILAC's direct separation reactor (From [36])

The LEILAC2 project (2020-2025) will scale up the technology to a 100 000 t_{CO_2}/y capture capacity, i.e. quadrupling the capacity of LEILAC1. During the LEILAC2 project, the full integration of the technology within an existing cement plant as well as the use of renewable energy for heat supply will be investigated [36].

3.4.1.5 Oxycombustion

The fuel combustion takes place in oxygen (between 95 and 99% purity [41]) –instead of air– with recycled flue gas [33] (to moderate temperature) leading to a decreased fuel consumption and an increased CO_2 concentration in the off-gases [11]. The obtained flue gas consists of mainly CO_2 (>80 vol%), H_2O, particulate matter, and traces of SO_x and NO_x. There is no need for solvents or sorbents for CO_2 capture in this case. In fact, particulate matter is removed by an electrostatic precipitator, H_2O is removed by condensation [41], while CO_2 is purified and compressed in a cryogenic CO_2 purification unit (CPU) [36].

The major drawback of the oxycombustion technology is the need of a cryogenic air separation unit (ASU) for oxygen production which drastically increases the energy requirements [41]. The ASU unit typically consumes between 150 and 800 kWh/t_{O_2} [42]. The implementation of oxycombustion allows to capture 90% of the CO_2 in the exhaust gases, with a specific energy consumption of around 1.6 GJ/t_{CO_2} [43].

The Zero-Carbon Lime (ZERCAL) pilot plant uses oxycombustion technology and captures the entirety of the CO_2 emitted by the lime production process. The pilot plant, located at Singleton Birch's Melton Ross site, is capable of producing 3000 tons of lime per year [3].

3.4.1.6 Calcium looping

The calcium looping technology is based on the reversibility of the carbonation reaction of CaO into $CaCO_3$. Off-gases containing CO_2 are contacted with a sorbent (CaO) in the carbonator. The reaction between the sorbent and the CO_2 leads to the formation of $CaCO_3$ which is fed to the calciner (operated under oxycombustion conditions). In the calciner, $CaCO_3$ is heated at around 900–950℃ [1] and decomposes into CaO, which is recycled back to the carbonator, and almost pure CO_2 [44], which is retrieved and either

stored or used. However, a periodical sorbent replacement is necessary accounting for the degradation of the CaO sorbent over time due to particle sintering during calcination [10]. A schematic representation of the calcium looping process is depicted in Figure 24.

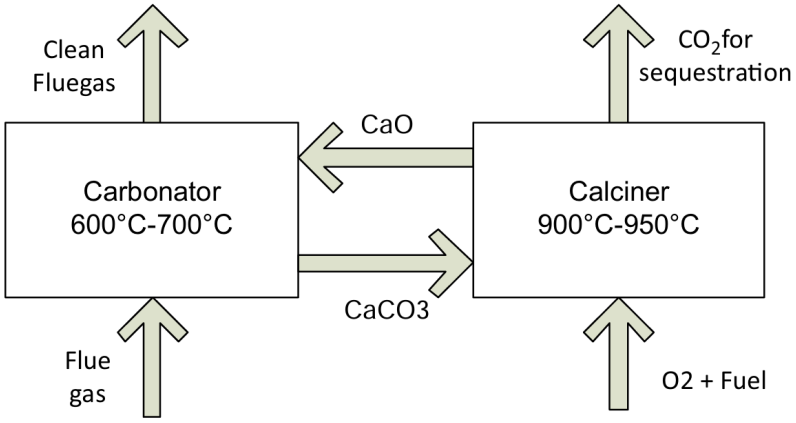

Figure 24: Calcium looping process (From [1])

A CO_2 capture of over 90% is possible and requires between 3 and 4 GJ/t_{CO_2} [10].

Calcium carbonate looping is investigated by Carmeuse and Endesa Generation in their CaO2 project (Calcium carbonate looping for coal power plants), by Carmeuse and Alstom in their CALENERGY project (Chemical Looping 4 Combustion Technology), and by TY Darmstadt and Lhoist in their CARINA project (Carbon Capture by Indirectly Heated Carbonate Looping Process) [3]. Moreover, between 2017 and 2023, the CLEANKER project demonstrated the integration of calcium looping technology in a cement plant in Vernasca (Italy) [45].

3.4.1.7 Cryogenic carbon capture

Cryogenic carbon capture is based on the cooling of flue gases at low temperature to separate CO_2 from other gases [33] by distillation, condensation or sublimation. Due to the low temperatures implemented in the separation process, moisture has to be removed from the treated flue gas, before the cryogenic separation, to avoid water freezing and blocking of the pipes [46]. However, cryogenic distillation is not suitable for CO_2 capture from flue gas due to its high temperature and low concentration. On the other hand, cryogenic sublimation is gaining interest in research due to its lower energy consumption compared to the cryogenic condensation technique as well as the wide range of acceptable CO_2 concentration of the treated effluent –between 10 vol% and 70%– which makes the technology reasonable for flue gas treatment [46].

Cryogenic sublimation is based on the high freezing point difference between CO_2 and other components contained in the flue gases. It has been shown that between 90 and 99% of CO_2 can be captured when operating temperature ranges from -135 ℃ to -120 ℃. The captured CO_2 is characterized by a purity exceeding 99%. Experimental setups required between 0.39 and 3.4 GJ/t_{CO_2} [46].

A collaboration between Air Liquide and Lhoist for cryogenic separation began in 2023 for the CalCC project [47]. Thanks to the Cryocap^{TM} FG technology developed by Air Liquide, Lhoist targets an emission reduction of 600 kt$_{CO_2}$/y, which will be transported and sequestrated in the North Sea [12].

3.4.1.8 Fuel cells

Molten Carbonate Fuel Cells (MCFC) are envisaged for CO_2 capture from flue gases. MCFCs are used to directly convert the chemical energy of a fuel, such as natural gas, into electricity through an electrochemical

process. Reaction 8 takes place at the anode, while reaction 9 takes place at the cathode.

$$CH_4 + 4CO_3^{2-} \longrightarrow 2H_2O + 5CO_2 + 8e^- \tag{8}$$

$$2O_2 + 4CO_2 + 8e^- \longrightarrow 4CO_3^{2-} \tag{9}$$

The net reaction in the fuel cell is:

$$CH_4 + 2H_2O + 4CO_2 + 2O_2 \longrightarrow 5CO_2 + 4H_2O + heat + electricity \tag{10}$$

The working principle of an MCFC is depicted in Figure 25, implying the following reactions. At the anode, natural gas (CH_4) reacts according to the steam reforming reaction (see eq. 11). The produced CO is then transformed into CO_2 according to the water-gas shift reaction (see eq. 12). Moreover, the produced hydrogen reacts, according to eq. 13, with the carbonate ion, produced at the cathode following the eq. 9.

$$CH_4 + H_2O \rightleftharpoons CO + 3H_2 \tag{11}$$

$$CO + H_2O \rightleftharpoons CO_2 + H_2 \tag{12}$$

$$H_2 + CO_3^{2-} \longrightarrow H_2O + CO_2 + 2e^- \tag{13}$$

The MCFC technology is interesting since it allows simultaneous CO_2 capture, H_2 production as well as power and heat generation, which can be valued internally or exported. With three fuel cells in series, nearly 70% of CO_2 emissions are avoided [10]. Depending on the configuration and number of MCFCs that are used, the CO_2 capture efficiency varies between 31 and 76% with a specific energy consumption between 0.4 and 1.2 GJ/t$_{CO_2}$ [48].

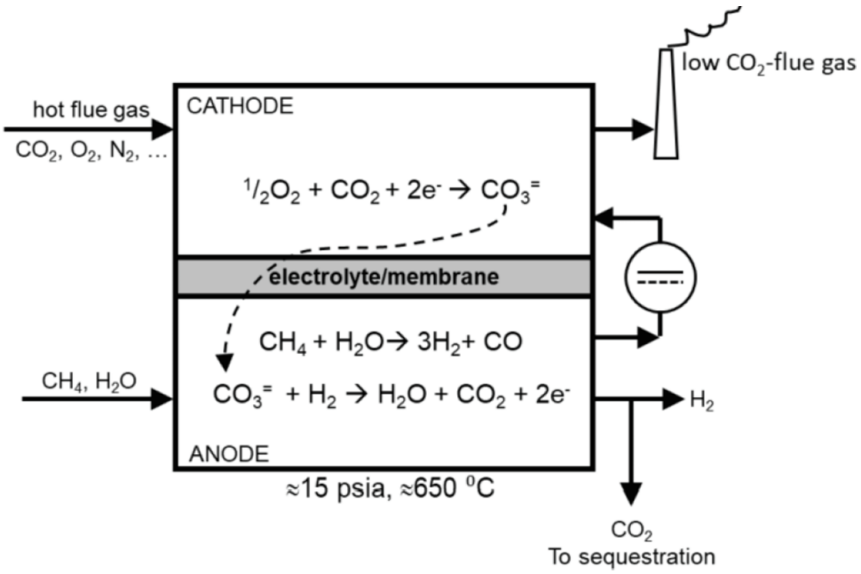

Figure 25: MCFC for CO_2 capture (From [49])

3.4.2 Bioenergy with carbon capture and storage

Bioenergy with carbon capture and storage (BECCS) represents one of the most advanced solutions for emission-intensive industries. Digestion or fermentation of biomass produces respectively gaseous and

liquid biofuels. Once burned, the generated heat can be used in industrial plants or for electricity production. Thus, CO_2 is captured through the photosynthesis of biomass, as well as by carbon capture processes [33]. BECCUS combined with product carbonation (see section 3.4.5) is expected to remove 250 000 tons of CO_2 per year from the atmosphere from 2040 [11].

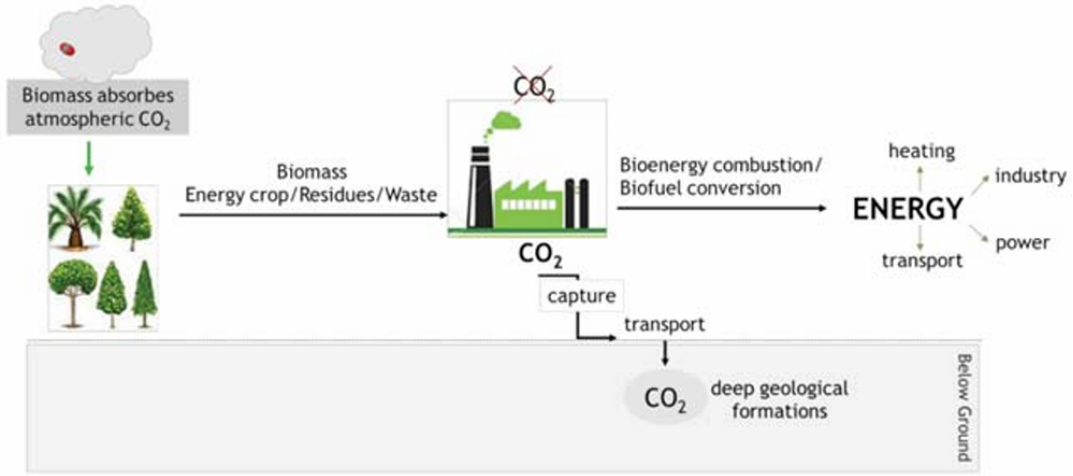

Figure 26: Bioenergy with carbon capture and storage (BECCS) (From [33])

3.4.3 Fuel switching

Another possibility for the reduction of CO_2 emissions related to lime production is fuel switching for the kiln. There is typically a desire to switch from solid fuels –such as lignite, coal, petroleum coke and anthracite– to natural gas to decrease the environmental impact [30]. Alternative fuels are predicted to provide 10 TWh by 2030 to lime kilns and more than 22 TWh by 2050 [12]. These alternative fuels [10] include:

- **Waste derived fuels**: waste derived fuels, such as plastics, paper or textiles [30], are more readily accessible in densely inhabited regions like Western Germany, Northern France, Belgium and the Netherlands [30] [12].
- **Biomass**: biomass constitutes a low-carbon and renewable fuel alternative. However, one must be careful about its availability. For example, Spanish Lhoist's facilities are fueled with grape seeds and olive derivatives, allowing an all-year-round fuel availability. Moreover, the required fuel quantity is quadrupled since biomass' calorific power and density are around half those of traditional solid fuels [30]. Typical calorific values for different fuels are listed in Table 1. Fuel switching to biomass is studied in various projects such as BIOXYSORB (Biomass co-combustion under both air- and oxy-fuel conditions) of IFK and Lhoist, or the ADIREN4LIME (Anaerobic Digestion as a Renewable Energy for the Lime Industry) project which aims at producing biogas directly fed to the kiln or used to produce electricity for electrified kilns [3].
- **Renewable electricity**: fully electrified kilns are expected to represent between 5 and 10% of the lime production by 2050 [12]. Electric alternative kilns are studied in various projects. Coolbrook patented the RotoDynamic Heater technology which heats air, nitrogen and process gases at very high temperatures, thanks to electricity instead of fossil fuel, and provides heat up to 1700 ℃ [50]. Moreover, SaltX Technology patented its Electric Arc Calciner (EAC) technology. The EAC consists of a plasma generator positioned at the center of a cylindrical chamber which directly converts electricity into high-temperature heat (>1600 ℃). The particularity of the SaltX's EAC technology is that the thermal energy is directly transferred to the raw material –by radiation and conduction– instead of a large volume of hot gases. In 2022, a 300 kW kiln pilot has been installed. In November 2023, a 2 MW electric kiln pilot

was commissioned in Hofors (Sweden). The first commercial application for quicklime production is expected for 2025 [51]. An electric rotary kiln has been developed by AGICO Cement. Silicon carbide rods allow an indirect heating of the raw material through the kiln wall [52] [53]. The inner structure of the electric kiln is shown in Figure 29.

- **Solar-powered kiln**: The SOLPART project focuses on the development of a solar reactor for high-temperature processes. Thus, calcination of limestone and dolomite could be performed thanks to concentrated solar heat. Figure 27 depicts the investigated configuration. A heliostat tilts its mirrors facets to reflect the sunlight towards the parabola all day long. The parabola concentrates the solar heat towards the reactor in which calcination takes place. Different types of reactors have been tested as part of the project. However, the shallow cross-flow bubbling fluidized bed, depicted in Figure 28, seems the most suitable option. First lab-scale experiments with gypsum and mete-kaolinite proved that a single pass operation allows to reach the required conversion. Satisfactory results have also been demonstrated with dolomite and limestone at a feed rate of 5–15 kg/h [54].
- **E-fuels**: E-fuels are synthetic fuels produced by the reaction between CO_2 and (preferentially green) hydrogen [10]. The use of such fuels enables net-zero CO_2 emissions without major infrastructure modifications.
- **Hydrogen**: the use of hydrogen for the manufacture of lime has been demonstrated in 2022 with a project at the Tarmac Tunstead [11]. Interest for hydrogen is growing due to its high calorific power and the absence of CO_2 during its combustion [10]. Several color labels of hydrogen exist, related to the production route: green for water electrolysis using renewable energy, blue for natural gas reforming coupled with carbon capture and storage, gray for natural gas reforming, black or brown for a production from coal, pink/purple/red for nuclear energy powered electrolysis, turquoise for methane pyrolysis, yellow for solar powered electrolysis, and white for natural occurrences of hydrogen [55]. Early applications of green hydrogen and e-fuels in lime kilns are expected for the end of the decade [12].

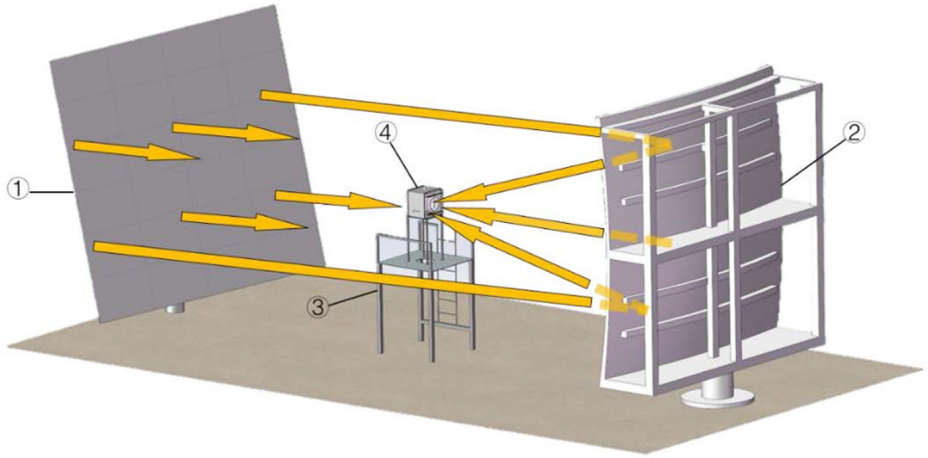

Figure 27: Layout for solar calcination of limestone 1) Sun-tracking heliostat; 2) Concentrating parabola; 3) Support structure of solar furnace (From [54])

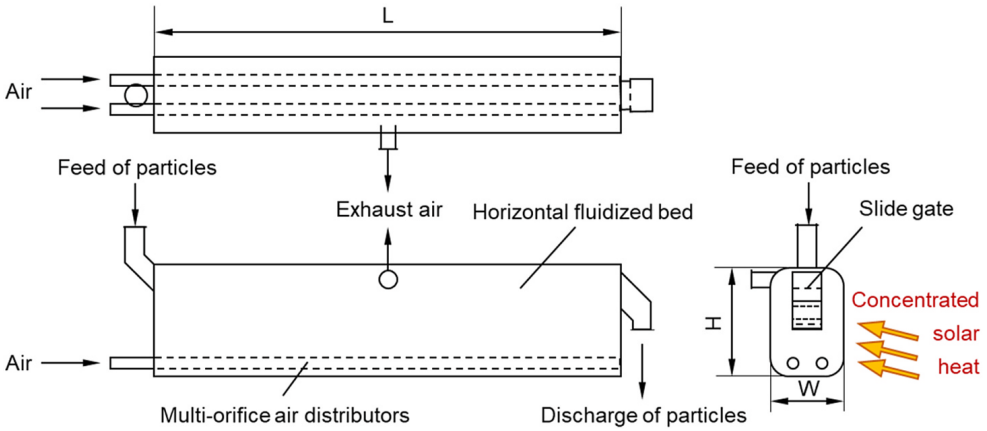

Figure 28: Representation of a shallow cross-flow bubbling fluidized bed (From [54])

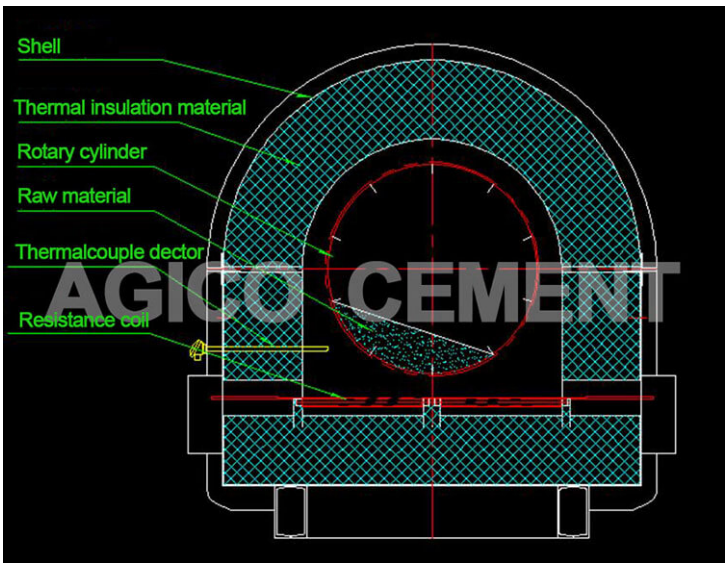

Figure 29: Electric rotary kiln by AGICO Cement (From [53])

Depending on the considered renewable energy source, the kiln operation will be impacted differently [56]. For **solid renewable fuels** such as wood, olive stones or almond shells, about 3% higher thermal energy will be required compared to a lignite-fired kiln. Moreover, a higher electricity consumption will be required due to the biomass processing, i.e. crushing, drying, and screening. Due to the lower calorific power and/or density of solid biomass compared to lignite, a threefold to sixfold fuel volume will be injected, leading to 20% higher off-gas volume. The temperature of the off-gases will be around 20 °C higher. For **liquid alternative fuels**, such as vegetable oil, bioethanol or biodiesel, no significant changes are expected. For **biogas**, the thermal energy and electricity consumption will be respectively 3% and 10% higher, compared to a PFRK fired with natural gas. Due to its lower calorific power compared to natural gas, two to three times higher fuel volume will be necessary. This leads to a higher off-gas volume (+6%) and a higher off-gas temperature (+20 °C). On the contrary, operating a kiln with **biomethane** instead of natural gas will induce no significant changes. The use of **pyrolysis gas** instead of natural gas will increase the thermal energy consumption, the electricity requirement, the injected fuel volume, the off-gas volume and the kiln off-gas temperature by respectively 9%, a factor 2, a factor 8, a factor 1.5 and more than 100 °C. The use of **hydrogen** in a lime kiln requires a lower thermal energy input of around 8% to avoid lime overburning or sintering, leading to kiln blockages [57].

Table 1: Lower calorific value of traditional and alternative fuels

Fuel type	Lower Calorific Value [MJ/kg]	Reference
Hydrogen	120	[58]
Torrefied biomass	20–30	[58]
Lignin	17–26	[58]
Wood	12–19	[58]
Straw	17	[59]
Corncob	18	[59]
Peanut shell	21.5	[59]
Natural gas	50	[58]
Oil	41	[58]
LPG	46	[60]
Hard coal	21	[59]
Municipal Solid Waste	10.5	[10]
Sewage Sludge	3.5	[10]
Medical Waste	13.9	[10]
Olive stones	19.8	[56]
Almond shells	13.3	[56]
Tail oil	41.4	[56]
Biodiesel	37	[56]
Bioethanol	37	[56]
Biogas (50% CH_4 – 50% CO_2)	13.3	[56]
Biogas (75% CH_4 – 25% CO_2)	26	[56]
Biomethane	50	[56]
Pyrolysis gas	4.17	[56]

3.4.4 Alternative "cold" production routes

Alternative production routes avoiding, or reducing, CO_2 emissions of the process are also investigated [10]. These alternatives include an electrochemical decarbonation of $CaCO_3$ and a chemical decarbonation by reaction with $NaOH$.

3.4.4.1 Electrochemical decarbonation

Ellis et al. [61] demonstrated the decarbonation of $CaCO_3$ and the precipitation of $Ca(OH)_2$ by an electrochemical process operated at ambient temperature, according to equation 14. A schematic representation of the process is shown in Figure 30. A maximum yield of 85% has been assessed.

$$CaCO_{3(s)} + 2H_2O_{(l)} \longrightarrow Ca(OH)_{2(s)} + H_{2(g)} + \frac{1}{2}O_{2(g)} + CO_{2(g)} \tag{14}$$

At the anode and cathode of a water electrolyzer occur respectively reaction 15 and 16.

$$2H_2O \longrightarrow O_2 + 4H^+ + 4e^- \tag{15}$$

$$2H_2O + 2e^- \longrightarrow H_2 + 2OH^- \tag{16}$$

The generated pH gradient allows the decarbonation of $CaCO_3$ at low pH, via reactions 17–20, and the precipitation of $Ca(OH)_2$ at high pH, via reaction 21 which is favored at pH > 12.5.

$$CaCO_{3(s)} \rightleftharpoons Ca^{2+}_{(aq)} + CO^{2-}_{3(aq)} \tag{17}$$

$$CO_3^{2-} + H^+ \rightleftharpoons HCO_3^- \tag{18}$$

$$HCO_3^- + H^+ \rightleftharpoons H_2CO_3 \tag{19}$$

$$H_2CO_{3(aq)} \rightleftharpoons CO_{2(g)} + H_2O \tag{20}$$

$$Ca^{2+} + 2OH^- \longrightarrow Ca(OH)_2 \tag{21}$$

From this process, a gaseous mixture of O_2 and CO_2 is produced at the anode, whereas H_2 is produced at the cathode. The obtained carbon dioxide can be separated and stored. One advantage of this cold production route is that the associated production of hydrogen might fulfill a large portion of the process energy demand or be used as feedstock for ammonia or fertilizers production. Moreover, even if CO_2 would still be produced, CO_2 capture would be facilitated by its higher volumetric concentration. In addition, the O_2/CO_2 stream could be used in an oxy-fuel lime manufacturing process or in a solid-oxide fuel cell whose generated electricity could power the necessary grinding and mixing steps of the process [61]. The key benefit of the electrochemical production of $Ca(OH)_2$ is that it doesn't require any energy input to produce the intermediate CaO [13].

An electrochemical process is studied in the FARADAY project (Integrated reactor for $H_2/O_2/CO_2$ production for CCU applications). The aim is the electrified production of lime and concentrated CO_2 which can be combined with green hydrogen for the production of e-fuels for example. This project has a double advantage: the emissions mitigation of the lime sector and the production of low-carbon-footprint chemicals [62]. In this project, Carmeuse, John Cockerill, UCL and UMons are involved.

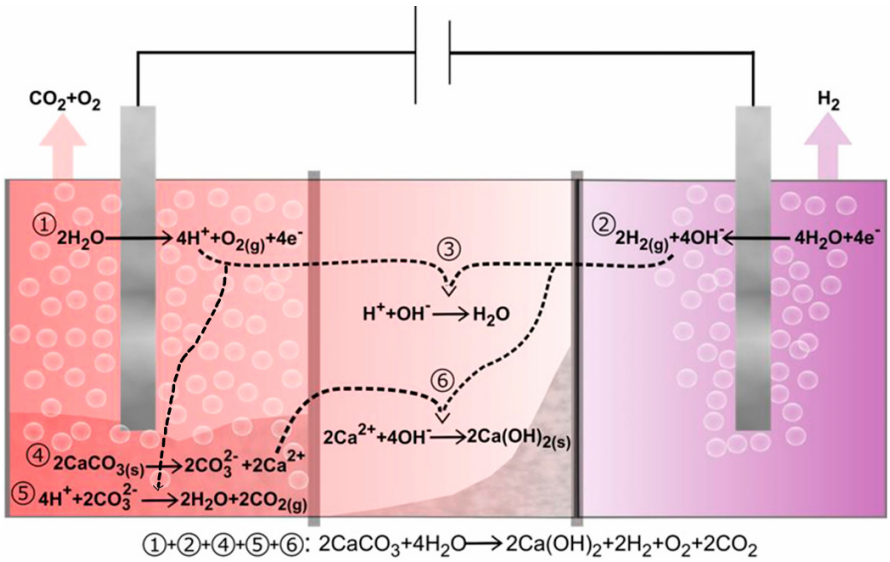

Figure 30: Electrochemical production of $Ca(OH)_2$ (From [61])

3.4.4.2 Chemical decarbonation

A room-temperature production of $Ca(OH)_2$ through a liquid-solid reaction between $CaCO_3$ and $NaOH$ (see equation 22, i.e. the reverse of the causticisation reaction [63]) is also investigated since it avoids both the fuel emissions –as no combustion is required– and the process emissions –as CO_2 is stored in mineral form $Na_2CO_3.xH_2O$, which can be valued as raw material for the glass, detergent, and chemical industries.

$$CaCO_3 + 2NaOH + xH_2O \longrightarrow Ca(OH)_2 + Na_2CO_3.xH_2O \ (x\text{=}0,\ 1) \tag{22}$$

The mixture obtained after the reaction contains $CaCO_3$, $Ca(OH)_2$, $NaOH$, Na_2CO_3 and/or $Na_2CO_3.H_2O$. Thus, further separation operations are necessary to obtain sufficiently pure calcium hydroxide.

For low initial amounts of sodium hydroxide (see Figure 31a), the unreacted $NaOH$ is firstly removed by selective dissolution in alcohol. Then, exploiting the difference of solubility in water between Na_2CO_3 and other calcium-containing components, Na_2CO_3 is removed from the product mixture. Finally, water excess is evaporated. When high amounts of sodium hydroxide are used (see Figure 31b), Na_2CO_3 and $NaOH$ are jointly dissolved and separated from the slurry, from which $Ca(OH)_2$ is recovered by water evaporation. The obtained mixture of Na_2CO_3 and $NaOH$ is dried, before removing $NaOH$ by its selective dissolution in alcohol.

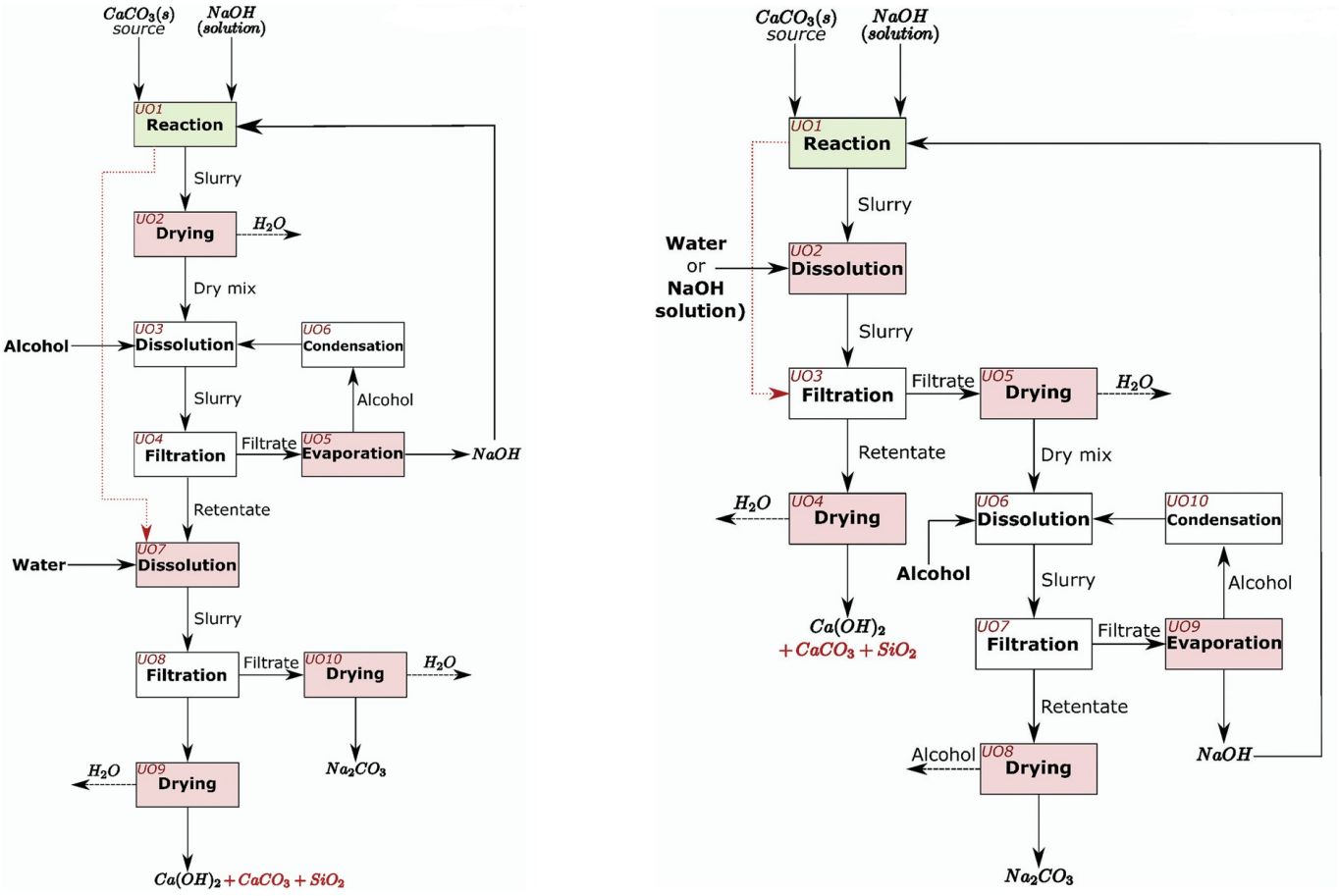

(a) High amount of $NaOH$ (b) Low amount of $NaOH$

Figure 31: Separation units necessary after reaction (From [63])

The avoided CO_2 emissions and the maximum conversion of 96% for the optimal $CaCO_3$:$NaOH$:H_2O ratio are promising for the up-scaling of this alternative production route, still at laboratory scale. However, the

emissions linked to the $NaOH$ production by the chlor-alkali process –that is the electrolysis of brine leading to the production of $NaOH$, H_2 and Cl_2– emitting 0.78 t_{CO_2}/t_{NaOH} if fossils fuels are used [10], have to be also considered for the environmental impact assessment of the overall process. Currently, there are no plans to deploy this alternative production method on a large scale, due to the higher cost of $NaOH$ compared to CaO [13].

3.4.5 Product carbonation

It has been determined that lime can be used as carbon sink. In its final application, lime is often exposed to the atmosphere, leading to its chemical reaction with CO_2 (see eq. 23).

$$CaO + CO_2 \longrightarrow CaCO_3 \tag{23}$$

Thus, it has been showed that around 33% of the CO_2 emitted by the lime production process is permanently captured [11] [12]. Depending on the application, the percentage of process CO_2 that is absorbed during use varies between 5–28% for steelmaking and 80–92% for lime mortar. This percentage reaches 93% for pulp and paper, and 100% for lime used in drinking water treatment [30].

Carbon storage by mineralization is studied by Nordkalk, Politecnico di Milano and EuLA [3].

4 Modeling of the lime sector and its identified energy transition pathways

To achieve the objective of the thesis, a superstructure optimization methodology is utilized, which was developed by Salman et al. [64] in their similar analysis for the decarbonization of the glass industry. The methodology consists of literature review, data collection, model development and validation and optimization (utilizing the OSMOSE Lua tool). Initially, mass and energy balances have been set up for the production of lime and its derivatives, i.e., hydrated lime, milk of lime and lime putty. The data necessary for the model –such as temperatures, energy requirements, and necessary raw materials– were sourced from open literature and the best available techniques (BAT, 2013) reference document of lime sector [9]. Furthermore, a validation of model is also conducted through the industry. The second part of the work consisted of modeling identified energy transition pathways for the lime sector. These include fuel-switching, carbon capture and alternative "cold" production routes.

4.1 Introduction to the OSMOSE tool

OSMOSE ('OptimiSation Multi-Objectifs de Systèmes Énergétiques intégrés', i.e. Multi-Objective Optimization of Integrated Energy Systems) is a tool developed by the IPESE group of EPFL, Ecole Polytechnique Fédérale de Lausanne.

The OSMOSE tool provides a combined mass, heat, and power integration and is able to optimize simultaneously environmental, economic, and thermodynamic elements [65]. OSMOSE is a research tool coupling databases, optimization methods and solvers, simulation tools, as well as post-analysis methods [66].

4.2 OSMOSE workflow

The OSMOSE workflow is depicted in Figure 32

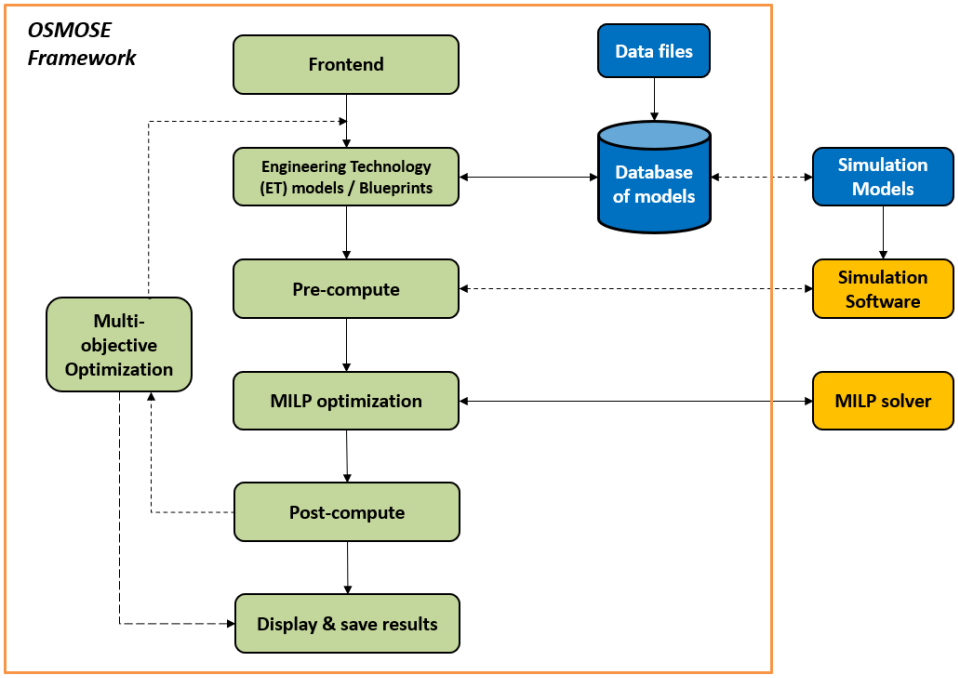

Figure 32: OSMOSE workflow (From [67])

The **frontend** is the routine launched for the execution of the OSMOSE workflow. In this file is defined the

problem: the objective function, the choice of the solver and its settings, the choice of the decision variables and their value range in case of a multi-objective optimization, the loading of models and the definition of the superstructure (i.e. assembling of several ET models), the values of model parameters, the post-compute functions [65].

The **ET models** represent technologies converting material and/or energy inputs into "material and/or energy products, by-products, waste and services" [66]. These models consist of:

- *Units*: elementary black boxes of the system, containing mass and energy balances and costing details (e.g., a reactor, a distillation column, ...);
- *Streams*: heat, electricity or material flowing into/out of a unit;
- *Layers*: "pipelines" allowing the streams to flow from one unit to another;
- *Parameters*: used in the definitions of the streams or units (e.g., size, temperature, cost, ...).

The **pre-compute** consists of all the necessary calculations performed before the problem optimization, e.g., the determination of a boiler's fuel consumption depending on its efficiency and heat production. The use of external software, e.g., Aspen, for the computation of state variables, such as specific consumption, unit cost or efficiency, is possible [66].

After the execution of the pre-compute, the Mixed-Integer Linear Programming (**MILP**) **Optimization** is carried out which occurs as shown in Figure 33. The different ET models are gathered into a data structure. The data are then parsed into *.MOD* files, storing equations, and *.DAT* files, storing parameters. The *.MOD* and *.DAT* files are sent as input to the MILP solver which solves the optimization problem and generates a *.OUT* file. Finally, the output file is parsed into a data structure, before being sent to the post-compute module. The MILP problem consists of an objective function, mass and energy balances constraints, heat cascade constraints, and unit sizing constraints [65].

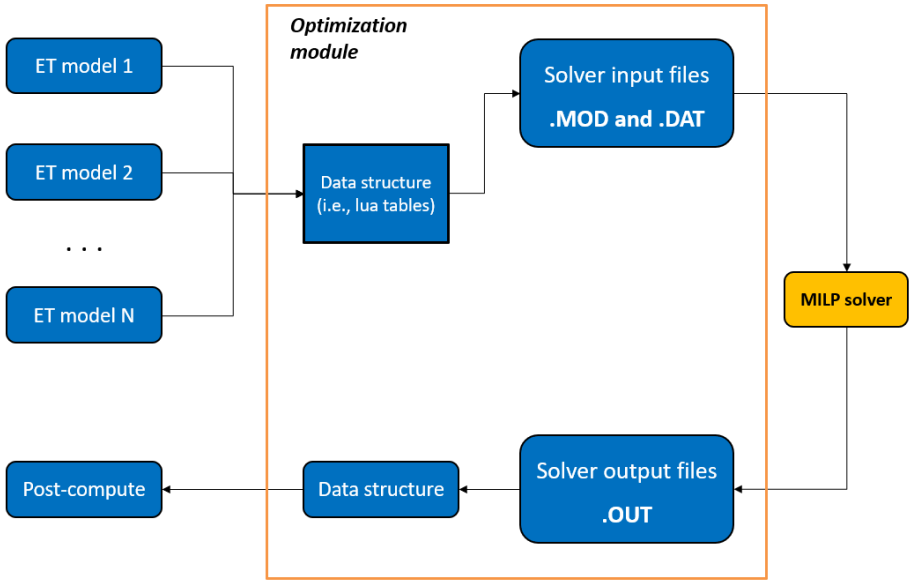

Figure 33: MILP optimization (From [67])

The **post-compute** functions allow the computation of various indicators (energy efficiency, environmental impact, cost, ...), as well as the displaying and saving of the obtained results (e.g., composite curves).

Multi-objective optimizations can also be carried out with the OSMOSE tool. In this case, the problem is divided into a master problem and a slave sub-problem. The master problem uses an evolutionary algorithm to change the values of the process variables/parameters. These values serve as input data for the slave

optimization sub-problem, i.e. a mono-objective MILP problem [68]. Once the results are retrieved, the objectives are evaluated, and the master optimization is re-iterated.

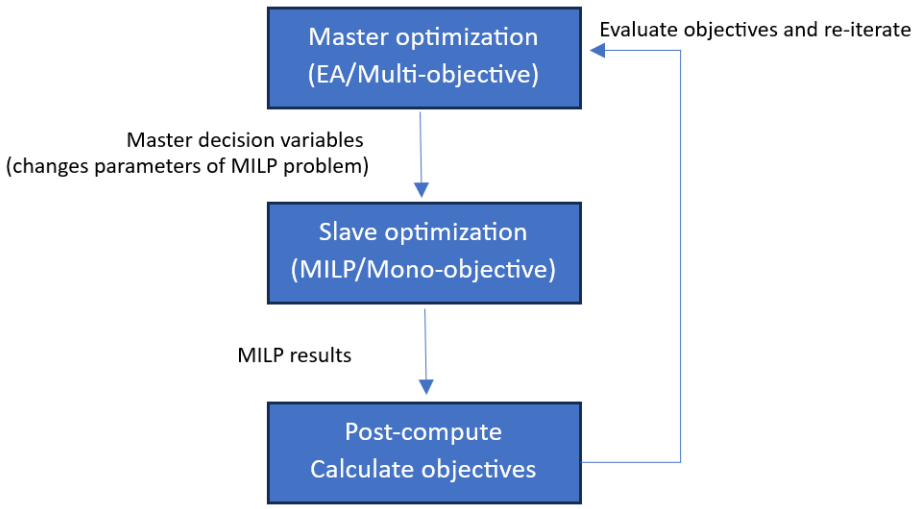

Figure 34: Multi-Objective Optimization (From [66])

4.3 Development of the blueprint of the lime sector

In the following, the blueprint of the lime sector and its details are presented. The hypothesis, simplifications and considered data are reported for the production of quicklime, dolime, hydrated lime, milk of lime and lime putty.

4.3.1 Economics: general considerations

The cost related to a process can be decomposed into two terms: capital expenditure (CAPEX) and operational expenditure (OPEX). The CAPEX can be estimated by multiplying the equipment cost –obtained from textbooks, previous purchases or vendor's quotes– by a factor taking into account additional necessary expenses such as the installation, the land or the design and engineering. The OPEX, expressed in M€/y, consists of fixed costs –such as labor, insurance and maintenance– and variable costs –electricity, steam, cooling water, and raw materials [69].

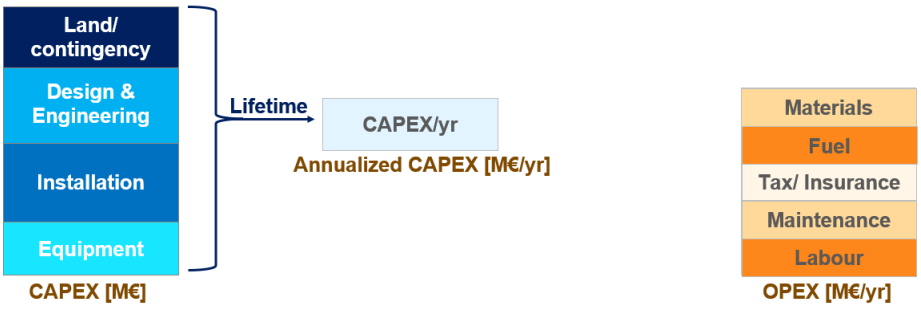

Figure 35: CAPEX and OPEX (From [69])

4.3.1.1 CAPEX

The capital investment cost C_a of an apparatus of size A_a can be estimated from the cost C_b of the apparatus of size A_b according to the six-tenth rule (as presented in eq. 24).

$$\frac{C_a}{C_b} = \left(\frac{A_a}{A_b}\right)^n \tag{24}$$

where a and b relate to different apparatus capacities, C is the cost, A is the size and n is the size factor typically between 0.6 and 0.7 for a chemical plant [70]. A value of 0.6 has been considered for the model.

The CAPEX, expressed in M€, can be annualized over its lifetime according to equation 25.

$$\text{Annualized CAPEX} = \text{CAPEX} \cdot \left(\frac{i(1+i)^n}{(1+i)^n - 1}\right) \tag{25}$$

where i is the discount rate (6% for the model) and n is the lifetime of the installation.

The cost can be updated from one year to another using a ratio of Chemical Engineering Plant Cost Indexes (CEPCI) –i.e., a composite index taking into account equipment, construction labor, buildings as well as engineering and supervision [71]– according to equation 26, where A and B relate to two different periods [72]. Table 2 lists the values of the considered CEPCIs.

$$\text{Cost}_B = \text{Cost}_A \cdot \frac{\text{CEPCI}_B}{\text{CEPCI}_A} \tag{26}$$

Remark: As a rule of thumb, the cost update is relatively accurate if periods A and B are less than 5 years apart [73].

Table 2: CEPCI for different years

Year	2002	2008	2014	2015	2018	2019	2020	2023
CEPCI	395.6	575.4	576.1	556.8	603.1	607.5	596.2	798.04

4.3.1.2 OPEX

For the model of the lime sector, fixed operating costs are discarded. The variable costs related to raw materials and utilities are computed as in equation 27 by multiplying their reference flow with their specific price.

$$\text{OPEX} = \sum_i (C_{en,i} \cdot \dot{Q}_i) + (C_{CO_2} \cdot \dot{m}_{CO_2}) + \sum_j (C_{rm,j} \cdot \dot{m}_j) \tag{27}$$

with C_{en} and C_{rm} the specific cost of energy resources and raw materials respectively, C_{CO_2} the carbon price, $\dot{Q}$ and $\dot{m}$ respectively the energy and mass flow rate.

4.3.2 Model of high-calcium quicklime production

As explained in section 3.3.2, the calcination of limestone (see eq. 28) produces quicklime CaO and CO_2.

$$CaCO_3 + heat \rightleftharpoons CaO + CO_2 \tag{28}$$

The lime kiln is represented as a black box in Figure 36.

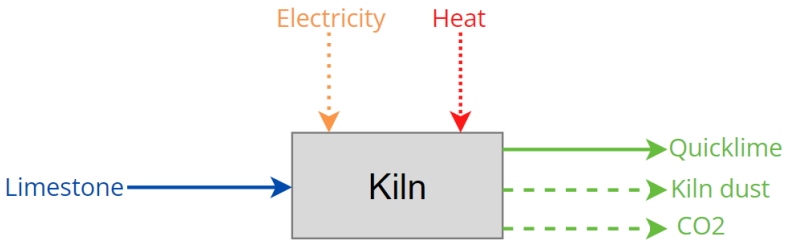

Figure 36: Lime kiln for limestone calcination represented as a black box

Given that the molar mass of $CaCO_3$, CaO and CO_2 (the so-called "process CO_2") are respectively 100, 56 and 44 g/mol, it comes from equation 28 that 1.786 kg of high-calcium limestone are needed for and 0.786 kg of CO_2 (reaction-related only) are generated by the production of 1 kg of quicklime. However, since 8% loss as kiln dust is observed, the effective limestone mass flow rate $\dot{m}_{SL}$ which is fed to the kiln is computed as in equation 29.

$$\dot{m}_{LS} = wr_{th} \cdot \dot{m}_{QL} \cdot \frac{1}{X} \tag{29}$$

where wr_{th} is the theoretical limestone-to-lime weight ratio (1.786 kg_{CaCO_3}/kg_{CaO}), $\dot{m}_{QL}$ is the mass flow rate of produced quicklime and X is the conversion (92%).

Heat and electricity requirements depend on the type of kiln that is used to perform calcination. Each of them have been briefly described in sections 3.3.2.1 to 3.3.2.5. For the model, the most common type of kiln, i.e., Parallel Flow Regenerative Kiln (PFRK) [9] [13], has been considered. The base case is a kiln fueled by natural gas, whose combustion leads to additional CO_2 emissions (the so-called "fuel-related CO_2"). The model considers an average electricity consumption of 30 kWh/t_{lime}. For preheating the limestone –from 20 ℃ to the reaction temperature (typically between 900 ℃ and 1100 ℃ [9])– and performing the calcination reaction respectively 0.514 kWh/kg_{CaO} and 0.852 kWh/kg_{CaO} are necessary [15], considering a reaction temperature of 1000 ℃. The cooling duty associated to the temperature decrease of quicklime down to 100 ℃ in the last portion of the kiln amounts to 0.458 kWh/kg_{CaO} [15].

The CAPEX computation related to the lime kiln is described in section 4.4.1.

4.3.3 Model of dolime production

As explained in section 3.3.2, dolime $CaO.MgO$ is produced by calcination of dolomitic limestone $CaCO_3.MgCO_3$, according to the reaction equation 30. The lime kiln is represented as a black box in Figure 37.

$$CaCO_3.MgCO_3 + heat \rightleftharpoons CaO.MgO + 2CO_2 \tag{30}$$

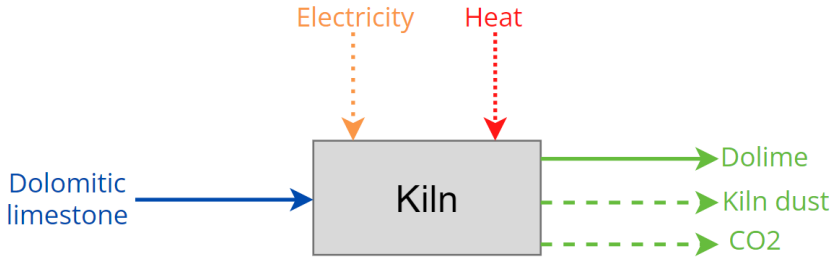

Figure 37: Lime kiln for dolomite calcination represented as a black box

Given that the molar mass of $CaCO_3.MgCO_3$, $CaO.MgO$ and CO_2 are respectively 184, 96 and 44 g/mol, it comes from equation 30 that 1.916 kg of dolomitic limestone are needed for and 0.917 kg of CO_2 are

generated by the production of 1 kg of dolime. However, once again, 8% loss as kiln dust is observed.

Due to a lower enthalpy of reaction and a lower dissociation temperature for $MgCO_3$, the energy requirement for –non-sintered– dolime production is lower than the one for high-calcium quicklime. In fact, the dolomite calcination requires 723 kcal/kg $CaO.MgO$ (at 25℃) and typically takes place between 750℃ and 900℃ [15] [54]. A PFRK is, once again, considered with a heat requirement of 3200 MJ/t_{lime} and an average electricity consumption of 30 kWh/t_{lime} [9].

The cost computation is carried out similarly to the high-calcium quicklime case, assuming an identical investment cost for the lime kiln.

4.3.4 Model of pebble and ground lime production

Quicklime is fed to impact mills to produce coarser grades, and to ball mills or high-pressure mills to obtain finer grades. No material losses are assumed [13] for this comminution step. The electricity requirements to produce coarser and finer particles vary respectively between 4–10 kWh/t and 10–40 kWh/t [9]. An average electricity consumption of 20 kWh/t_{lime} has been considered for the model.

In Figure 38 is depicted the black box representation of a milling unit.

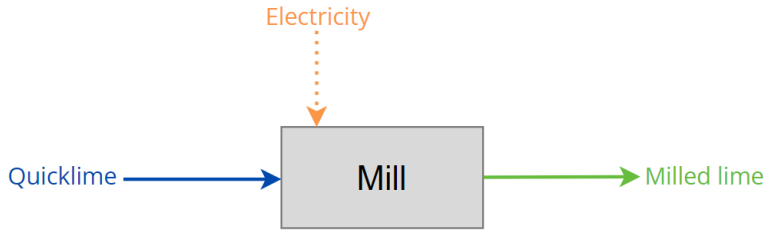

Figure 38: Lime mill represented as a black box

A ball mill with a capacity of 30 t/h typically costs between $200 000 and $1.5 million [74]. An average cost of $850 000, or equivalently €790 500, is considered for the model. A lifetime of 25 years is assumed for the CAPEX annualization.

4.3.5 Model of hydrated lime production

Considering the hydrator as a black box –as depicted in Figure 39– quicklime, water and electricity flow into the hydrator, while hydrated lime and steam exit the aforementioned unit. Hydrated lime, $Ca(OH)_2$, is produced by the exothermic reaction of quicklime, CaO, and water, H_2O, according to equation 31.

$$CaO + H_2O \rightleftharpoons Ca(OH)_2 + heat \tag{31}$$

Given that the molar mass of CaO, H_2O and $Ca(OH)_2$ are respectively 56.1, 18 and 74.1 g/mol, one may deduct that the required amounts of quicklime and water for the reaction are 0.757 kg_{CaO}/$kg_{Ca(OH)_2}$ and 0.243 kg_{H_2O}/$kg_{Ca(OH)_2}$. However, for the production of hydrate, twice the stoichiometric amount of water is added [15] and the excess of water will be evaporated and vented to the atmosphere as steam [13]. Thus, a water-to-lime weight ratio of 0.486 kg_{H_2O}/$kg_{Ca(OH)_2}$ is considered.

The electricity requirement for the operation of the hydrator, air classifiers and conveyors ranges from 5 to 30 kWh/t_{CaO} [9]. An average value of 17.5 kWh/t_{CaO} has been considered.

The heat released by the reaction is not recovered currently. This heat is evacuated mainly via steam and by the increase in temperature of the product [13]. The generated steam, at around 100℃, is released into

the atmosphere [75] since no low-grade heat is required in the lime plant. Moreover, the steam temperature and quantity are too low to be used for an urban heating network or electricity generation with an ORC [13].

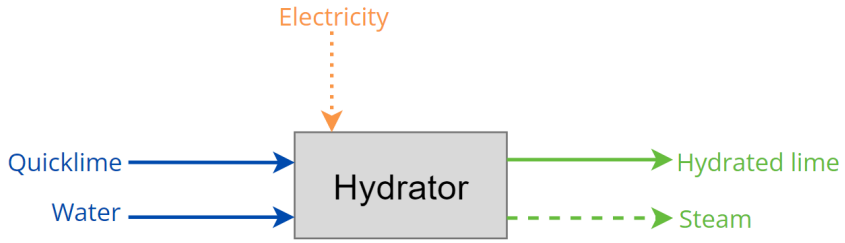

Figure 39: Hydrator represented as a black box

The cost of a hydrator is assumed to be identical to the one of a detention slaker (see section 4.3.6).

4.3.6 Model of milk of lime production

Milk of lime is produced according to the same reaction as for hydrated lime (see equation 31). The modeling is thus quite similar. The main difference is the considerable excess of water that is used. The typical water-to-lime weight ratio lies between 3:1 and 4:1 [15]. An average ratio of 3.5:1 is considered. Thus, 1 kg CaO and 3.5 kg H_2O yield 4.5 kg of milk of lime.

The slaker in which takes place the production of milk of lime is represented as a black box in Figure 40. The cost of a detention slaker, with a capacity of 2.5 t/h, is estimated at $1 000 000 [76], or equivalently €899 300. A lifetime of 25 years is considered.

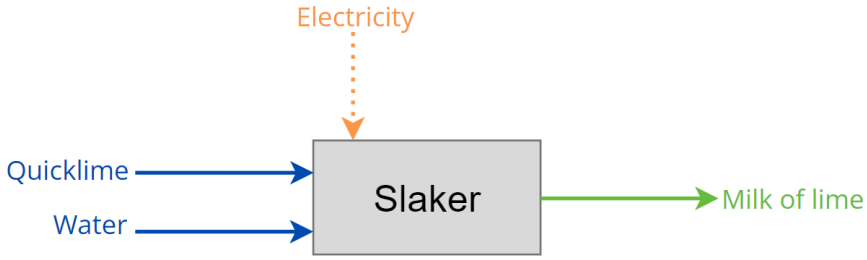

Figure 40: Slaker represented as a black box

4.3.7 Model of lime putty production

Lime putty production can be modeled with a black box representing a mixer, as depicted in Figure 41. The hydrated lime is mixed with water to reach a lime putty of the desired consistency. Typically, 3 kg of hydrated lime is mixed with 0.7 to 1 kg of water [15]. An average mass of water, i.e., 0.85 kg, is considered for the model. Thus, 0.779 kg of hydrated lime and 0.221 kg of water are necessary to produce 1 kg of lime putty. No heating or cooling steps are involved in lime putty production.

For the computation of the investment cost, an industrial mixer for viscous pastes is considered. For a capacity of 1300 L, €7500 have to be invested [77]. To apply equation 24, the lime putty volume has to be specified instead of its mass. This conversion can be done knowing that lime putty has a density of 1350 kg/m^3 [78]. The annualization of the CAPEX is performed considering a lifetime of 25 years.

Figure 41: Mixer for lime putty represented as a black box

4.4 Development of blueprints related to the energy transition pathways

In the following sections, the blueprints related to the identified energy transition pathways for the lime sector are presented. The hypothesis, simplifications and considered data are reported for fuel switching possibilities –from natural gas to biogas, biomethane, hydrogen or biomass–, kiln electrification, the implementation of a carbon capture unit –post-combustion with monoethanolamine (MEA), or natural gas oxycombustion– and two "cold" production routes.

4.4.1 Base case: Natural gas-fired kiln

In a natural gas-fired lime kiln, the heat necessary to perform the calcination reaction at a temperature between 900 and 1100 ℃ is provided by the combustion of natural gas with air. This combustion yields 1 mol of CO_2 per mol of fuel, or equivalently 2.75 kg_{CO_2}/kg_{fuel}s.

The heat balance within the kiln considers radiation, convection, stack losses, wall losses and air preheating. The adiabatic flame temperature of natural gas in air is 1957 ℃ [79]. The stoichiometric molar air-to-fuel ratio for natural gas is 9.52. The exhaust gases leave the lime kiln at 150 ℃ [24].

In terms of economics, a specific investment cost of £665/kW, or equivalently €778.05/kW, was observed for a natural gas-fired kiln in 2018 [80]. The kiln's lifetime is 40 years [9].

4.4.2 Fuel switching

4.4.2.1 Biogas-fired kiln

Biogas is a mixture of mainly CH_4 (typically between 45 and 75 vol%) and CO_2 produced by anaerobic digestion of organic matter [81]. Biogas is envisaged as alternative fuel for lime kilns since its combustion generates "net-zero CO_2 emissions" which are not subjected to carbon price.

The original code related to the natural gas-fired kiln has been modified for firing biogas. The major modifications are related to parameter values. The lower heating value, the adiabatic flame temperature, the final flue gas temperature, the molecular weight of the fuel as well as the air-to-fuel ratio have been adapted. The values considered in the model for "rich biogas" (75% CH_4 – 25% CO_2) are listed in Table 3.

Table 3: Model parameters for the biogas-fired kiln

	Value	Reference
Lower Heating Value [kJ/kg]	26 000	[56]
Adiabatic flame temperature [℃]	1593	[82]
Molecular weight [g/mol]	23	
Air-to-fuel ratio [mol_{air}/mol_{fuel}]	8.84	

Another modification concerns the CO_2 flow related to the heat supply. In fact, the released CO_2 does not only come from the combustion reaction but also from the CO_2 initially in the biogas feed. However, these emissions are considered as biogenic and, thus, not accounted for carbon price. Finally, the flue gas

temperature is increased by 20℃ compared to the one observed during natural gas combustion [56]. Thus, a stack temperature of 170℃ is considered in the model.

Due to lack of information in terms of kiln conversion cost, it is assumed that the investment cost related to the biogas-fired lime kiln remains unchanged compared to the natural gas-fired one.

4.4.2.2 Biomethane-fired kiln

Biomethane, obtained by upgrading biogas –i.e., removing CO_2 and other contaminants– or by thermal gasification of biomass and methanation [81], can be used instead of natural gas without significant changes [56]. For a higher model flexibility, a mixture of natural gas and biomethane is fed to the kiln. The original code related to the natural gas-fired kiln is modified to take into account that the CO_2 related to the combustion of biomethane is considered as "biogenic CO_2" and not "scope 1 CO_2". This can be done by virtually separating the "biogenic CO_2" from the "scope 1 CO_2" as follows.

$$CO_{2,scope1} = x_{NG} \cdot CO_{2,total} \tag{32}$$

$$CO_{2,biog} = (1 - x_{NG}) \cdot CO_{2,total} \tag{33}$$

where $CO_{2,scope1}$ and $CO_{2,biog}$ are the CO_2 produced by the combustion of respectively natural gas and biomethane, $CO_{2,total}$ is the total CO_2 produced, and x_{NG} is the fraction of natural gas in the feed.

Since biomethane can replace natural gas without technical constraints [80], the investment cost of the kiln partially fed with biomethane is assumed to be identical to the one of a lime kiln burning natural gas.

4.4.2.3 Electrically-heated kiln

Kilns based on plasma technology are investigated by the lime sector [50] [51]. The plasma generator converts electricity into high-temperature heat with a typical thermal efficiency of 90% [80]. An electric arc heats up gas –such as helium, neon or argon for example [83]– at very high temperature (4000℃ for the model) inducing its transition to the plasma state [84].

In 2019, the investment cost for the calcination reactor and plasma generators with a total capacity of 25 MW was estimated to, respectively, €1.7 M and €9.5 M [84]. The expected lifetime of the plasma generators is 25 years and the one of the reactor is 40 years.

4.4.2.4 Hydrogen-fired kiln

The model for hydrogen firing was derived from the natural gas-fired kiln model. The model parameters that have been modified are listed in Table 4. However, in the case of a 100% substitution of natural gas by hydrogen, the temperature within the kiln is expected to increase. Overburning and sintering can be avoided by reducing the energy input by around 8% [57]. The main advantage of hydrogen-fired kilns is the avoided CO_2 related to fuel combustion.

Table 4: Model parameters for the hydrogen-fired kiln

	Value	Reference
Lower Heating Value [kJ/kg]	120 000	[58]
Adiabatic flame temperature [℃]	2061	[79]
Molecular weight [g/mol]	2	
Air-to-fuel ratio [mol_{air}/mol_{H_2}]	2.38	

For a hydrogen-fired kiln with a 10 MW capacity, the investment cost amounted to £732/kW [80], or equivalently €859/kW, in 2018. The CAPEX can be annualized considering a lifetime of 25 years [80].

4.4.2.5 Biomass-fired kiln

Biomass is considered as an alternative fuel for lime kilns. In the model, pine wood, olive stones and almond shells are considered. The parameter values that have been modified compared to the natural gas-fired kiln can be found in Table 5. Moreover, the emitted biogenic CO_2 is tax-free. Finally, as for the biogas case, the considered flue-gas temperature is 170℃ [56].

The CO_2-to-fuel ratio is determined based on the carbon content of the considered fuel ($wt\%_C$). This carbon content represents the mass of carbon per kilogram of fuel, which can be transformed as the amount (mol) of carbon per kilogram of fuel based on its molar mass (eq. 34). Given that each mol of carbon will generate one mol of CO_2, one may determine the mass of CO_2 released by the combustion of one kilogram of fuel (according to eq. 35). The total flow of emitted CO_2 is obtained by multiplying the CO_2-to-fuel ratio (cfr) with the mass flow of biomass that is fed into the kiln.

$$mf_{CO_2} = wt\%_C \cdot \frac{1000}{12.011} \tag{34}$$

$$cfr = mf_{CO_2} \cdot MW_{CO_2} \tag{35}$$

where cfr is the CO_2-to-fuel ratio (mass basis), MW_{CO_2} is the molar mass of CO_2 and mf_{CO_2} is the number of mol of CO_2 per kilogram of fuel.

Table 5: Model parameters for the biomass-fired kiln

	Pine wood	**Olive stones**	**Almond shells**	**Reference**
Lower Heating Value [kJ/kg]	19 000	19 800	13 300	[56] [59]
Adiabatic flame temperature [℃]	2149	2288	2172	[85]
Carbon content [wt% C]	52.7	48.8	44.98	[85]
Air-to-fuel ratio [mol_{air}/mol_{fuel}]	6.02	5.75	5.4	[85]

The conversion cost to fire biomass instead of natural gas was estimated to £62.5/kW [80] –i.e., €72.92/kW– for a 120 MW capacity (in 2018). The total investment cost for a biomass-fired kiln is thus computed as the sum of the CAPEX of a natural gas-fired kiln and the additional cost for fuel switching.

4.4.3 Oxycombustion of natural gas

Another alternative that is considered for the future of the lime sector is a natural gas oxycombustion kiln. The use of pure oxygen instead of air induces an increase in the adiabatic flame temperature –from 1957℃ to 2770℃ [79]– and a fuel consumption reduction of 15–20% [86].

The necessary oxygen is provided by a cryogenic Air Separation Unit (ASU) which is fed with compressed air and produces oxygen (95 vol% purity). The electricity consumption amounts to 226 kWh/t_{O_2}. Moreover, a front end purification of air by adsorption is necessary, requiring 58.3 kJ/kg_{O_2} for the regeneration of the adsorption bed and provided by low-pressure steam [87]. The oxycombustion and ASU models were already available.

The investment cost of a natural gas oxycombustion kiln is assumed to be the investment cost of a "traditional" natural gas-fired kiln (see section 4.4.1) to which is added the investment cost of the ASU. For a ASU with a 24 t_{O_2}/h capacity, an investment cost of €27 900 000 was necessary in 2002. The CAPEX annualization is performed for a lifetime of 40 years.

Oxycombustion yields a much higher CO_2 concentration (>80 vol% [41]) than with natural gas combustion in air, allowing a much easier CO_2 capture. A CO_2 capture of 90% (with a cryogenic purification unit yielding a CO_2 stream pure at 95% [36]) and a compression up to 152 bar are achievable with an electricity

consumption of 1.24 MJ/kg$_{CO_2}$[1]. The CO_2 capture and compression further adds €128 M to the CAPEX (for a capacity of 765 Mt$_{CO_2}$/y, in 2014) which can be annualized based on a lifetime of 25 years [88].

4.4.4 CO_2 capture with MEA chemical absorption

Various carbon capture technologies exist and are presented in section 3.4.1. For the present model, a MEA-based carbon capture process is implemented. The post-capture CO_2 compression is also considered in terms of energy consumption and investment cost. The flue gas pretreatment, i.e. the NO_x and SO_x removal as well as the dehydration, is not taken into account in the model. The Carbon Capture and Storage (CCS) unit is represented as a black box in Figure 42.

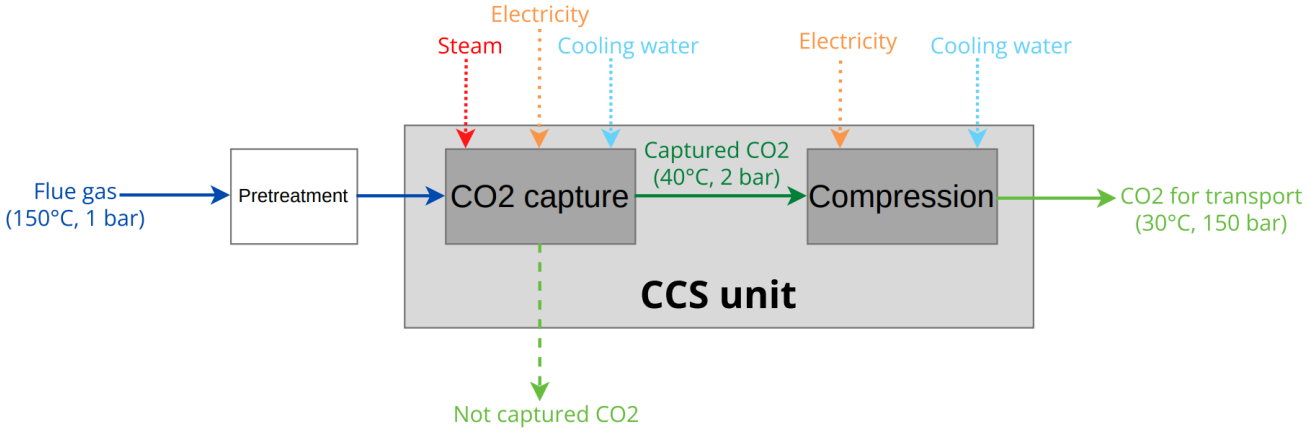

Figure 42: Carbon capture unit represented as a black box

The CO_2 capture with MEA is schematically represented in Figure 43. The flue gas is first cooled down from 150 ℃ to 40 ℃ before entering the absorption column. Within this column, CO_2 dissolves selectively in the MEA solution, leaving an almost CO_2-free gas stream at the top of the column. The CO_2-rich MEA is preheated from 51 ℃ to 107 ℃ by the CO_2-lean MEA coming from the bottom of the desorption column. The preheated CO_2-rich MEA stream enters the desorption column in which the MEA solvent is regenerated – and leaves at the bottom at 119 ℃– and the captured CO_2 is retrieved at the top at 101 ℃. The captured CO_2 undergoes a cooling step –with a temperature decrease down to 40 ℃– prior a multi-stage compression. After a heat exchange with the CO_2-rich MEA, the regenerated MEA at 61 ℃ and make-up solvent are cooled down to 40 ℃ before entering the absorption column [89].

The CO_2 compression process is depicted in Figure 44. The captured CO_2 enters the compression process at 40 ℃ and 2 bar. Carbon dioxide undergoes a pressure increase in a compressor up to 4.3 bar, is cooled down to 28 ℃ and the condensed water is removed thanks to a flash. These three steps are repeated but with a pressure increase from 4.3 bar to 18.6 bar. Once the CO_2 stream has reached 80 bar after a third compressor, the pressure of the supercritical CO_2 is brought up to 152 bar with a pump. The compressed CO_2 leaves the process at 30 ℃ after passing through a fourth cooler [89].

[1] The electricity requirement amounts to 1.22 MJ/kg$_{CO_2}$ when a compression up to 110 bar is considered [43]. To reach the same final pressure as in the case of a MEA-based CCS, an additional electricity input of 0.02 MJ/kg$_{CO_2}$ is necessary (value computed by an Aspen simulation)

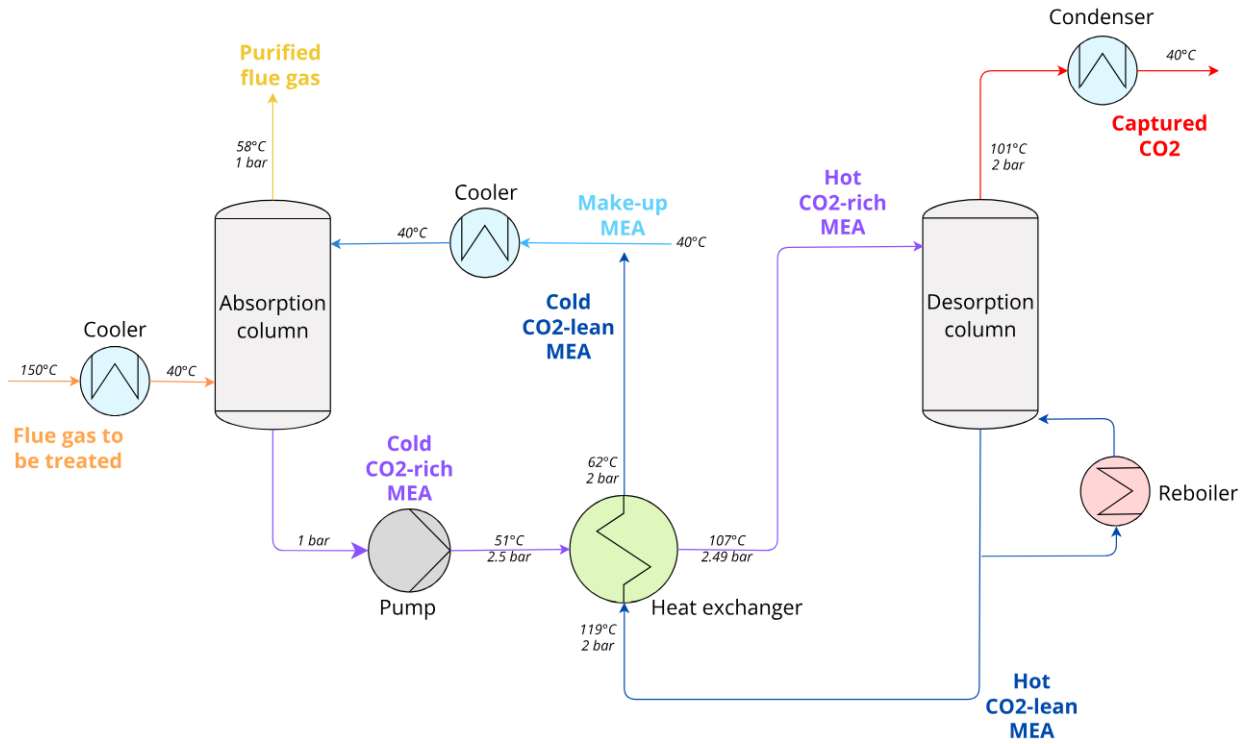

Figure 43: CO_2 capture with MEA

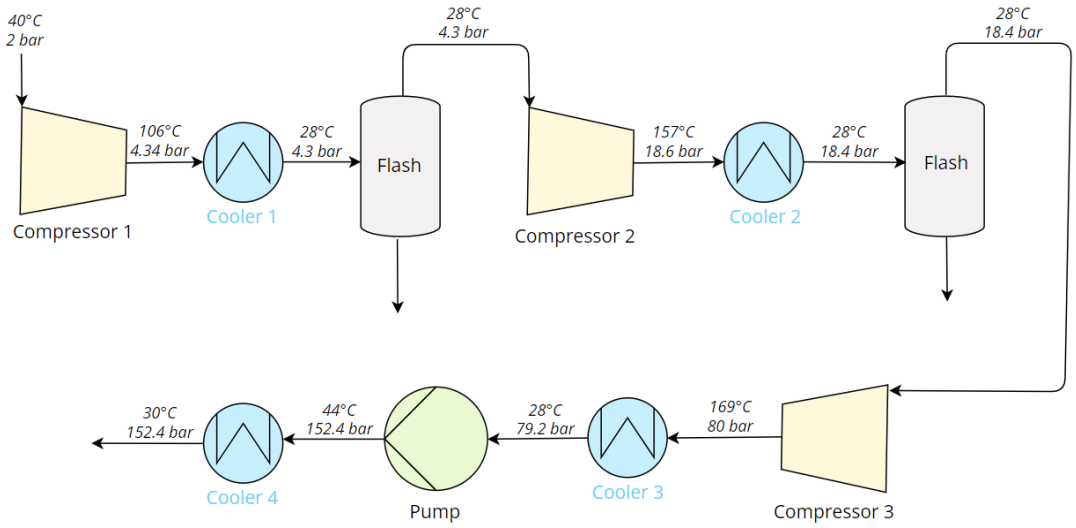

Figure 44: CO_2 compression

The capture process requires steam (for the reboiler of the desorption column) produced by a natural gas-fired boiler, cooling water (for the coolers), and electricity (for the pump operation). For the CO_2 compression process, electricity (for the compression stages) and cooling water (for the intercooling steps) are necessary. The capture efficiency of the unit is assumed to be 90%. The energy requirements (steam, cooling water and electricity) and the investment costs for the CO_2 capture and compression processes are based on correlations developed by Kim et al. [90]. These correlations depend on the flue gas flow rate, temperature and CO_2 concentration. The data used in the model are listed in Table 8 (see Appendix A).

4.4.5 Cold production routes

4.4.5.1 Electrochemical production of Ca(OH)$_2$

The electrochemical process described by Ellis et al. [61] is schematically represented in Figure 45. The overall reaction involved in the aforementioned process is equation 36. From this, it comes that 1.351 kg $CaCO_3$ and 0.486 kg H_2O are necessary to produce 1 kg $Ca(OH)_2$. For each kilogram of calcium hydroxide are produced 0.027 kg H_2, 0.216 kg O_2 and 0.594 kg CO_2.

$$CaCO_3 + 2H_2O \longrightarrow Ca(OH)_2 + H_2 + \frac{1}{2}O_2 + CO_2 \tag{36}$$

The electricity requirements of the process are related to the water electrolysis. In the literature, values between 51.2 kWh/kg$_{H_2}$ [91] and 55 kWh/kg$_{H_2}$ [92] are reported. An average value of 53.1 kWh/kg$_{H_2}$ is considered for the model.

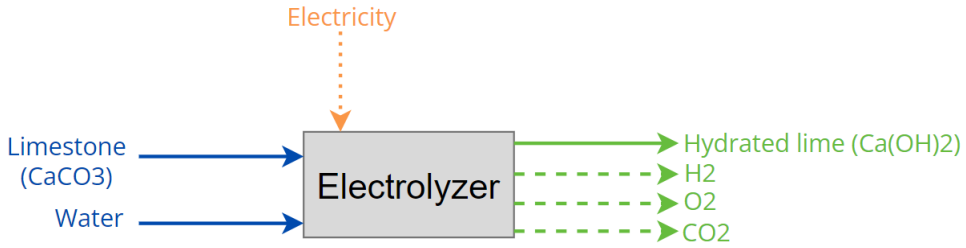

Figure 45: Electrolyzer-reactor for hydrated lime represented as a black box

4.4.5.2 Production of Ca(OH)$_2$ with NaOH

The production of $Ca(OH)_2$ by reaction between $CaCO_3$ and $NaOH$, carried out at room temperature, has been investigated [63]. The implemented reaction is equation 37. From that equation, it comes that 1.351 kg $CaCO_3$ and 1.081 kg $NaOH$ are required to produce 1 kg $Ca(OH)_2$ and 1.432 kg Na_2CO_3.

$$CaCO_3 + 2NaOH \longrightarrow Ca(OH)_2 + Na_2CO_3 \tag{37}$$

Further separation steps are required for separating the final product ($Ca(OH)_2$) from the obtained co-product (Na_2CO_3), the unreacted reagents and water –since the reaction takes place in an aqueous medium– which are not taken into account in the current model. Depending on the initial amount of $NaOH$ added, between 19 400 and 42 201 kJ/kg$_{Ca(OH)_2}$ are necessary for the separation steps. This low-grade heat requirement can be fulfilled by waste heat sources [63].

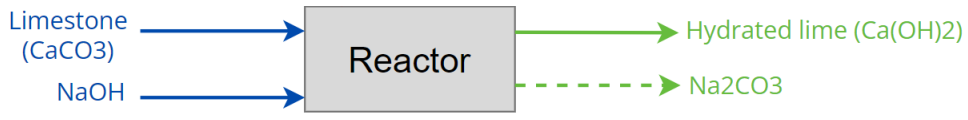

Figure 46: NaOH-based production of hydrated lime represented as a black box

5 Evaluation of energy transition pathways for the lime sector

5.1 Superstructure of the lime sector

In Figure 47, the superstructure of lime production with all the identified energy transition pathways is presented.

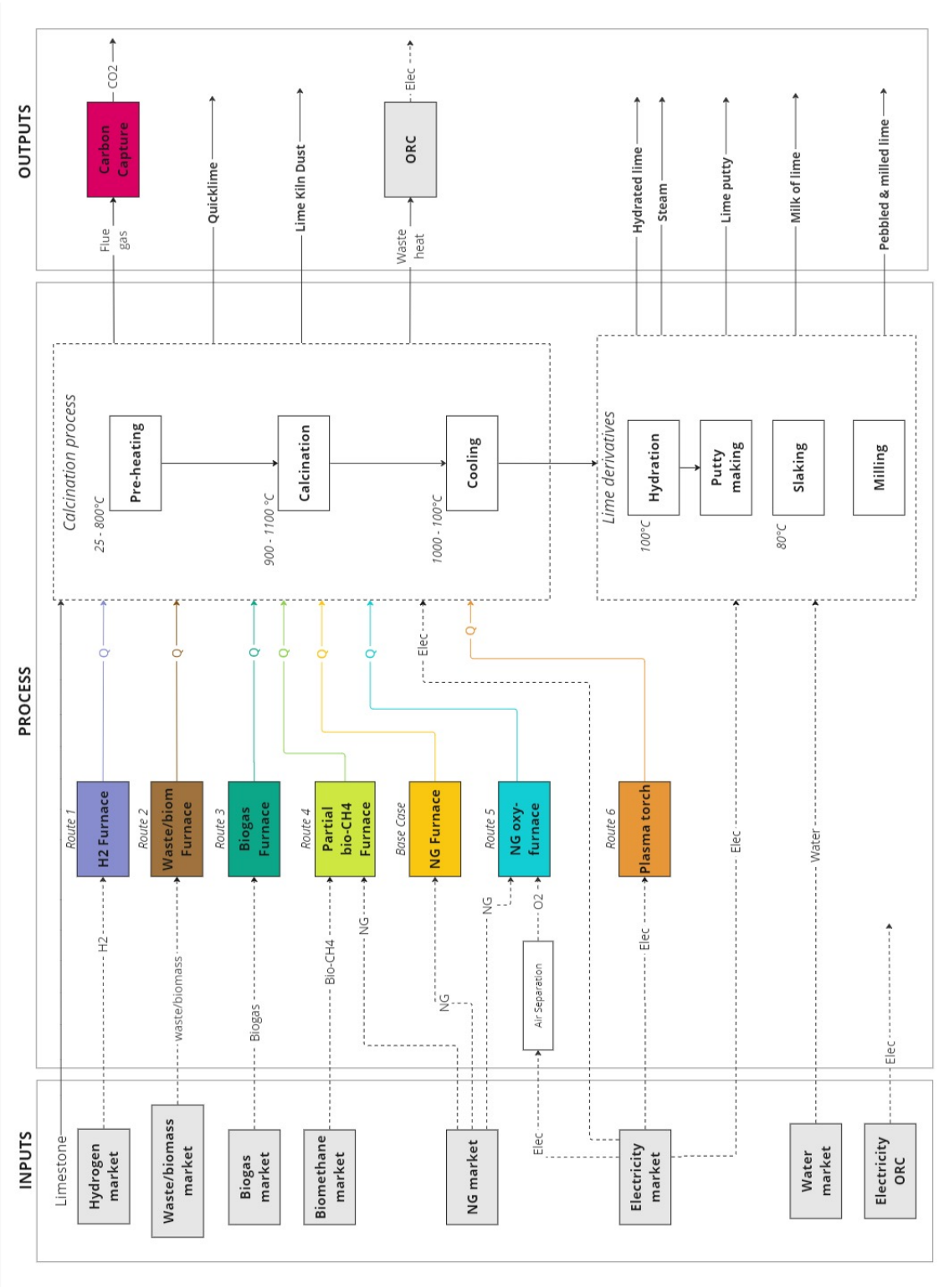

Figure 47: Superstructure of the lime sector

The lime sector consists mainly of quicklime production, which can then be milled. The produced quicklime can also be hydrated (to produce hydrated lime) or slaked (to produce milk of lime) depending on the water excess used. Lime putty can also be produced by mixing water and hydrated lime in desired quantities.

The CO_2 emissions of the lime sector are almost entirely related to limestone calcination. This reaction takes place at high temperatures around 1000°C. The heat required to perform calcination is usually provided by natural gas combustion (base case for the following analyses). Only about 25% of the total CO_2 emissions are related to fuel combustion, while the remaining 75% are due to the calcination reaction itself. As previously mentioned, to reduce the CO_2 emissions of the lime sector, three main transition routes are investigated: fuel switching, carbon capture and alternative "cold" production routes. While the cold production routes are still at lab scale, fuel switching and carbon capture are studied at large scales. Various carbon-neutral fuels –such as hydrogen, solid biomass or biogas/biomethane– as well as kiln electrification with plasma torches are considered. For capturing the emitted CO_2, chemical absorption with MEA as well as oxycombustion are included in the superstructure.

Heat recovery from lime kiln off-gases with an Organic Rankine Cycle (ORC) is considered for rotary kilns. For PFRKs, heat recovery is not implemented. In fact, no low-grade heat is necessary in the quicklime production facility. Moreover, the flue gas temperature and volume are insufficient for an economically interesting heat recovery with an ORC [13].

5.2 CO_2 emission reduction potential and energy requirements

In the following analyses, fourteen different routes are considered. The heat necessary for limestone calcination can be provided by burning natural gas –with air (*'NG'*) or oxygen (*'NGOxy'*)–, hydrogen (*'H2'*), biogas (*'Biogas'*), solid biomass –specifically wood– (*'Biomass'*), a mixture of 50% natural gas and 50% biomethane (*'BioCH4'*) or by using plasma technology (*'Plasma'*). For each of the seven options previously mentioned, a coupling with a carbon capture (CC) process is considered. When the lime kiln is fired with hydrogen, biogas, biomethane, solid biomass or natural gas for combustion with air, carbon capture by absorption with MEA is implemented. In the case of natural gas oxycombustion, the CO_2 capture is facilitated by the higher CO_2 concentration in the fumes and is performed by cryogenic separation. On top of reducing energy requirements for CC, the oxycombustion configuration suppresses the health hazard related to the MEA-based CC[2]. For plasma-based kilns, it is assumed that the exhaust gases have a sufficiently high CO_2 concentration to perform CC with the same method as for natural gas oxycombustion. The specific energy requirements (kWh/t_{lime}), the specific net CO_2 emissions (kg_{CO_2}/t_{lime}) and the emission reduction potential (%) compared to a natural gas-fired kiln are listed in Table 6.

The total energy requirement for limestone calcination varies between 1038.6 kWh/t_{lime} for the plasma technology and 3579.8 kWh/t_{lime} for biogas combustion coupled with MEA-based chemical absorption for carbon capture. The three less energy-consuming technologies are plasma-based kilns (with or without further CO_2 capture), natural gas oxycombustion and natural gas combustion in air. The three most energy-intensive technologies are MEA-based carbon capture coupled with a hydrogen-, solid biomass- or biogas-fired kiln.

When MEA-based carbon capture is implemented, an increase in natural gas and electricity consumption, for steam generation and compression steps respectively, is observed compared to the equivalent kiln technology without CC. When oxycombustion and plasma technologies are coupled with CC, only electricity requirements are affected by the fully-electric carbon capture process implemented.

[2]MEA may induce eye and skin irritation at high concentrations, as well as nasal irritation, pulmonary edema or central nervous system problems after inhalation or swallowing [93].

Moreover, from Table 6, it comes that the 'NGOxy' configuration allows a decrease in natural gas consumption of around 11% compared to the 'NG' case. In fact, using oxygen instead of air for combustion results in a fuel use reduction of 20% in the lime kiln. However, the ASU requires an additional heat requirement for oxygen production.

The net CO_2 emissions related to quicklime production lie between -0.261 t_{CO_2}/t_{lime} for a biogas-fired kiln with end-of-pipe carbon capture and 1.067 t_{CO_2}/t_{lime} for the natural gas-fired kiln without CC. Without the implementation of a carbon capture unit, the CO_2 emission reduction potential allowed by fuel switching compared to the base case (natural gas-fired kiln) is bounded to 26% due to the 0.786 t_{CO_2}/t_{lime} released by the calcination reaction. Carbon capture coupled with natural gas combustion in air, hydrogen combustion, combustion of a natural gas/biomethane mixture, natural gas oxycombustion and plasma technology allows an emission reduction of respectively 69%, 77%, 82%, 90% and 93% compared to 'NG'. Significant CO_2 emissions reductions are achieved for biogas- and biomass-fired lime kilns combined with MEA-based carbon capture, enabling respectively 124% and 115% lower CO_2 emissions than a natural gas-fired kiln. Both configurations result in net negative CO_2 emissions.

Table 6: Comparison of various technologies in terms of specific energy consumption and CO_2 emissions

Case	NG use (kWh/t)	H2 use (kWh/t)	Biogas use (kWh/t)	BioCH$_4$ use (kWh/t)	Solid biomass use (kWh/t)	Electricity use (kWh/t)	Net CO_2 emissions (kg/t)	Emission reduction potential
NG	1419.7	0	0	0	0	30	1067.1	–
NG-CC	2533.9	0	0	0	0	115.8	327.3	69%
NGOxy	1253.5	0	0	0	0	113.2	1034.2	3%
NGOxy-CC	1253.5	0	0	0	0	434.3	103.4	90%
H2	0	1748.0	0	0	0	30	786	26%
H2-CC	823.0	1748.0	0	0	0	93.4	241.6	77%
Plasma	0	0	0	0	0	1038.6	786	26%
Plasma-CC	0	0	0	0	0	1282.6	78.6	93%
Biogas	0	0	1857.1	0	0	30	786	26%
Biogas-CC	1571.6	0	1857.1	0	0	151.1	-261.3	124%
BioCH4	709.9	0	0	709.9	0	30	926.6	13%
BioCH4-CC	1824.1	0	0	709.9	0	115.8	186.8	82%
Biomass	0	0	0	0	1642.3	30	786	26%
Biomass-CC	1414.2	0	0	0	1642.3	138.9	-156.4	115%

Remark: The cold production routes previously identified (see section 3.4.4) are not included in the following analyses, since these technologies are not expected to be deployed on a large scale currently. In fact, these processes are still at lab scale (TRL 2–3 [94]). Moreover, production of Ca(OH)$_2$ through reaction between limestone and caustic soda seems unlikely for now, according to sector's experts, due to the higher price of $NaOH$ compared to CaO [13].

5.3 Scenarios for 2030, 2040 and 2050

To identify the best energy transition pathways for the lime sector in the upcoming years, the evaluation of the various technologies is performed considering price scenarios for three different years: 2030, 2040 and 2050.

Considered costs for natural gas, electricity, hydrogen, biomass, biogas, biomethane and emitted CO_2 are listed in Table 7. According to TIMES-BE model of EnergyVille, natural gas prices are expected to decrease compared to current levels. Biomass prices will remain relatively constant until 2050, according to the European Heat Roadmap [95]. The International Energy Agency (IEA) [81] estimates European biogas and

biomethane prices in 2040 at respectively $9/MBtu (or equivalently €28.56/MWh) and $14/MBtu (or equivalently €44.43/MWh). Finally, an increase in carbon tax is assumed, reaching €350/t_{CO_2} in 2050.

The EnergyVille TIMES-BE model considers supply and demand variations for electricity and hydrogen, and computes the related cost for ten representative days. This model considers three different scenarios: "central scenario", "electrification scenario" and "clean molecules scenario". In the **central scenario**, carbon-neutrality is reached in Belgium by 2050 thanks to investments in energy efficiency improvement or new technologies such as fuel switching, electrification and CCUS. Moreover, unlimited access to CO_2-storage sites is assumed. In the **electrification scenario**, a higher offshore wind capacity and investments in nuclear energy (Small Modular Reactors) are considered. The **clean molecules scenario** is based on the possibility of importing low-cost synthetic molecules –such as hydrogen– from outside the EU, where renewable energy is abundant. Moreover, access to cross-border CO_2 storage in the Netherlands or Norway is assumed to be limited to 5 Mt/y [95]. Average electricity and hydrogen prices for each scenario can be found in Table 7.

Table 7: Prices for electricity, hydrogen, natural gas, biogas, biomethane, biomass and CO_2 emissions for different years and scenarios (E = electrification; C = central; M = clean molecules)

	2030			2040			2050				
Scenario	**E**	**C**	**M**	**E**	**C**	**M**	**E**	**C**	**M**	**Units**	**Source**
Electricity	106.95	121.26	121.09	87.36	101.73	98.30	65.67	105.29	95.31	€/MWh	[96]
Hydrogen	94.53	101.72	78.00	70.21	81.20	65.77	47.31	67.22	58.50	€/MWh	[96]
Natural gas	38.52			35			35			€/MWh	[95]
Biogas [3]	39.61			28.56			28.56			€/MWh	[81]
Biomethane [4]	52.30			44.43			44.43			€/MWh	[81]
Biomass	16.92			18			18			€/MWh	[95]
CO_2 tax	0.15			0.25			0.35			€/kg	[95]

Each alternative technology will be compared to the base case (natural gas-fired kiln, without CC) based on three KPIs: net specific CO_2 emissions (kg_{CO_2}/t_{lime}), specific energy consumption (kWh/t_{lime}) and specific total cost (€/t_{lime}). The specific CO_2 emissions include only scope 1 emissions. The total specific cost is computed according to equation 38.

$$\text{total specific cost} = \frac{\text{annualized CAPEX + OPEX}}{\text{tons of lime produced}} \tag{38}$$

The specific energy requirement takes into account the fuel consumption for heat supply to the lime kiln, as well as the natural gas and electricity requirements for the carbon capture unit (if included). It was decided to consolidate fuel and electricity requirements to calculate the overall energy consumption for each configuration. This approach facilitates the comparison between configurations considering different fuels. Moreover, the impact on energy consumption of the implementation of a carbon capture unit becomes clearer. Analyses could be improved by evaluating fuel and electricity demands separately.

Remark: One must note that limestone, compressed air and cooling water costs as well as the CAPEX for the different technologies are assumed identical regardless of the considered year or scenario. Only energy and carbon prices vary.

[3] The 2030 price is an average between the biogas cost in 2020 ($16/MBtu [81]) and 2040 ($9/MBtu[81]). The biogas price in 2050 is assumed to be identical to the one in 2040.

[4] The 2030 price is an average between the biomethane cost in 2020 ($19/MBtu [81]) and 2040 ($14/MBtu[81]). The biomethane price in 2050 is assumed to be identical to the one in 2040.

5.4 Evaluation of energy transition pathways

5.4.1 Results for 2030

The evaluation of energy transition pathways for year 2030 is presented in Figure 48. Pareto plots for each scenario (see Figures 49a, 49b and 49c) facilitate the visualization of trade-offs between KPIs.

The specific total cost in the base case amounts to €269/t_{lime} for the electrification scenario, and €270/t_{lime} for the clean molecules and central scenarios. For all three scenarios, the cheapest configuration is the biomass-fired kiln coupled with CC, characterized by a specific total cost below €200/t. The second cheapest alternative is the 'Biomass' configuration. However, the corresponding emissions are relatively high (0.786 t_{CO_2}/t_{lime}) since only the fuel-related CO_2 emissions are addressed. The next optimal energy transition pathway from an economic point of view is 'NGOxy-CC' for clean molecules and central scenarios, and 'Plasma-CC' for the electrification scenario (closely followed by 'NGOxy-CC'), emitting respectively 0.103 and 0.079 t_{CO_2}/t_{lime}. Finally, in the central and clean molecules scenarios, the specific total cost of 'BioCH4-CC' is almost identical to the 'Plasma-CC' one (€240/t for 'BioCH4-CC' vs. €237/t for 'Plasma-CC'), with sensibly higher CO_2 emissions (0.186 t_{CO_2}/t_{lime} for 'BioCH4-CC' vs. 0.079 t_{CO_2}/t_{lime} for 'Plasma-CC'). The cost difference between both configurations increases in the electrification scenario due to lower electricity prices. Conversely, 'H2' and 'H2-CC' are the most expensive options in all three scenarios with a specific total cost exceeding €300/t.

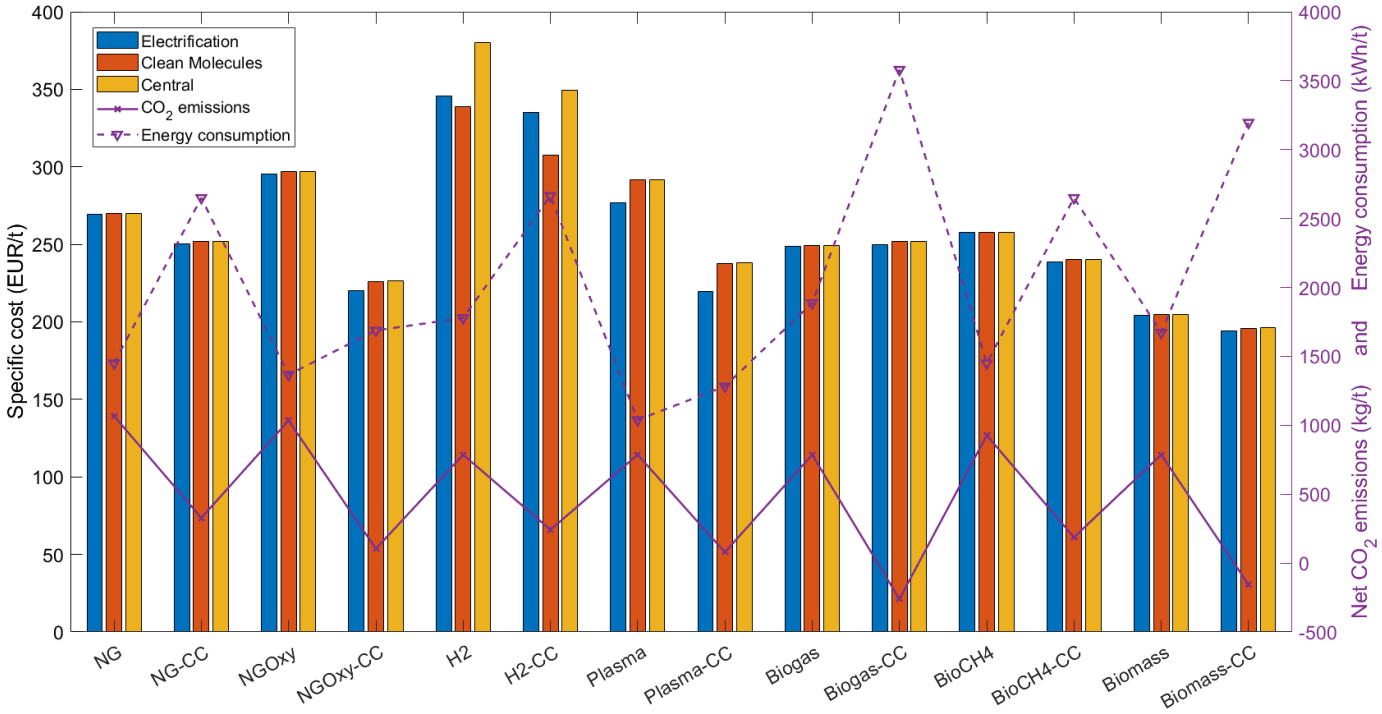

Figure 48: Specific total cost (€/t_{lime}), specific net CO_2 emissions (kg_{CO_2}/t_{lime}) and specific energy requirements (kWh/t_{lime}) for different technologies in 2030

As can be seen in Figure 48, the specific total cost is almost unaffected by the studied scenario –electrification, clean molecules or central– except for hydrogen-fired kilns (with or without CC), plasma generators (with or without CC), and oxycombustion of natural gas coupled with carbon capture to a lesser extent. This can be attributed to a larger share of hydrogen and electricity costs, whose prices are the only ones to vary between scenarios.

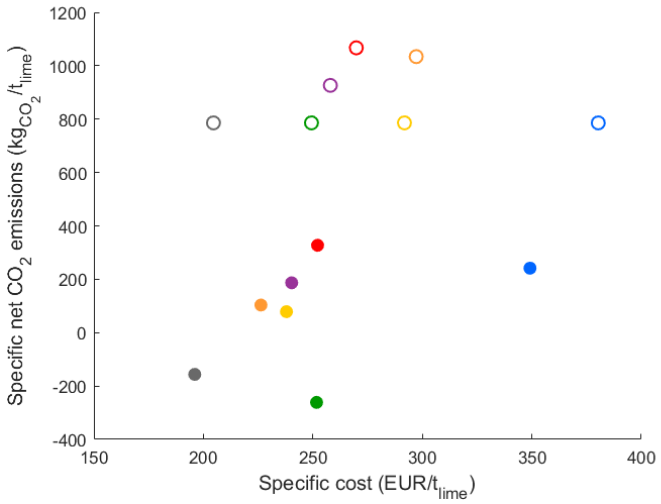

(a) Central scenario – 2030

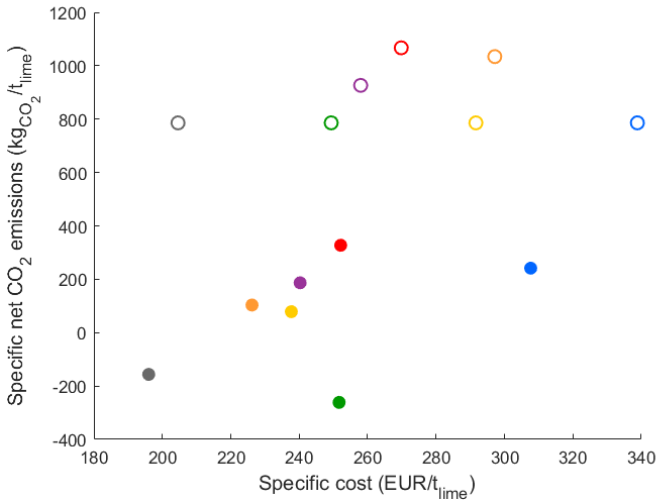

(b) Clean molecules scenario – 2030

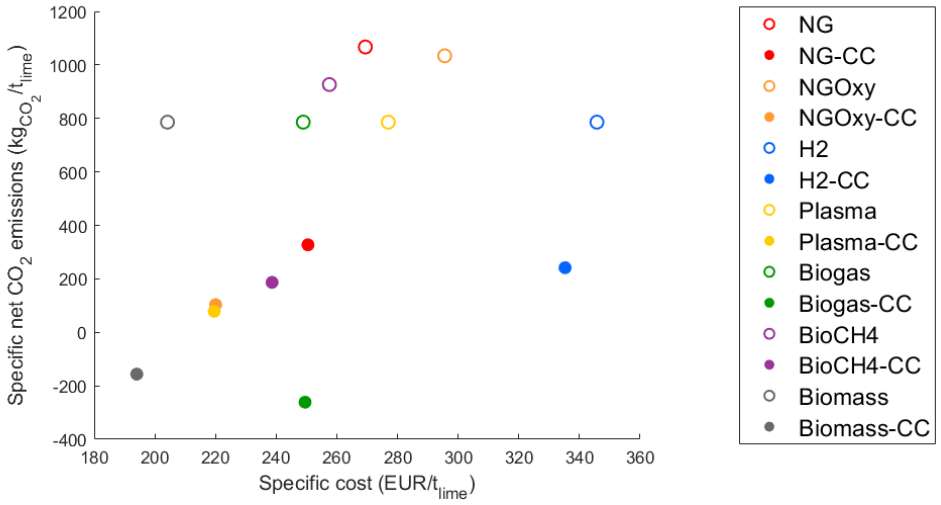

(c) Electrification scenario – 2030

Figure 49: Specific CO_2 emissions (kg_{CO_2}/t_{lime}) and specific total cost (€/t_{lime}) for different technologies and different scenarios in 2030

Moreover, all the considered alternatives lead to an increased energy consumption –due to a lower kiln efficiency or additional energy requirements to perform CO_2 capture and compression– except the 'NGOxy', 'Plasma-CC' and 'Plasma' configurations which are characterized by an energy consumption reduction of 6%, 12% and 28%, respectively, compared to the base case. The fact that no heat is wasted in heating nitrogen explains the lower energy consumption for the 'NGOxy' case. The reduced energy consumption for the plasma-based configurations stems from the absence of gases to be heated and the larger high-grade heat available.

Implementing a MEA-based CC unit for a natural gas-fired kiln decreases the scope 1 emissions by 69% and the total specific cost by 7%, but increases the specific energy consumption by 83% compared to the base case. Despite the higher CAPEX and higher energy consumption of the 'NG-CC' configuration compared to the base case, the cost reduction can be explained by the decreased amount EU-ETS quotas needed to cover scope 1 emissions. Moreover, it is worth noting that, even though the MEA-based CC unit is characterized by a capture rate of 90%, the CO_2 emission reduction potential compared to the base case is less than 90%. This observation can be explained by the fact that the CO_2 emitted by the combustion of natural

gas required for the carbon capture process (specifically for steam generation) cannot be captured.

The implementation of oxy-fuel technology without CC is not interesting for the lime sector since CO_2 emissions are only reduced by 3% compared to the base case, while the related specific total cost rises by 10% (due to the additional investment cost related to the ASU). However, depending on the considered scenario, scope 1 CO_2 emissions can be decreased by 90% and the specific total cost can be reduced by 16–18% compared to the base case when the 'NGOxy-CC' configuration is considered, which requires only 16% more energy than natural gas-fired kilns. The savings resulting from the reduction of the quantity of CO_2 emissions subjected to carbon tax outweigh the additional costs associated with the increased energy consumption compared to the base case. The 90% CO_2 emission reduction potential for the 'NGOxy-CC' configuration can be attributed to the fully-electric carbon capture process, which does not contribute to scope 1 emissions, unlike CO_2 capture with MEA.

Using hydrogen instead of natural gas implies a CO_2 emission reduction of 26% (since only fuel-related emissions are addressed), a specific energy consumption increase of 23% (due to a lower kiln efficiency), and a specific total cost increase of 26%, 28% and 41% in, respectively, the clean molecules scenario, the electrification scenario and the central scenario. When a hydrogen-fired kiln is followed by a MEA-based carbon capture, CO_2 emissions are reduced by 77%, the specific energy consumption increases by 84% and, depending on the considered scenario, the specific total cost increases by 14–29% compared to the base case.

Plasma technology coupled with CC decreases the scope 1 emissions by 93%, the energy consumption by 12% and the specific total cost by 12–18%, depending on the scenario, compared to the base case. The CO_2 emission reduction potential is over 90% since energy-related emissions are completely removed and the fully-electric carbon capture process does not emit scope 1 CO_2. When kiln electrification takes place and the CO_2 emitted by the calcination reaction is not captured, a decrease of 26% and 28% is observed respectively for specific CO_2 emissions and specific energy consumption whereas the specific cost slightly increases compared to 'NG' by 3% in the electrification scenario and by 8% in the clean molecules and central scenarios.

Scope 1 CO_2 emissions are cut-off by 26% in the case of a biogas-fired kiln. This decrease can be explained by biogenic CO_2 emissions resulting from biogas combustion which are not accounted in scope 1 emissions. As for hydrogen-fired kilns, even if energy-related emissions are removed, process-related emissions remain unchanged, limiting the emission reduction potential of fuel switching alone. Moreover, the specific total cost is around 8% lower than for a natural gas-fired kiln (due to a lower amount of CO_2 subjected to carbon tax) while the specific energy consumption is increased by 30% (due to higher losses at the stack). Biogas-fired kilns coupled with MEA-based CC lead to net negative CO_2 emissions (-124% compared to the base case). Even though the related energy requirement is 147% higher than for the base case, this configuration is 7% less expensive. This cost reduction can be attributed to the absence of scope 1 CO_2 emissions.

In the case of a kiln partially fueled with biomethane (50% NG–50% bioCH4), scope 1 emissions are reduced by 13% since half of the energy-related emissions (i.e., coming from biomethane combustion) are considered as biogenic. Moreover, the specific total cost is 4% lower than the base case. When 'BioCH4-CC' configuration is implemented, CO_2 emissions are cut-off by 82% compared to the base case, while the total specific cost is reduced by 11%. However, this configuration requires 83% more energy than a natural gas-fired kiln. The CO_2 emission reduction potential is higher for the 'BioCH4-CC' configuration (82%) than for the 'NG-CC' configuration (69%) due to the captured biogenic CO_2 accounted as negative emissions and partially compensating scope 1 emissions uncaptured by the CC unit.

Firing the lime kiln with solid biomass decreases the scope 1 emissions by 26%, as biomass combustion releases biogenic CO_2. The specific total cost decrease (-24% compared to the base case) can be attributed

to lower scope 1 emissions and a lower biomass price compared to natural gas. However, the specific energy requirement is increased by 15% due to a lower kiln efficiency than for natural gas combustion. A biomass-fired kiln followed by a CC unit requires around 120% more energy than the base case, but allows reaching net negative CO_2 emissions (-115% compared to the 'NG' case). Combined with lower prices for biomass than for natural gas, the absence of scope 1 emissions results in a specific total cost 27–28% lower than for 'NG'.

The aforementioned impacts of the various technologies on CO_2 emissions, energy requirements and total cost compared to the 'NG' configuration are listed in Table 9 (see Appendix B).

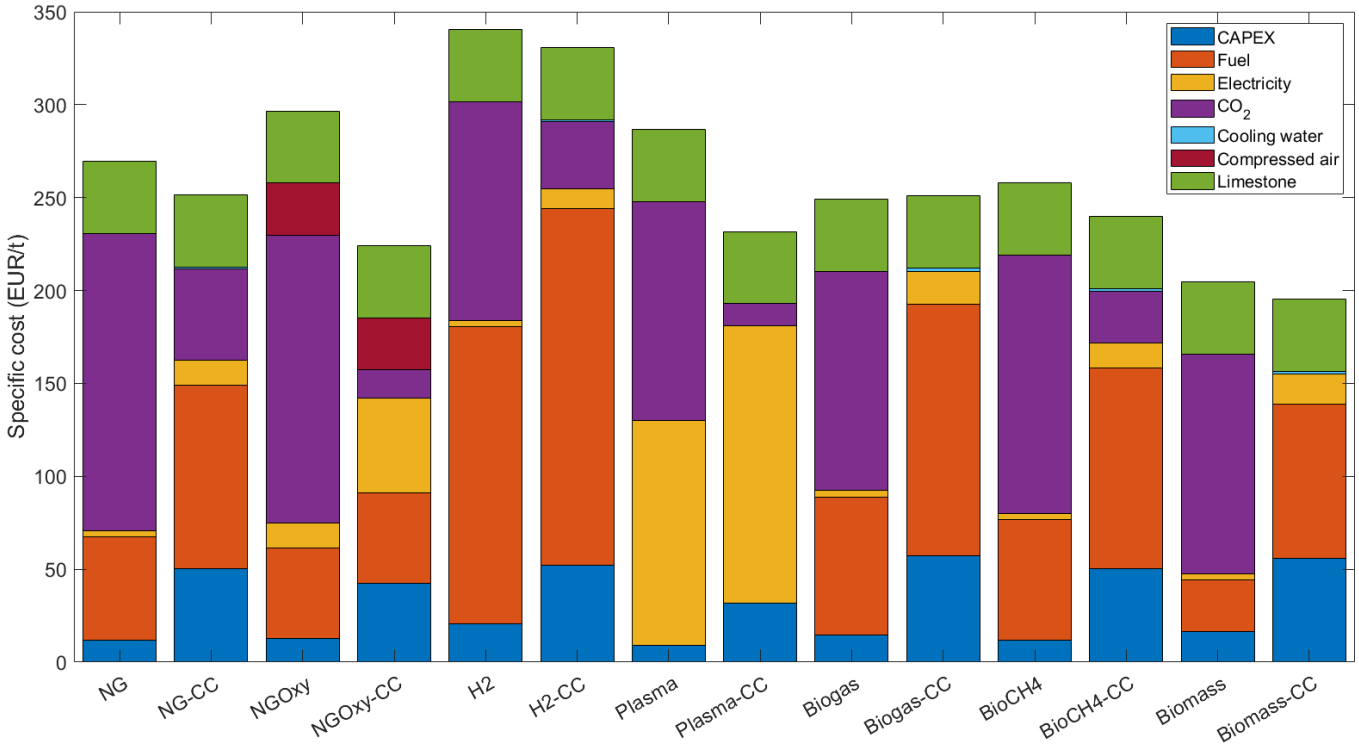

Figure 50: Breakdown of the specific cost for various configurations in 2030

The breakdown of the specific cost[5] for different configurations in 2030 is depicted in Figure 50. The relative share of CAPEX, fuel (i.e., natural gas, hydrogen, biogas, biomethane or solid biomass), electricity, emitted CO_2, cooling water, compressed air (necessary for oxygen production) and limestone can be observed. These relative shares are also summarized in Table 12 (see Appendix C).

The CAPEX represents between 3% (for 'Plasma') and 29% (for 'Biomass-CC') of the total specific cost. When comparing a particular kiln technology with and without CC, the higher CAPEX related to configurations implementing carbon capture makes sense due to the need for additional units to separate and purify CO_2. In general, carbon capture increases the relative share of fuel and electricity due to the associated additional energy requirements for CO_2 removal from flue gases and its compression[6].

Natural gas-, hydrogen-, biogas-, biomethane-, and solid biomass-fired kilns can all be coupled or not with MEA-based carbon capture. The observed cost difference –in terms of CAPEX, fuel and electricity– between both configurations varies depending on the burned fuel. This variation can be explained by differences in capture capacity and CO_2 concentration in the fumes for the different fuel options. In fact, for lime kilns fueled with hydrogen, the carbon dioxide to be captured comes only from the reaction, which explains the smaller

[5]Computed as the mean of the specific total costs obtained for the electrification, clean molecules and central scenarios
[6]Transportation and sequestration of CO_2 are not included in the system boundaries.

additional investment cost needed compared to a natural gas-fired kiln where CO_2 is emitted by both the calcination reaction and the fuel combustion. On the other hand, a much bigger CC unit capacity is needed in case of biogas combustion, since CO_2 results from the calcination reaction, the biogas combustion and the CO_2 initially present in the fuel feed. The same conclusions hold for fuel and electricity requirements.

Among the depicted configurations, those implying carbon capture are all cheaper than their counterparts without the CC unit, except for biogas-fired kilns. Indeed, the specific total cost is reduced by 7% when 'NG-CC' is implemented instead of 'NG', by 3% when considering 'H2-CC' instead of 'H2', by 7% when the 'BioCH4' configuration is replaced by the 'BioCH4-CC' one, and by 4% for 'Biomass-CC' compared to 'Biomass'. The largest cost savings after CC implementation are obtained for 'NGOxy-CC' and 'Plasma-CC' configurations (-24% for 'NGOxy-CC' compared to 'NGOxy', -19% for 'Plasma-CC' compared to 'Plasma'). This observation can be explained by significantly higher CO_2 concentrations in the fumes obtained by oxycombustion or plasma-based kilns than for other configurations, facilitating the carbon capture process. Thus, the benefit of reducing the amount of emitted CO_2 subject to carbon tax outweighs even more the additional costs associated with the CC unit. Furthermore, the facilitated carbon capture makes the 'Plasma-CC' and 'NGOxy-CC' cases much less costly than most of the other configurations involving carbon capture. In fact, only 'Biomass-CC' is more cost-effective, possibly thanks to lower biomass and natural gas prices (necessary for biomass-based kilns with carbon capture) than electricity (required to perform CC for oxy-fuel and plasma-based configurations). Finally, biogas-fired kilns with CC remain slightly more expensive (+1%) than those without, owing to larger CC capacities required than for 'NG'.

For configurations not implementing carbon capture (except hydrogen-fired and plasma-based kilns), the specific cost related to CO_2 emissions is preponderant, representing between 47% (for 'Biogas') and 59% (for 'NG'). While the largest contribution to the specific total cost for 'H2' and 'Plasma' cases is fuel (47%) and electricity (42%) respectively, CO_2 ranks as the second most significant factor contributing for respectively 35% and 41% of the specific total cost.

When CC is included, the specific total cost is primarily influenced by fuel expenses, except 'NGOxy-CC' and 'Plasma-CC' cases for which the fully-electric carbon capture process implemented leads to electricity expenses significantly impacting the total cost. In fact, fuel-related expenses for 'NG-CC', 'H2-CC', 'Biogas-CC', 'BioCH4-CC' and 'Biomass-CC' account for respectively 39%, 58%, 54%, 45% and 43% of the specific total cost. The 'NGOxy-CC' cost is dominated by electricity (23%), closely followed by fuel costs (22%), while for 'Plasma-CC', electricity represents 64% of the total specific cost. Moreover, no fuel-related expenses are observed for plasma-based options since the process is considered as entirely electric.

The relative share of CO_2 for configurations including CC is lower than the one for the corresponding kiln technologies without CC. This decrease can be explained by the reduced scope 1 emissions when carbon capture is considered. The CO_2-related cost for 'BioCH4-CC' is lower than the one for 'NG-CC' due to the biogenic CO_2 that is captured and considered as negative CO_2 emissions. Thus, less EU-ETS quotas are needed to cover the remaining CO_2 emissions. No CO_2-related cost is observed for 'Biogas-CC' and 'Biomass-CC', which can be explained by the net negative CO_2 emissions enabled by both configurations. In addition, thanks to a fully electric carbon capture process, lower CO_2 costs are observed for 'NGOxy-CC' and 'Plasma-CC' configurations compared to MEA-based options. The steam necessary for chemical absorption CC with MEA is provided by natural gas boilers whose CO_2 emissions cannot be treated.

Even if energy consumption is only increased by 23% compared to the base case, the fuel-related expenses for the 'H2' configuration are almost three times higher than for natural gas combustion. This observation can be attributed to a more than twofold hydrogen price compared to the natural gas one in 2030 (€78–102/MWh$_{H_2}$ vs. €38.5/MWh$_{NG}$). The higher fuel-related costs for 'Biogas' and 'BioCH4' configurations stem from, respectively, an increased energy consumption (+30% compared to 'NG') and a higher fuel price

(€52/MWh$_{BioCH4}$ vs. €38.5/MWh$_{NG}$). Lower fuel costs can be observed for the 'Biomass' case, even though specific energy requirements are 15% higher than for 'NG'. This observation can be explained by biomass availability at less than half the price of natural gas (€17/MWh$_{Biomass}$ vs. €38.5/MWh$_{NG}$). Finally, even if the 'Plasma' configuration is characterized by a specific energy consumption 28% lower than that of 'NG', the energy-related expense (i.e., fuel and electricity combined) in the 'Plasma' case is approximately double that of 'NG' due to much higher electricity prices compared to natural gas prices in 2030 (€107–121/MWh$_e$ vs. €38.5/MWh$_{NG}$).

Cooling water has a minor impact of less than 1% whatever the configuration. Compressed air being used for oxygen production[7], it appears only for options implementing natural gas-oxycombustion (9% for 'NGOxy' and 12% for 'NGOxy-CC'). Finally, limestone represents between 11% (for 'H2') and 20% (for 'Biomass-CC') of the specific total cost for all studied configurations.

5.4.2 Results for 2040

Figure 51 shows the specific total cost (€/t$_{lime}$), the specific net CO_2 emissions (kg$_{CO_2}$/t$_{lime}$) and the specific energy consumption (kWh/t$_{lime}$) of the various alternatives considered for the lime sector in 2040. The specific CO_2 emissions and specific energy consumption are identical to the ones mentioned in section 5.4.1. Pareto plots –represented in Figures 52a, 52b and 52c– provide a clear view of trade-offs between KPIs.

In all three scenarios, the 'Biomass-CC' configuration is the cheapest one, with a specific cost below €200/t. 'Plasma-CC', 'NGOxy-CC' and 'Biogas-CC' configurations come next. These alternatives are characterized by a specific total cost of, respectively, €202–221/t, €217–223/t, and €220–222/t. Again, hydrogen-fired kilns –with or without CC– are part of the most expensive configurations.

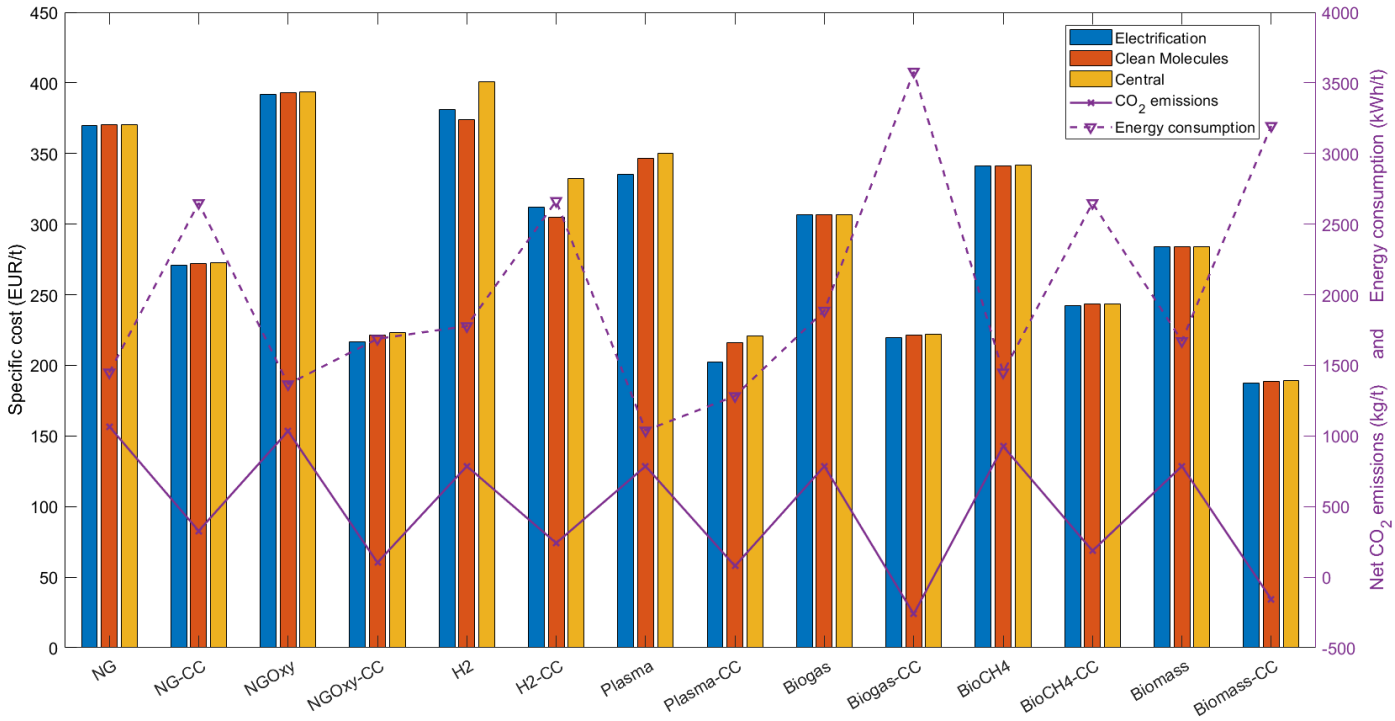

Figure 51: Specific total cost (€/t$_{lime}$), specific net CO_2 emissions (kg$_{CO_2}$/t$_{lime}$) and specific energy requirements (kWh/t$_{lime}$) for different technologies in 2040

[7] As a reminder, compressed air is sent to the ASU to be separated into oxygen and other inert gases.

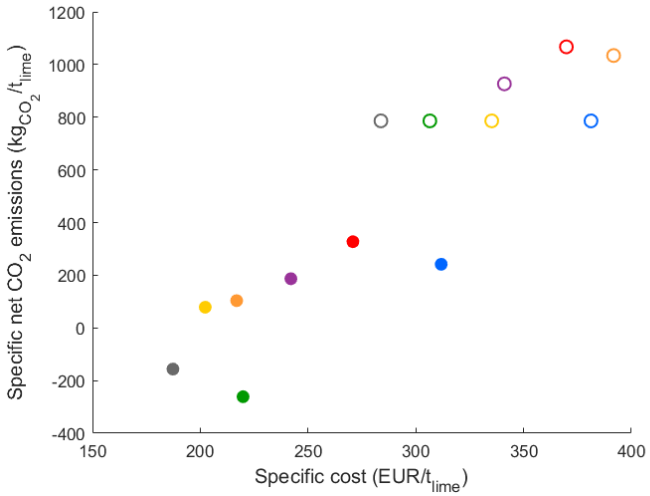

(a) Electrification scenario – 2040

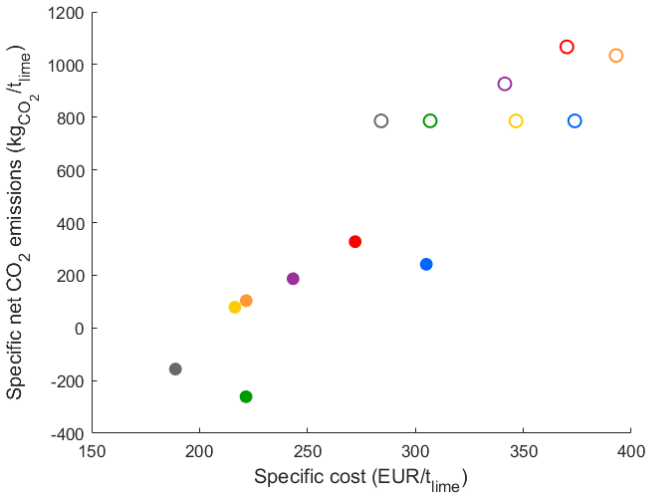

(b) Clean molecules scenario – 2040

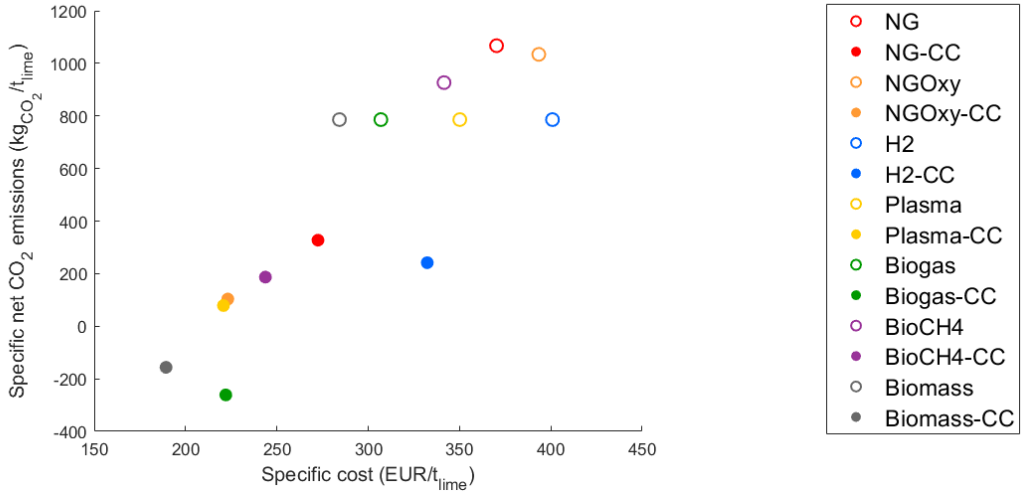

(c) Central scenario – 2040

Figure 52: Specific CO_2 emissions (kg_{CO_2}/t_{lime}) and specific total cost (€/t_{lime}) for different technologies and different scenarios in 2040

The base case-specific total cost amounts to €370/t for all three 2040 scenarios, as can be seen in Figure 51. The high carbon price (€250/t_{CO_2}) favors the implementation of carbon capture units in the lime sector. In fact, the specific total cost of all configurations with CC is lower than the one of their equivalents without CC. Moreover, all the studied alternatives become cheaper than the natural gas-fired kiln, except 'NGOxy' and 'H2' cases which remain respectively 6% and 1–8% more expensive than the base case, depending on the scenario. The higher cost of 'NGOxy' compared to 'NG' can be attributed to a higher CAPEX (due to the ASU), a higher energy requirement (for oxygen production) and almost no benefit in terms of CO_2 emissions (-3% compared to 'NG'). The high specific total cost related to 'H2' can be explained by 2.5 to 3 times higher prices for hydrogen than natural gas. However, the specific cost difference between hydrogen and natural gas is less marked in the clean molecules scenario due to the availability of cheaper hydrogen.

Without carbon capture, the biogas-, biomethane- and solid biomass-fired kilns as well as plasma-based calcination cases are characterized by respectively 17%, 8%, 23% and 5–9% lower specific total cost than the base case. When the aforementioned alternative kilns are coupled with CC units, the cost reduction compared to the 'NG' case amounts to 41% in the electrification scenario and 40% in the clean molecules

and central scenarios for 'Biogas-CC'; 35% in the electrification scenario and 34% in the clean molecules and central scenarios for 'BioCH4-CC'; 49% in all scenarios for 'Biomass-CC'; and 45%, 42% and 40% for 'Plasma-CC' in the electrification, clean molecules and central scenarios, respectively. Finally, the 'NG-CC', 'NGOxy-CC' and 'H2-CC' configurations reduce the specific total cost compared to the base case by respectively 27%, 41% and 16% in the electrification scenario; by respectively 26%, 40% and 18% in the clean molecules scenario; and by respectively 26%, 40% and 10% in the central scenario.

The specific net CO_2 emissions and the specific total cost of 'Plasma-CC' and 'NGOxy-CC' configurations are very close. The biggest cost difference between both cases is observed for the electrification scenario, due to favorable electricity prices.

The CO_2 emissions, energy requirements and total cost reductions compared to the base case for the various configurations are listed in Table 10 (see Appendix B).

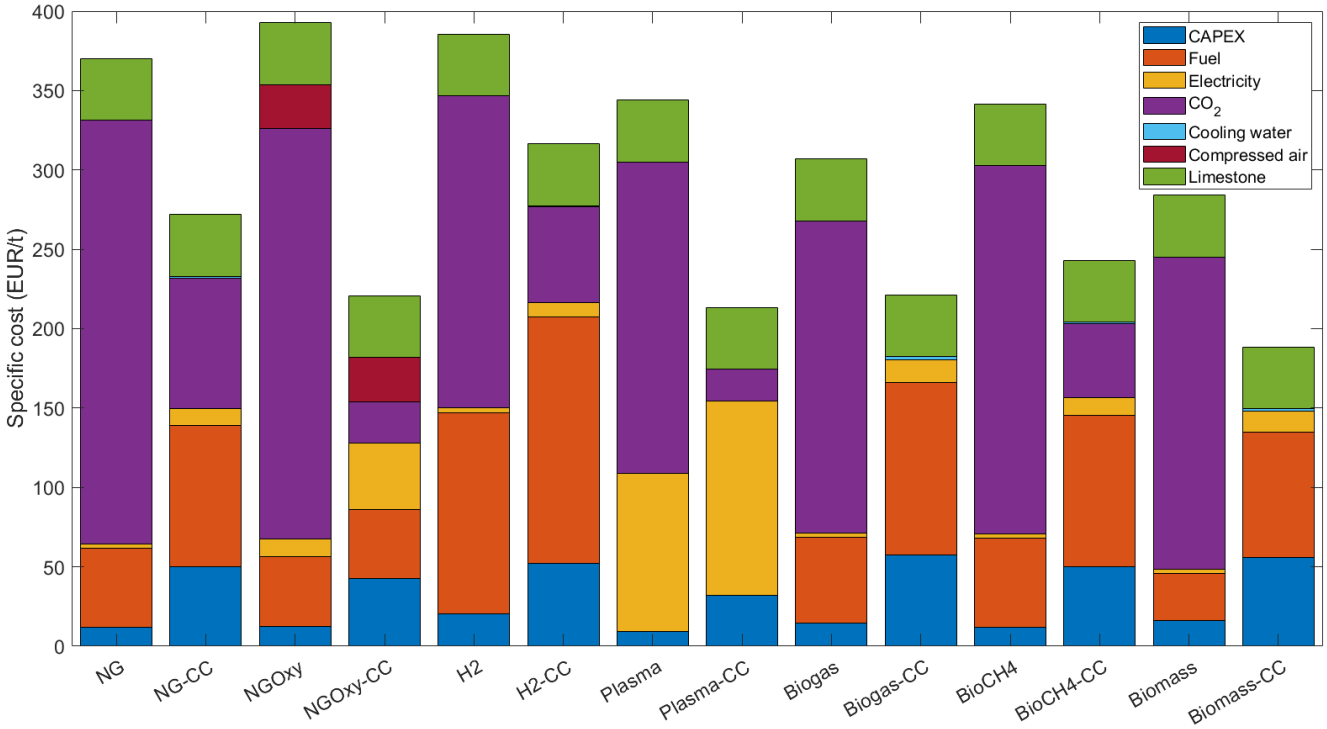

Figure 53: Breakdown of the specific cost for various configurations in 2040

The breakdown of the specific cost[8] for different configurations, in 2040, is depicted in Figure 53. The relative shares of CAPEX, fuel (i.e., natural gas, hydrogen, biogas, biomethane or solid biomass), electricity, CO_2, cooling water, compressed air and limestone are summarized in Table 13 (see Appendix C).

The relative share of CAPEX remains almost identical to the 2030 scenarios, and varies between 3% (for 'NG', 'NGOxy', 'Plasma' and 'BioCH4') and 30% (for 'Biomass-CC') of the specific total cost.

When no carbon capture takes place, the specific total cost comes mainly from scope 1 emissions (51–72%) whereas for configurations where CO_2 is captured, the largest contribution to the specific cost comes from fuel (20–49%), except for 'Plasma-CC', where electricity is predominant (58%).

The relative share of CO_2 cost is higher in 2040 than in 2030, ranging between 51% (for 'H2') and 72% (for 'NG') for configurations without CC *(vs. 35% for 'H2' and 59% for 'NG' in 2030)*, and between 9% (for 'Plasma-CC') and 30% (for 'NG-CC') when a CC unit is included *(vs. 5% for 'Plasma-CC' and 20% for*

[8]Computed as the mean of the specific total costs obtained for the electrification, clean molecules and central scenarios.

'NG-CC' in 2030). This observation can be explained by an increased carbon price compared to 2030. As expected, no CO_2-related cost is observed for 'Biogas-CC' and 'Biomass-CC' since both configurations enable achieving net negative CO_2 emissions.

Moreover, the relative shares of fuel and electricity costs are lower in 2040 than in 2030. Indeed, fuel costs vary between 10 and 49% for 'Biomass' and 'H2-CC' cases respectively *(vs. 14–58% in 2030)*. Electricity costs represent only 1% when no CC is taken into account, except for 'NGOxy' and 'Plasma' options where, respectively, 3% and 29% of the specific total cost is related to electricity *(vs. 1% for 'NG', 'H2', 'Biogas' and 'BioCH4'; 2% for 'Biomass'; 4% for 'NGOxy'; 42% for 'Plasma' in 2030)*. The higher impact of electricity in the 'Plasma' configuration is obvious, as the kiln is electrically heated. The larger share of electricity in the 'NGOxy' configuration can be attributed to the requirements of the ASU. When CC is implemented, the impact of electricity on the specific total cost varies between 3% for 'H2-CC' and 58% for 'Plasma-CC' *(vs. 3–64% in 2030)*. These observations can be explained by a decreased price of fuels and electricity compared to 2030, as can be seen in Table 7.

The primary distinction between the results for 2030 and 2040 scenarios lies in the specific total cost variation between lime kilns coupled or not with carbon capture. In 2040, the cost savings after CC implementation are much more considerable than in 2030. In fact, looking at Figure 53, one may realize that, in 2040, all configurations including CC are cheaper than their counterparts without CC, and the gap widened compared to 2030. Indeed, the specific total cost is reduced by 27% when implementing 'NG-CC' instead of 'NG' *(vs. -7% in 2030)*, by 18% when considering 'H2-CC' instead of 'H2' *(vs. -3% in 2030)*, by 29% when the 'BioCH4' configuration is replaced by the 'BioCH4-CC' one *(vs. -7% in 2030)*, by 28% when implementing 'Biogas-CC' instead of 'Biogas' *(vs. +1% in 2030)* and by 34% for 'Biomass-CC' compared to 'Biomass' *(vs. -4% in 2030)*. The highest cost reduction is achieved for 'NGOxy-CC' (-44% compared to 'NGOxy', vs. -24% in 2030) and for 'Plasma-CC' (-38% compared to 'Plasma', vs. -19% in 2030) due to the facilitated carbon capture process.

5.4.3 Results for 2050

Figure 54 shows the specific total cost (€/t_{lime}), the specific net CO_2 emissions (kg_{CO_2}/t_{lime}) and the specific energy consumption (kWh/t_{lime}) of the various alternatives considered for the lime sector in 2050. Energy consumption and CO_2 emissions are identical to the ones mentioned in section 5.4.1. Comparisons –in terms of CO_2 emissions, energy requirements and costs– between the identified alternatives and the base case are summarized in Table 11 (see Appendix B). Moreover, the Pareto plots for each scenario (see Figures 55a, 55b and 55c) facilitate the visualization of trade-offs between KPIs.

In the 2050 electrification scenario, 'Plasma-CC' is the least expensive configuration (€182/t), closely followed by 'Biomass-CC' (€184/t). The next two most cost-effective alternatives are 'Biogas-CC' and 'NGOxy-CC' (€217/t and €218/t respectively). In the 2050 clean molecules and central scenarios, the cheapest option is the 'Biomass-CC' case (€188–189/t), followed by 'Biogas-CC' (€221–223/t). The 'Plasma-CC' and 'NGOxy-CC' cases come at the third and forth positions, with very similar costs (respectively €220/t and €231/t for the clean molecules scenario; €233/t and €235/t respectively for the central scenario). Hydrogen-fired kilns are once again among the most expensive options for the sector (depending on the scenario, €419–455/t for 'H2' and €294–332/t for 'H2-CC'), even if a slight improvement compared to 2030 and 2040 is observed. In fact, 'H2-CC' becomes cheaper than 'NG-CC' for the electrification scenario. Moreover, the 'H2' configuration is cheaper than the 'NG' and 'NGOxy' cases in all three scenarios. This can be attributed to lower CO_2 emissions for hydrogen-fired kilns.

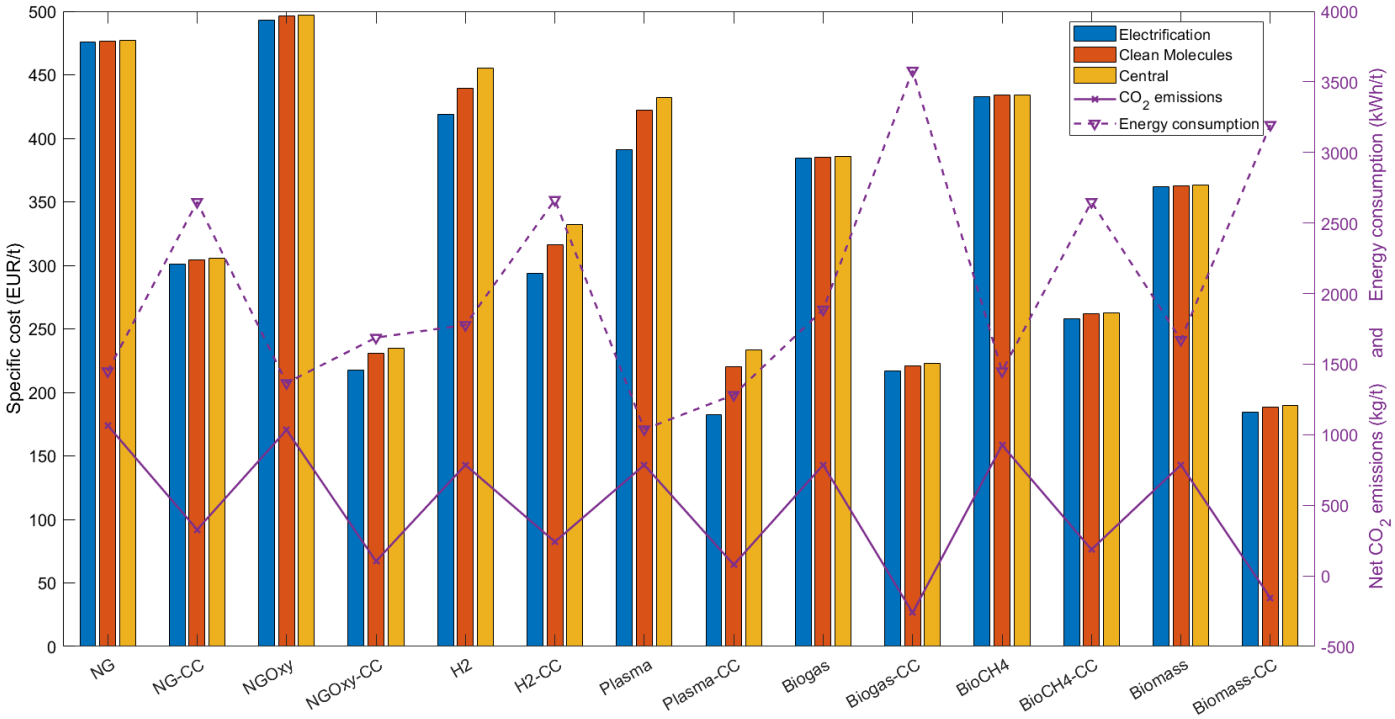

Figure 54: Specific total cost (€/t_{lime}), specific net CO_2 emissions (kg_{CO_2}/t_{lime}) and specific energy requirements (kWh/t_{lime}) for different technologies in 2050

In 2050, the specific total cost in the base case reaches €476/t for the electrification scenario and €477/t for the clean molecules and central scenarios. With a carbon price of €350/t_{CO_2}, only the 'NGOxy' option is more expensive (+4%) than the base case. In fact, depending on the considered scenario, the 'Plasma-CC', 'NGOxy-CC', 'Biomass-CC', 'Biogas-CC', 'H2-CC', 'NG-CC' and 'BioCH4-CC' configurations result in a specific total cost decrease of respectively 51–62%, 51–54%, 60–61%, 53–54%, 30–38%, 36–37% and 45–46% compared to the natural gas-fired kiln. When no CC unit is implemented, the cost reduction compared to the base case for the biomass-, biogas- and biomethane-fired kiln amounts to 24%, 19% and 9%, respectively. In addition, when hydrogen combustion or plasma technology are implemented for limestone calcination, without CC, the specific total cost is respectively 5–12% and 9–18% lower than the base case, depending on the scenario.

Increasing the carbon price up to €350/t_{CO_2} leads to CC-based configurations even more cost-effective than their counterparts without the CC unit, compared to 2030 and 2040 scenarios. Indeed, depending on the considered scenario, the specific total cost is reduced by 36–37% when implementing 'NG-CC' instead of 'NG' and by 27–30% when considering 'H2-CC' instead of 'H2'. Choosing 'BioCH4-CC' over 'BioCH4' leads to cost savings of 39–40%, while opting for 'Biogas-CC' instead of 'Biogas' enables a specific cost reduction of 42–44%, depending on the scenario. Replacing the 'Biomass' configuration with the 'Biomass-CC' one results in a cost reduction of 48–49%. Similarly, depending on the scenario, cost savings after CC implementation of 53–56% and 46–53% can be achieved by implementing, respectively, 'NGOxy-CC' instead of 'NGOxy', and 'Plasma-CC' instead of 'Plasma'.

Moreover, in Figures 55a, 55b, 55c, it can be observed that the most expensive CC configurations ('NG-CC' for the electrification scenario and 'H2-CC' for clean molecules and central scenarios) are characterized by a lower specific total cost than the cheapest configuration without CC (i.e., 'Biomass' for all three scenarios). Thus, a carbon price of €350/t_{CO_2} is a sufficient incentive to widely implement carbon capture facilities in lime plants.

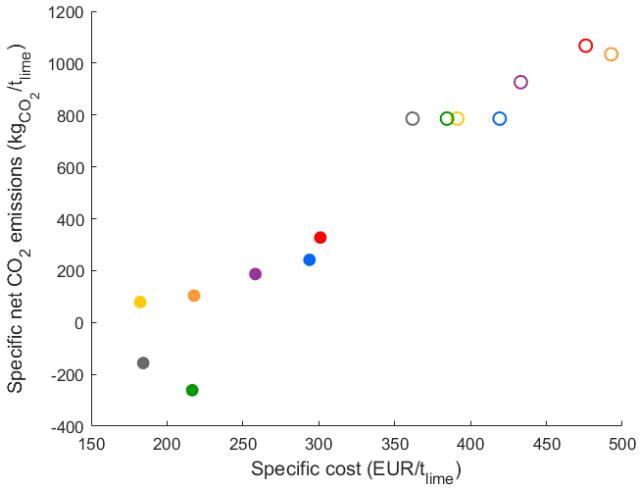

(a) Electrification scenario – 2050

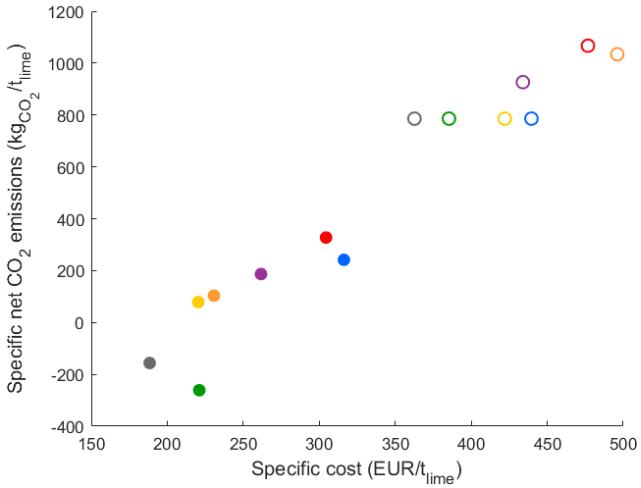

(b) Clean molecules scenario – 2050

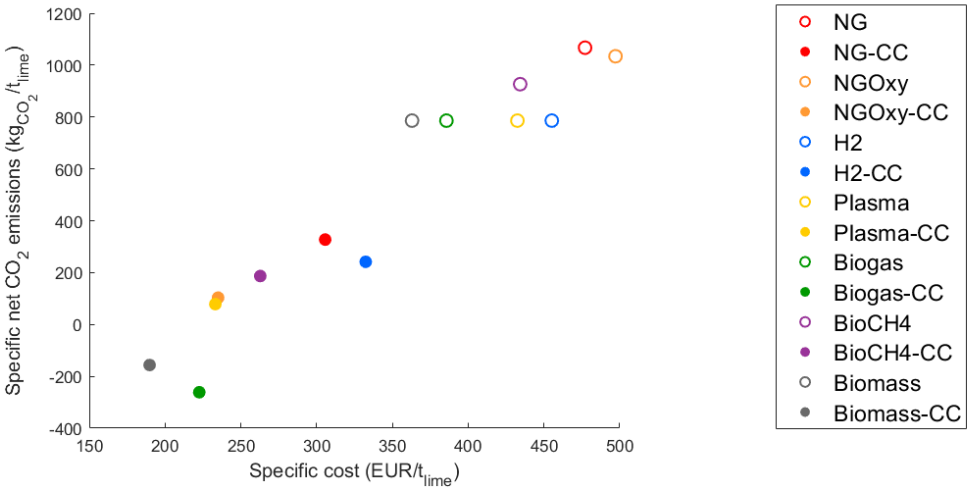

(c) Central scenario – 2050

Figure 55: Specific CO_2 emissions (kg_{CO_2}/t_{lime}) and specific total cost (€/t_{lime}) for different technologies and different scenarios in 2050

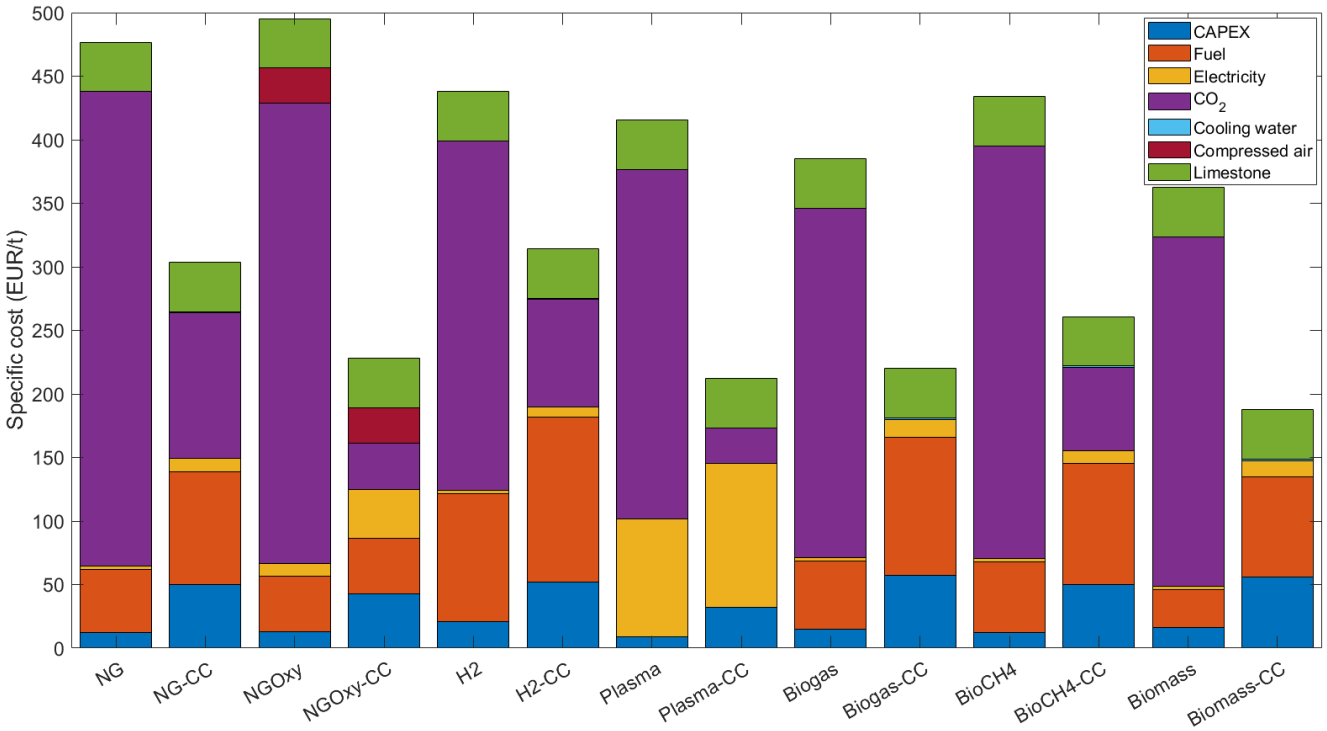

Figure 56: Breakdown of the specific cost for various configurations in 2050

The specific cost[9] breakdown between CAPEX, fuel (i.e., natural gas, hydrogen, biogas, biomethane or solid biomass), electricity, emitted CO_2, cooling water, compressed air and limestone for different configurations in 2050 can be seen in Figure 56. These relative shares are also listed in Table 14 (see Appendix C).

The relative share of CAPEX remains essentially the same in both previous years and varies between 2% (for 'Plasma') and 30% (for 'Biomass-CC') of the specific total cost. Generally speaking, the relative share of CO_2 is higher in 2050 than in 2040, whereas fuel and electricity have a diminished impact. This observation stems from the downward trend in fuel and electricity prices between 2040 and 2050, combined with an increasing CO_2 tax as can be seen in Table 7.

Considering a carbon price of €350/t_{CO_2} in 2050, the specific cost of all configurations not implementing CO_2 capture is dominated by CO_2-related expenses. In fact, in the absence of carbon capture, the relative share of CO_2 ranges from 63% (for 'H2') to 78% (for 'NG'), while it drops down to values between 13% (for 'Plasma-CC') and 38% (for 'NG-CC') when CC is implemented. The relative share of CO_2 for 'Biogas-CC' and 'Biomass-CC' is 0% due to the net negative CO_2 emissions achieved by both configurations. A majority of lime kiln technologies followed by CC units exhibit a specific cost primarily driven by fuel-related expenses, representing 41% for 'H2-CC', 49% for 'Biogas-CC', 36% for 'BioCH4-CC', and 42% for 'Biomass-CC'. Electricity and CO_2 have the largest impact on the specific total cost of, respectively, 'Plasma-CC' and 'NG-CC' configurations. The specific total cost of the 'NGOxy-CC' configuration is almost equally distributed among CAPEX (19%), fuel (19%), electricity (17%), limestone (17%), CO_2 (16%) and compressed air (12%).

5.4.4 Final remarks

Various energy transition pathways have been identified and evaluated for different years and scenarios. Since it would only tackle around 25% of the total CO_2 emissions, fuel switching alone is not sufficient. Thus, carbon capture implementation in lime plants is inevitable.

[9]Computed as the mean of the specific total costs obtained for the electrification, clean molecules and central scenarios

From the previously obtained results, it comes that a carbon price of €150/t_{CO_2} favors configurations implementing CC over their counterparts without CC, while prices exceeding €350/t_{CO_2} completely rule out configurations emitting CO_2 directly to the atmosphere, regardless of the kiln technology. However, current carbon prices are far too low to incentivize the implementation of carbon capture in lime plants. In fact, in February 2024, the EU-ETS carbon price plummeted to around €55/t_{CO_2}. Since then, it has experienced a slight increase, exceeding €70/t_{CO_2} in May 2024 [97].

The most cost-effective option for the lime sector to decrease its CO_2 emissions is a solid biomass combustion for heat supply coupled with CC. This configuration is investigated since it enables net negative CO_2 emissions, compensating the process CO_2 uncaptured in other kilns. Combustion of solid biomass is, nonetheless, associated with some minor problems. In fact, NO_x emissions are drastically increased, and sometimes above permitted levels. Currently, some derogations exist, considering that the benefit obtained for CO_2 emissions reduction outweighs the undesired NO_x production. However, these derogations will soon be finalized. Moreover, ashes produced by solid biomass combustion may affect the product quality. Finally, the use of solid biomass increases the maintenance requirements [13]. However, these challenges are not insurmountable, given that 100% biomass-fired kilns already exist [13] [30]. In fact, the biggest issue with using biomass is its availability. Since several sectors are considering biomass as a means of reducing their CO_2 emissions, all lime kilns would not be able to be fired with 100% biomass. In fact, according to Eurostat data, a maximum biomass availability in Belgium of 13.89 TWh/y [95] should be considered. For Carmeuse's lime production sites in Moha and Aisémont, producing respectively 200 000 t_{lime}/y and 400 000 t_{lime}/y [13], the yearly biomass demand would be 0.33 TWh/y and 0.66 TWh/y, respectively. These two plants alone would require 7% of the global biomass availability. Limitations for biogas and biomethane availability also exist. According to IEA [81], the global biogas potential in 2020 amounted to 600 Mtoe (i.e., $\sim$7 TWh), with the European Union representing roughly 9%. In 2040, this potential could be 50% higher. Moreover, in 2020, the biomethane potential amounted to 700 Mtoe (i.e., $\sim$8 TWh), with 16% related to Europe, according to IEA. The global biomethane potential is expected to reach 1000 Mtoe (i.e., $\sim$11.6 TWh) by 2040 [81].

From 2040, 'Biogas-CC' is part of the cheapest configurations, also enabling net negative CO_2 emissions. However, one must keep in mind that the CAPEX related to biogas-fired kilns is assumed to be identical to the natural gas-fired one. Thus, real CAPEX values may be lower or higher than currently considered, which may affect its position in the ranking.

'Plasma-CC' and 'NGOxy-CC' are also among the cheapest energy transition pathways for the lime sector in 2030, 2040 and 2050 scenarios. Both configurations are relatively close in terms of specific CO_2 emissions and specific total cost. The plasma technology is always favored over the oxy-fuel configuration, except in the central and clean molecules scenarios in 2030. However, one must realize that plasma and oxy-fuel technologies are at different Technology Readiness Levels (TRL)[10] for lime production: TRL 3 for kiln electrification with plasma torches [94] [98]; TRL 6–8 for oxy-fuel [94] [3]. This means that, even if the expected CAPEX of the plasma technology is relatively low, the first-of-a-kind plasma-based kilns will probably be more expensive. Moreover, due to the low TRL of the plasma technology, the related CAPEX may be associated with greater uncertainty than mature technologies, such as natural gas-fired kilns. Currently, the oxycombustion pathway is strongly favored by sector's experts [13] [56].

One must know that 'Plasma-CC' and 'NGOxy-CC' configurations separate CO_2 with a cryogenic method, while the other configurations use MEA-based chemical absorption to capture CO_2. For the MEA-based carbon capture, steam generation requires additional natural gas combustion. The related CO_2 emissions can not be captured and are thus subject to high carbon prices. In contrast, the cryogenic CO_2 separation

[10] TRL are described in Appendix D

requires only an additional electricity input. Moreover, the energy requirements and total costs related to carbon capture with MEA have been carefully studied for correlations development by Kim et al. [90] whereas data related to the oxycombustion carbon capture are sourced from literature and are often underestimated [99]. Therefore, MEA-related data are more reliable.

Even if it is often envisaged as an alternative fuel, regardless of the considered year or scenario, hydrogen is one of the most expensive configurations. Moreover, according to experts of the lime sector, a sharp increase of temperature within the kiln compared to a natural gas-fired one is expected, which has a negative impact on the lifespan of installations [13]. Hydrogen-fired kilns also need further development since the TRL ranges from 3 to 6 [3]. The limited reduction of CO_2 emissions, shortened lifespan of equipment and high investment costs make hydrogen an unviable option according to experts [13]. Moreover, one must keep in mind that, currently, hydrogen is almost entirely produced from fossil fuels. In fact, in 2022, 62% of the global hydrogen production was coming from natural gas reforming without CC, while 21% of the hydrogen was produced from coal without CC. Hydrogen production from fossil fuels with CC and from electricity amounted to, respectively, 0.6% and 0.1% of the global production [100].

Finally, the last remark concerns the model limitations. All the presented results rely on assumed costs for energy commodities such as hydrogen, electricity, natural gas, biomass and carbon price. These costs come from EnergyVille scenarios and may not reflect reality. Unexpected events can greatly affect energy prices. For instance, after the Russian invasion of Ukraine, a sharp increase of natural gas and electricity prices was experienced in Europe. Considering this uncertainty, a sensitivity study on energy commodities prices could be beneficial for more in-depth analyses. Specifically, scenarios where the EU-ETS carbon price is much lower than expected, or where natural gas or biomass prices are higher than those assumed by EnergyVille, could be explored.

6 Conclusion and perspectives

The ever-increasing atmospheric CO_2 concentration intensifies the greenhouse effect endangering our ecosystem. Alarming phenomena are being observed: Arctic Sea ice is melting, ocean acidification is occurring and extreme weather events –such as heatwaves, floods, hurricanes and cyclones– are becoming more and more frequent. As stated in the Paris Agreement, it is crucial to limit the global average temperature increase by the end of the century below 1.5℃ compared to pre-industrial levels.

To reach Paris Agreement targets and mitigate climate change, significant efforts on CO_2 emission reduction must be realized through innovative solutions and collective actions. While the decarbonization of the power sector takes rapidly place by transitioning to renewable energy sources, emissions reduction in hard-to-abate sectors –such as cement, steel or lime– is much more complex.

In response to the climate crisis, several energy transition projects have been launched all around the world, such as the TRILATE project studying the potential of energy transition and possible symbiosis in Belgian industrial clusters. The project's goal consists in determining the investments and the planning needed for the energy transition in the Belgian industry. To reach this goal, a comprehensive modeling of process blueprints for the various sectors present on Belgian territory –such as sugar refining, cement production or glass-making process– is carried out by ULiège. The lime sector being also part of these, the present master's thesis focused on the evaluation of energy transition pathways for the Belgian lime sector.

The lime sector, emitting between 1 and 1.8 t_{CO_2}/t_{lime} depending on the kiln design [9] and representing alone around 1% of the global anthropogenic CO_2 emissions [8], is described as hard-to-abate and thus plays a crucial role in achieving Paris Agreement targets. Nonetheless, the lime sector faces huge challenges in terms of CO_2 emissions reduction. In fact, the high-temperature heat required to perform limestone calcination (900–1200℃ [9]) is provided by the combustion of fossil fuels, such as natural gas, emitting a substantial amount of CO_2 into the atmosphere. However, the majority of CO_2 emissions stems from the calcination reaction itself (see eq. 39) and is thus considered unavoidable.

$$CaCO_3 + heat \rightleftharpoons CaO + CO_2 \tag{39}$$

As a net-zero emissions economy is targeted by 2050, CO_2 emissions reduction efforts must be actively implemented by the lime industry. A number of energy transition projects have been launched in the sector. Some of them are investigating heat recovery (e.g. Lhoist's and Steetley's WHeatRec4PG project [3]). Other projects are focusing on fuel switching: BIOXYSORB (*Lhoist*) is studying biomass combustion in air and oxygen; ADIREN4LIME (*Birch Energy UK*) investigates the use of biomethane –upgraded from biogas produced by anaerobic digestion– in lime kilns [3]; heat supply by plasma generators is investigated by *SaltX* [51]. Finally, various carbon capture techniques are considered: amine-based capture (DINAMX (*Lhoist*)); direct separation (LEILAC (*Lhoist*)); calcium looping (CALENERGY (*Carmeuse, Alstom*), CARINA (*Lhoist*)) [3].

This master thesis explored several energy transition pathways identified by the lime sector to address these CO_2 emissions. After a thorough literature review on quicklime and derivatives production as well as on identified energy transition pathways, a superstructure of the sector was realized. This superstructure consists of process blueprints, i.e., mass and heat balances as well as economics in steady-state. The obtained models could then be evaluated for three different years (2030, 2040, 2050) and three different scenarios (electrification, clean molecules, central), impacting energy prices, to determine the most suitable energy transition pathways for the lime sector based energy requirements, CO_2 emissions and total cost. Fourteen different configurations have been analyzed. Natural gas combustion in air (*'NG'*) or oxygen (*'NGOxy'*) could be im-

plemented for heat supply. Lime kilns could also be fired with carbon-neutral fuels such as hydrogen (*'H2'*), biogas (*'Biogas'*), solid biomass (*'Biomass'*) or even a mixture of natural gas and biomethane (*'BioCH4'*). Moreover, kiln electrification with plasma generators (*'Plasma'*) has also been considered. Finally, all the aforementioned kiln technologies could be combined with carbon capture (*'CC'*).

Firstly, fuel-related CO_2 emissions can be tackled with fuel-switching opportunities. The use of hydrogen, biomass-based fuels as well as electrification options are investigated for the lime sector. However, fuel switching allows a maximum CO_2 emissions reduction of 26% due to the 786 kg_{CO_2}/t_{lime} emitted by the calcination reaction. Thus, to reach carbon neutrality by 2050, implementation of carbon capture (such as MEA-based chemical absorption or oxycombustion) in lime production facilities is inevitable. Carbon capture coupled with a natural gas-fired kiln, a hydrogen-fired kiln or a lime kiln partially fed with biomethane (50% NG – 50% BioCH4) allows a CO_2 emission reduction of respectively 69%, 77% and 82% compared to the base (i.e., natural gas-fired kiln without CC), or equivalently emits 327 kg_{CO_2}/t_{lime}, 242 kg_{CO_2}/t_{lime} and 187 kg_{CO_2}/t_{lime} respectively. Plasma and natural gas oxycombustion technologies coupled with CC allow reaching net scope 1 CO_2 emissions of, respectively, 79 kg_{CO_2}/t_{lime} and 103 kg_{CO_2}/t_{lime}. Only biomass- and biogas-fired kilns followed by CC units enable net negative CO_2 emissions (respectively -156 kg_{CO_2}/t_{lime} and -261 kg_{CO_2}/t_{lime}).

According to analyses, the configuration characterized by the lowest specific total cost, in 2030, is the biomass-fired kiln coupled with MEA-based CC ('Biomass-CC'). The next two cheapest alternatives resulting in significantly lower CO_2 emissions are natural gas oxycombustion with CC ('NGOxy-CC') and plasma-based kilns followed by CC units ('Plasma-CC'). In 2040, the cheapest energy transition pathway for the lime sector remains 'Biomass-CC'. The 'Plasma-CC' configuration ranks second, closely followed by 'NGOxy-CC' and 'Biogas-CC'. In 2050, 'Biomass-CC', 'Biogas-CC', 'Plasma-CC' and 'NGOxy-CC' are again the most cost-effective configurations to reduce CO_2 emissions in the lime sector. The low cost and considerable reduction in CO_2 emissions make biomass-based configurations very attractive for the lime sector. However, availability problems are holding back widespread use, even if some biomass-fired kilns are already in use [13] [30]. While natural gas oxycombustion and plasma technology are both relatively close in terms of CO_2 emissions and specific costs, oxycombustion technology is favored by sector's experts [56] [13]. Finally, hydrogen-based configurations are among the most expensive options for the sector, regardless the considered year or scenario, which is consistent with the lime industry's conclusions [13].

Even if this study provides a comprehensive investigation of a wide variety of energy transition pathways for the lime sector, there is still room for improvement. In fact, other carbon capture processes could be investigated such as calcium looping, which is widely studied [3], or CO_2 capture with membranes. Moreover, more precise economic data, especially for oxycombustion CC and biomass-based alternatives, could further improve the conclusions. More precise information about CO_2 concentration in the exhaust gases exiting a plasma-based kiln could also increase confidence in the obtained results. Furthermore, prior to carbon capture, acid gases removal (NO_x and SO_x) is necessary. This treatment has not been considered in the present work but represents additional energy requirements and investment costs which may not be negligible. In addition, it could be interesting to also consider scope 2 CO_2 emissions, notably for electrified and hydrogen-based kilns. In fact, hydrogen is considered as a carbon-neutral fuel. However, currently, hydrogen is almost exclusively produced from fossil fuels (without carbon capture), while electrolysis-based hydrogen production represented only 0.1% of the global production in 2022 [100]. Finally, a sensitivity study on commodities prices could be carried out.

References

[1] J. Chen, L. Duan, and Z. Sun, "Review on the development of sorbents for calcium looping," *Energy & Fuels*, Apr. 2020. DOI: 10.1021/acs.energyfuels.0c00682.

[2] T. Gaudiaut. "Le rythme d'accroissement du CO2 dans l'atmosphère s'accélère," [Online]. Available: https://fr.statista.com/infographie/31279/evolution-concentration-atmospherique-co2-et-niveau-ere-pre-industrielle/ (visited on Apr. 3, 2024).

[3] "CO2 innovation in the lime sector 3.0," The European Lime Association, Tech. Rep., 2022.

[4] I. Tiseo. "Distribution of carbon dioxide emissions worldwide in 2022, by sector," [Online]. Available: https://www.statista.com/statistics/1129656/global-share-of-co2-emissions-from-fossil-fuel-and-cement/ (visited on Apr. 23, 2024).

[5] "Distribution of electricity generation in belgium in 2023, by source," [Online]. Available: https://www.statista.com/statistics/1234898/belgium-distribution-of-electricity-production-by-source/ (visited on Apr. 23, 2024).

[6] "Share of energy from renewable sources in electricity generation in belgium from 2007 to 2020," [Online]. Available: https://www.statista.com/statistics/419420/belgium-share-of-electricity-from-renewable-sources/ (visited on Apr. 23, 2024).

[7] "IFC at COP28: Decarbonization of hard-to-abate sectors," Dec. 2023. [Online]. Available: https://www.ifc.org/en/events/2023/decarbonizing-hard-to-abate-sectors#:~:text=The%20hard%2Dto%2Dabate%20sectors,meeting%20the%20Paris%20Agreement%20targets..

[8] A. Laveglia, S. Luciano, N. Ukrainczyk, N. De Belie, and E. Koenders, "Hydrated lime life-cycle assessment: Current and future scenarios in four EU countries," *Journal of Cleaner Production*, vol. 369, 2022. DOI: https://doi.org/10.1016/j.jclepro.2022.133224.

[9] F. Schorcht, I. Kourti, B. M. Scalet, S. Roudier, and L. Delgado Sancho, "Best available techniques (BAT) reference document for the production of cement, lime and magnesium oxide: Industrial emissions directive 2010/75/EU (integrated pollution prevention and control)," Publications Office of the European Union, Tech. Rep., 2013. DOI: 10.2788/12850.

[10] M. Simoni, M. D. Wilkes, S. Brown, J. L. Provis, H. Kinoshita, and T. Hanein, "Decarbonising the lime industry: State-of-the-art," *Renewable and Sustainable Energy Reviews*, vol. 168, 2022. DOI: https://doi.org/10.1016/j.rser.2022.112765.

[11] "MPA lime – net negative 2040 roadmap," Mineral Products Association, Tech. Rep., 2023.

[12] "A pathway to negative CO2 emissions by 2050: The contribution of the lime industry to a carbon-neutral europe," European Lime Association, Tech. Rep., 2023. [Online]. Available: https://eula.eu/resources/a-pathway-to-negative-co2emissions-by-2050/.

[13] Personal communication with Alex Aubert (Carmeuse).

[14] "High calcium quicklime," [Online]. Available: https://www.carmeuse.com/na-en/products/high-calcium-quicklime (visited on Feb. 6, 2024).

[15] J. A. Oates, *Lime and Limestone: Chemistry and Technology, Production and Uses*. Wiley-VCH Verlag GmbH, 1998. DOI: 10.1002/9783527612024.

[16] "Competitiveness of the european cement and lime sectors: Final report," Publications Office of the European Union, Tech. Rep., 2018. DOI: 10.2873/300170.

[17] "Milk of lime," [Online]. Available: https://www.carmeuse.com/na-en/references/case-studies-success-stories/milk-lime (visited on Feb. 6, 2024).

[18] "Lime kiln dust," [Online]. Available: https://www.carmeuse.com/na-en/products/lime-kiln-dust-lkd (visited on Feb. 6, 2024).

[19] "Lime products," [Online]. Available: https://www.carmeuse.com/na-en/products/lime-products (visited on Feb. 21, 2024).

[20] "Quicklime market analysis: Industry market size, plant capacity, production, operating efficiency, demand & supply, end-user industries, sales channel, regional demand, company share, foreign trade, 2015–2032: Decode the future of quicklime." (2023), [Online]. Available: https://www.chemanalyst.com/industry-report/quicklime-market-768#:~:text=Testimonials%20Disruption%20Tracker-,Description,of%20Quicklime%20in%20H1%202023. (visited on Feb. 8, 2024).

[21] "Lime production by country in 2022 (in thousand metric tons)," [Online]. Available: https://www.statista.com/statistics/657049/production-of-lime-worldwide/ (visited on Feb. 7, 2024).

[22] "What is hot mix asphalt pavement," [Online]. Available: https://www.apa-mi.org/what_is_hot_mix_asphalt_paveme.php#:~:text=Hot%20Mix%20Asphalt%20(HMA)%20is,aggregate%20at%20an%20HMA%20facility. (visited on Feb. 13, 2024).

[23] *Energy and Environmental Profile of the U.S. Mining Industry*. Department of Energy, 2013, ch. 9–Limestone and Crushed Rock.

[24] A. Bes, "Dynamic process simulation of limestone calcination in normal shaft kilns," Ph.D. dissertation, Otto von Guericke Universität Magdeburg, 2005.

[25] G. Kehse, "Simplifying the geometry of a parallel flow regenerative (PFR) kiln to achieve both long-term cost savings and process advantages," *ZKG*, vol. 12, 2018.

[26] M. Massad, M. Kavvaji, H. Tran, and K. Lock, "Heat transfer in the chain section of lime kilns," *International Chemical Recovery Conference*, vol. 1, pp. 162–174, Jan. 2010.

[27] A., Rettig, M. A. Lagler, *et al.*, "Application of organic rankine cycles (ORC)," 2011. [Online]. Available: https://api.semanticscholar.org/CorpusID:173170220.

[28] M. Radaker, "Lime slaking 101," Tech. Rep., Jan. 2022.

[29] A. Sagastume Gutiérrez, J. B. Cogollos Martínez, and C. Vandecasteele, "Energy and exergy assessments of a lime shaft kiln," *Applied Thermal Engineering*, vol. 51, no. 1, 2013. DOI: https://doi.org/10.1016/j.applthermaleng.2012.07.013.

[30] "Carbon action 2030," Lhoist, Tech. Rep., 2023. [Online]. Available: www.lhoist.com.

[31] L. Grégoire, *CO2 capture and storage*, Lecture notes from 'Gestion durable des Combustibles' (ULiège), 2021.

[32] U. Khan, C. C. Ogbaga, O.-A. O. Abiodun, *et al.*, "Assessing absorption-based CO2 capture: Research progress and techno-economic assessment overview," *Carbon Capture Science & Technology*, vol. 8, 2023. DOI: https://doi.org/10.1016/j.ccst.2023.100125.

[33] M. J. Regufe, A. Pereira, A. F. P. Ferreira, A. M. Ribeiro, and A. E. Rodrigues, "Current developments of carbon capture storage and/or utilization–looking for net-zero emissions defined in the paris agreement," *Energies*, vol. 14, no. 9, 2021. DOI: 10.3390/en14092406.

[34] H. Hekmatmehr, A. Esmaeili, M. Pourmahdi, *et al.*, "Carbon capture technologies: A review on technology readiness level," *Fuel (Guildford)*, vol. 363, 2024. DOI: 10.1016/j.fuel.2024.130898.

[35] A.-M. Cormos, C. Dinca, L. Petrescu, D. Andreea Chisalita, S. Szima, and C.-C. Cormos, "Carbon capture and utilisation technologies applied to energy conversion systems and other energy-intensive industrial applications," *Fuel (Guildford)*, vol. 211, pp. 883–890, 2018.

[36] M. G. Plaza, S. Martínez, and F. Rubiera, "CO2 capture, use, and storage in the cement industry: State of the art and expectations," *Energies*, vol. 13, no. 21, 2020. DOI: 10.3390/en13215692.

[37] M.-B. Hägg, A. Lindbråthen, X. He, S. Nodeland, and T. Cantero, "Pilot demonstration-reporting on co2 capture from a cement plant using hollow fiber process," *Energy Procedia*, vol. 114, pp. 6150–6165, 2017, 13th International Conference on Greenhouse Gas Control Technologies, GHGT-13, 14-18 November 2016, Lausanne, Switzerland. DOI: https://doi.org/10.1016/j.egypro.2017.03.1752.

[38] G. Schöny, J. Fuchs, M. Infantino, J. van de Graaf, S. van Paasen, and H. Hofbauer, "Pilot scale demonstration of solid sorbent CO2 capture technology at a biomass power station," Oct. 2018.

[39] "Leilac – technology," [Online]. Available: https://www.leilac.com/technology/ (visited on Feb. 19, 2024).

[40] "Techno-economics report summary: A cost-effective path to carbon neutral industrial production," Tech. Rep., Jun. 2021, Version 1.01. [Online]. Available: https://www.calix.global/wp-content/uploads/2021/10/LEILAC-Techno-economic-Summary-2021.pdf.

[41] W. Y. Hong, "A techno-economic review on carbon capture, utilisation and storage systems for achieving a net-zero CO2 emissions future," *Carbon Capture Science & Technology*, vol. 3, 2022. DOI: https://doi.org/10.1016/j.ccst.2022.100044.

[42] "Cryogenic air separation: Costs and energy economics?" [Online]. Available: https://thundersaidenergy.com/downloads/cryogenic-air-separation-the-economics/ (visited on Mar. 19, 2024).

[43] M. Voldsund, S. Gardarsdottir, E. D. Lena, *et al.*, "Comparison of technologies for CO2 capture from cement production—part 1: Technical evaluation," *Energies*, vol. 12, 2019. DOI: doi:10.3390/en12030559.

[44] A. Nurdiawati and F. Urban, "Towards deep decarbonisation of energy-intensive industries: A review of current status, technologies and policies," *Energies*, vol. 14, Apr. 2021. DOI: 10.3390/en14092408.

[45] "CLEAN clinKER production by calcium looping process," [Online]. Available: https://cordis.europa.eu/project/id/764816 (visited on Mar. 11, 2024).

[46] M. Shen, L. Tong, S. Yin, *et al.*, "Cryogenic technology progress for CO2 capture under carbon neutrality goals: A review," *Separation and Purification Technology*, vol. 299, 2022. DOI: https://doi.org/10.1016/j.seppur.2022.121734.

[47] "CALCC project summary," [Online]. Available: https://www.lhoist.com/en/calcc (visited on Mar. 2, 2024).

[48] M. Spinelli, M. C. Romano, S. Consonni, S. Campanari, M. Marchi, and G. Cinti, "Application of molten carbonate fuel cells in cement plants for CO2 capture and clean power generation," *Energy Procedia*, vol. 63, pp. 6517–6526, 2014, 12th International Conference on Greenhouse Gas Control Technologies, GHGT-12. DOI: https://doi.org/10.1016/j.egypro.2014.11.687.

[49] T. A. Barckholtz, K. M. Taylor, S. Narayanan, S. Jolly, and H. Ghezel-Ayagh, "Molten carbonate fuel cells for simultaneous CO2 capture, power generation, and H2 generation," *Applied Energy*, vol. 313, 2022. DOI: https://doi.org/10.1016/j.apenergy.2022.118553.

[50] "Industrial process heating: Replacing fossil fuels with rotodynamic heater," [Online]. Available: https://coolbrook.com/electrification-solutions/rdh-industrial-process-heating/ (visited on Apr. 12, 2024).

[51] C. Blackman, "Electrification's promising path," *International Cement Review*, May 2024. [Online]. Available: https://www.saltxtechnology.com/story/saltx-featured-in-international-cement-review/.

[52] "The electrified commercial cement kiln." (2023), [Online]. Available: https://www.cemnet.com/News/story/174030/the-electrified-commercial-cement-kiln.html (visited on Apr. 12, 2024).

[53] "Electric heating rotary kiln," [Online]. Available: https://www.rotarykilnfactory.com/electric-heating-rotary-kiln/ (visited on Apr. 12, 2024).

[54] Y. Deng, J. Liu, S. Li, *et al.*, "The steam-assisted calcination of limestone and dolomite for energy savings and to foster solar calcination processes," *Journal of Cleaner Production*, vol. 363, 2022. DOI: https://doi.org/10.1016/j.jclepro.2022.132640.

[55] "The hydrogen colour spectrum," [Online]. Available: https://www.nationalgrid.com/stories/energy-explained/hydrogen-colour-spectrum (visited on Feb. 20, 2024).

[56] H. Piringer and P. Bucher, "Is it sufficient to use renewable energy sources for lime kilns to achieve the climate goals?" Tech. Rep., 2022, Maerz Ofenbau AG. [Online]. Available: https://www.zkg.

de/en/artikel/is-it-sufficient-to-use-renewable-energy-sources-for-lime-kilns-to-achieve-the-climate-goals-3855845.html.

[57] "BEIS energy innovation programme – alternatives to natural gas for high calcium lime manufacturing: Hydrogen," British Lime Association, Tech. Rep., 2023, FS4243 (Final Report). [Online]. Available: https://assets.publishing.service.gov.uk/media/637e4d28e90e072346aae0cb/phase_3_alternatives_to_natural_gas_for_high_calcium_lime_manufacturing_hydrogen.pdf.

[58] K. Kuparinen and E. Vakkilainen, "Green pulp mill: Renewable alternatives to fossil fuels in lime kiln operations," *BioResources*, vol. 12, pp. 4031–4048, Apr. 2017. DOI: 10.15376/biores.12.2.4031-4048.

[59] "Calorific value of different wood pellets," [Online]. Available: http://www.pellet-making.com/blog/wood-pellets-calorific-value.html#:~:text=Compared%20with%20coal%20and%20diesel,biodiesel%2C%20and%20biomass%20molding%20fuel. (visited on Mar. 16, 2024).

[60] "Heat values of various fuels," [Online]. Available: https://world-nuclear.org/information-library/facts-and-figures/heat-values-of-various-fuels.aspx (visited on Mar. 16, 2024).

[61] L. Ellis, A. Badel, M. Chiang, R. Park, and Y.-M. Chiang, "Toward electrochemical synthesis of cement—an electrolyzer-based process for decarbonating CaCO3 while producing useful gas streams," *Proceedings of the National Academy of Sciences*, vol. 117, 2019. DOI: 10.1073/pnas.1821673116.

[62] "Greenwin: Handbook 2011-2023 (2nd edition)," Tech. Rep., Dec. 2023. [Online]. Available: https://www.greenwin.be/fr/news/consult/472/le-nouveau-handbook-de-greenwin-le-vrai-et-l-original-2eme-edition.

[63] T. Hanein, M. Simoni, C. L. Woo, J. L. Provis, and H. Kinoshita, "Decarbonisation of calcium carbonate at atmospheric temperatures and pressures, with simultaneous CO2 capture, through production of sodium carbonate," *Energy Environ. Sci.*, vol. 14, pp. 6595–6604, 12 2021. DOI: 10.1039/D1EE02637B.

[64] M. Salman, D. Flórez-Orrego, J. Correa-Laguna, F. Maréchal, and G. Léonard, "Systematic analysis of energy transition pathways for emission reduction in the flat glass industry using MILP formulation," in *Proceedings of the 34th European Symposium on Computer Aided Process Engineering (ESCAPE34)*, 2024.

[65] M.-J. Yoo, L. Lessard, M. Kermani, and F. Maréchal, "Osmoselua – an integrated approach to energy systems integration with LCIA and GIS," in *12th International Symposium on Process Systems Engineering and 25th European Symposium on Computer Aided Process Engineering*, ser. Computer Aided Chemical Engineering, K. V. Gernaey, J. K. Huusom, and R. Gani, Eds., vol. 37, Elsevier, 2015, pp. 587–592. DOI: https://doi.org/10.1016/B978-0-444-63578-5.50093-1.

[66] *[EPOS] osmose presentation*, Video by EPFL IPESE (10th August 2016).

[67] *Trilate: TRILATEral research on optimal investments in adequate cross-border energy infrastructure*, Slides by Muhammad Salman, So-Mang Kim and Grégoire Léonard.

[68] L. Gerber, S. Fazlollahi, and F. Maréchal, "A systematic methodology for the environomic design and synthesis of energy systems combining process integration, life cycle assessment and industrial ecology," *Computers & Chemical Engineering*, vol. 59, 2013. DOI: https://doi.org/10.1016/j.compchemeng.2013.05.025.

[69] *MEA correlations*, Slides by So-Mang Kim (April 2024).

[70] *Management of an industrial project – methodology, techniques, tools: From idea to start up*, Slides by Patrick Brennet (ULiège, 2023).

[71] "The chemical engineering plant cost index ®," [Online]. Available: https://www.chemengonline.com/pci-home#:~:text=The%20CEPCI%20consists%20of%20a,weighted%20sum%20of%20several%20components. (visited on Apr. 8, 2024).

[72] "Chemical plant cost indexes," [Online]. Available: https://en.wikipedia.org/wiki/Chemical_plant_cost_indexes (visited on Apr. 8, 2024).

[73] "Chemical engineering plant cost index," [Online]. Available: https://www.training.itservices.manchester.ac.uk/public/gced/CEPCI.html?reactors/CEPCI/index.html (visited on Apr. 8, 2024).

[74] "How much does a ball mill with an output of 30 tons per hour cost?" (2023), [Online]. Available: https://www.linkedin.com/pulse/how-much-does-ball-mill-output-30-tons-per-hour-cost-zenith-crusher (visited on Mar. 15, 2024).

[75] Personal communication with Cédric Van Liefferinge (Carmeuse).

[76] D. Michaud. "Lime slaking equipment." (2015), [Online]. Available: https://www.911metallurgist.com/blog/lime-slaking-system (visited on Mar. 15, 2024).

[77] "Cosmetics liquid soap cream mixing machine industrial high viscous paste hydraulic lifting disperser mixer," [Online]. Available: https://www.alibaba.com/product-detail/_1601042360860.html (visited on Apr. 11, 2024).

[78] "Lime putty," [Online]. Available: https://cornishlime.co.uk/products/lime-binders/lime-putty/ (visited on Mar. 12, 2024).

[79] A. M. Helmenstine. "Flame temperatures table for different fuels." (2019), [Online]. Available: https://www.thoughtco.com/flame-temperatures-table-607307 (visited on Mar. 3, 2024).

[80] "Industrial fuel switching market engagement study: Final report for business, energy & industrial strategy department," Element Energy Limited, Tech. Rep., 2018. [Online]. Available: https://assets.publishing.service.gov.uk/government/uploads/system/uploads/attachment_data/file/824592/industrial-fuel-switching.pdf.

[81] "Outlook for biogas and biomethane: Prospects for organic growth," International Energy Agency IEA, Tech. Rep., 2020. [Online]. Available: https://www.iea.org/reports/outlook-for-biogas-and-biomethane-prospects-for-organic-growth/sustainable-supply-potential-and-costs.

[82] C. Ghenai and I. Janajreh, "Combustion of renewable biogas fuels," *Journal of Energy and Power Engineering*, vol. 9, p. 831, Oct. 2015. DOI: 10.17265/1934-8975/2015.10.001.

[83] S. Ebnesajjad, "Chapter 9 - plasma treatment of polymeric materials," in *Surface Treatment of Materials for Adhesive Bonding (Second Edition)*, William Andrew Publishing, 2014, pp. 227–269, ISBN: 978-0-323-26435-8. DOI: https://doi.org/10.1016/B978-0-323-26435-8.00009-5.

[84] E. Andersson and A. Skogström, "Process integration of electric plasma calcination in pulp and paper plants: Techno-economic and greenhouse gas emission assessment including co2 utilisation options," Chalmers University of Technology, 2020. [Online]. Available: https://odr.chalmers.se/server/api/core/bitstreams/34f43b97-1e6f-485a-95ab-f825047c4fb9/content.

[85] M. Sami, K. Annamalai, and M. Wooldridge, "Co-firing of coal and biomass fuel blends," *Progress in Energy and Combustion Science*, vol. 27, no. 2, pp. 171–214, 2001. DOI: https://doi.org/10.1016/S0360-1285(00)00020-4.

[86] "Demonstration of thermochemical reforming of natural gas for reducing GHG emissions in energy intensive industries," [Online]. Available: https://webgate.ec.europa.eu/life/publicWebsite/project/details/4423#results (visited on Mar. 25, 2024).

[87] E. De Lena, M. Spinelli, I. Martínez, *et al.*, "Process integration study of tail-end ca-looping process for co2 capture in cement plants," *International Journal of Greenhouse Gas Control*, vol. 67, pp. 71–92, 2017, ISSN: 1750-5836. DOI: https://doi.org/10.1016/j.ijggc.2017.10.005.

[88] S. O. Gardarsdottir, E. De Lena, M. Romano, *et al.*, "Comparison of technologies for co2 capture from cement production—part 2: Cost analysis," *Energies*, vol. 12, no. 3, 2019. DOI: 10.3390/en12030542.

[89] Personal communication with So-Mang Kim (8th April 2024).

[90] S.-M. Kim and G. Léonard, "CO2 capture technologies and shortcut cost correlations for different inlet CO2 concentrations and flow rates: Chemical absorption," [Manuscript submitted for review], International Journal of Greenhouse Gas Control, 2024.

[91] N. Tenhumberg and K. Büker, "Ecological and economic evaluation of hydrogen production by different water electrolysis technologies," *Chemie Ingenieur Technik*, vol. 92, Aug. 2020. DOI: 10.1002/cite.202000090.

[92] A. Franco and C. Giovannini, "Recent and future advances in water electrolysis for green hydrogen generation: Critical analysis and perspectives," *Sustainability*, vol. 15, 2023. DOI: 10.3390/su152416917.

[93] Safety Data Sheet for Monoethanolamine. [Online]. Available: https://www.parchem.com/siteimages/attachment/ghs%20monoethanolamine%20msds.pdf.

[94] A. Gailani, S. Cooper, S. Allen, A. Pimm, P. Taylor, and R. Gross, "Assessing the potential of decarbonization options for industrial sectors," *Joule*, vol. 8, no. 3, pp. 576–603, 2024. DOI: https://doi.org/10.1016/j.joule.2024.01.007.

[95] J. C. Laguna, A. Moglianesi, P. Vingerhoets, W. Nijs, and P. Lodewijks, "PATHS 2050 - scenarios towards a carbon-neutral belgium by 2050," EnergyVille, Tech. Rep., Jul. 2023. [Online]. Available: https://energyville.be/wp-content/uploads/2024/03/Full-Fledged-Report_1.pdf.

[96] "Paths 2050: The power of perspective." EnergyVille, [Online]. Available: https://perspective2050.energyville.be/ (visited on May 10, 2024).

[97] "Daily european union emission trading system (EU-ETS) carbon pricing from 2022 to 2024," [Online]. Available: https://www.statista.com/statistics/1322214/carbon-prices-european-union-emission-trading-scheme/ (visited on May 22, 2024).

[98] "ETP clean energy technology guide." IEA (2023), [Online]. Available: https://www.iea.org/data-and-statistics/data-tools/etp-clean-energy-technology-guide (visited on May 9, 2024).

[99] Personal communication with Professor Grégoire Léonard (ULiège).

[100] "Global hydrogen review," International Energy Agency, Tech. Rep., 2023. [Online]. Available: https://iea.blob.core.windows.net/assets/ecdfc3bb-d212-4a4c-9ff7-6ce5b1e19cef/GlobalHydrogenReview2023.pdf.

[101] "Carbon dioxide - density and specific weight vs. temperature and pressure," [Online]. Available: https://www.engineeringtoolbox.com/carbon-dioxide-density-specific-weight-temperature-pressure-d_2018.html (visited on May 6, 2024).

[102] "Oxygen - density and specific weight vs. temperature and pressure," [Online]. Available: https://www.engineeringtoolbox.com/oxygen-O2-density-specific-weight-temperature-pressure-d_2082.html (visited on May 6, 2024).

[103] "Nitrogen - density and specific weight vs. temperature and pressure," [Online]. Available: https://www.engineeringtoolbox.com/nitrogen-N2-density-specific-weight-temperature-pressure-d_2039.html (visited on May 6, 2024).

[104] "Dry air and water vapor - density and specific volume vs. temperature - imperial units," [Online]. Available: https://www.engineeringtoolbox.com/densities-specific-volumes-dry-air-water-vapor-d_1575.html (visited on May 6, 2024).

Appendices

A MEA-based CO_2 capture and compression: correlation results

For a **natural gas**-fired kiln, a flue gas temperature of 150℃ [24] and a CO_2 concentration of 21 mol% [10] are considered. About 26% of the generated CO_2 comes from the natural gas combustion while the rest is related to the calcination reaction. Based on CO_2 emissions of Carmeuse's site of Moha in 2022 –232 029 t_{CO_2}/y (EU-ETS Union Registry)– and the typical composition of the lime kiln off-gas [10] –20.6 vol% CO_2, 8.2 vol% O_2, 63.9 vol% N_2 and 7.3 vol% H_2O– a flue gas flow rate of 0.81 kmol/s is used in the correlations developed by Kim et al. [90]. This molar flow rate corresponds to a volumetric flow rate of 26.94 m^3/s knowing that at 150℃ –i.e., the flue gas temperature for a natural gas-fired kiln– the molar density of CO_2, O_2, N_2 and H_2O are 0.03013 [101], 0.03007 [102], 0.03015 [103] and 0.02894 mol/dm^3 [104] respectively.

In case of **biogas** combustion, the volume of off-gases is increased by 6% compared to the natural gas-fired lime kiln [56]. A volumetric flow rate of 28.56 m^3/s, or equivalently 0.711 kmol/s[11], is thus considered. The molar fraction of CO_2 in the fumes is computed by dividing the CO_2 emissions of the biogas-fired kiln [12] with the aforementioned molar flowrate of off-gases. A CO_2 molar fraction of 28% is thus considered in the model.

Biomass combustion yields off-gases with a typical CO_2 composition of around 15%. Thus, it is assumed that the flue gases exiting a biomass-fired kiln are composed of 30 mol% CO_2. Knowing that 1358.2 kg CO_2 are released per ton of produced quicklime in a biomass-fired kiln and assuming a lime production of 0.006 t/s, it comes that the flowrate of off-gases is 0.6526 kmol/s.

When **hydrogen** is used, CO_2 comes only from the calcination reaction. Moreover, a decrease of the off-gases volume of 5% compared to the natural gas-fired kiln is expected [56]. Thus, a flowrate of 25.59 m^3/s, or equivalently 0.6910 kmol of fumes/s, is considered in the model. Knowing that 786 kg_{CO_2}/t_{lime} are released and considering the same production capacity as for the biogas case, the obtained molar fraction of CO_2 in the fumes is 16%.

The results of the correlations [90] for a solid biomass-, biogas- or hydrogen-fired lime kiln as well as for other fuels (i.e., natural gas or a mixture of natural gas and biomethane) are listed in Table 8.

Table 8: Correlations results for energy requirements, CAPEX and OPEX related to the MEA-based capture process and CO_2 compression

		Biomass	Biogas	Hydrogen	Others
	Flue gas flowrate (kmol/s)	0.6526	0.7711	0.6910	0.8096
	CO_2 in flue gas (mol%)	30	28	16	21
MEA capture process	***Electricity (kWh/t)***	1.5	1.55	2.02	1.76
	Steam (GJ/t)	3.54	3.54	3.56	3.55
	Cooling (GJ/t)	3.1	3.08	3.05	3.04
	Annualized CAPEX (M€/y)	6.77	7.44	5.53	6.86
	OPEX (M€/y)	18.22	20	11.35	16.16
CO2 compression	***Electricity (kWh/t)***	87.56	87.56	87.56	87.56
	Cooling (GJ/t)	0.59	0.59	0.59	0.59
	Annualized CAPEX (M€/y)	0.69	0.72	0.52	0.64
	OPEX (M€/y)	1.99	2.17	1.23	1.74

[11] This conversion is performed considering a density of 0.027 mol/dm^3, as the molar density of CO_2 and N_2 at 170℃ is respectively 0.0266[101] and 0.0276[103] mol/dm^3

[12] Knowing that 1.509 t_{CO_2}/t_{lime} are released when biogas is burned and considering quicklime production of Carmeuse's Moha site (200 000 t/y [13] or 0.006 t/s)

B Emissions, energy consumption and cost reduction of different configurations compared to a natural gas-fired kiln

In the following tables, the various energy transition pathways identified for the lime sector are compared to a natural gas-fired kiln in terms of specific CO_2 emissions, specific energy consumption and specific total cost for the electrification (ELEC), clean molecules (CLEAN) and central (CENTR) scenarios. Negative values indicate a decrease compared to the base case, while positive values indicate an increase compared to the base case.

Table 9: CO_2 emissions, energy consumption and cost reduction of different configurations compared to a natural gas-fired kiln – 2030

Case	CO_2 emissions	Energy consumption	Cost (ELEC)	Cost (CLEAN)	Cost (CENTR)
NG-CC	-69%	83%	-7%	-7%	-7%
NGOxy	-3%	-6%	10%	10%	10%
NGOxy-CC	-90%	16%	-18%	-16%	-16%
H2	-26%	23%	28%	26%	41%
H2-CC	-77%	84%	24%	14%	29%
Plasma	-26%	-28%	3%	8%	8%
Plasma-CC	-93%	-12%	-18%	-12%	-12%
Biogas	-26%	30%	-8%	-8%	-8%
Biogas-CC	-124%	147%	-7%	-7%	-7%
BioCH4	-13%	0%	-4%	-4%	-4%
BioCH4-CC	-82%	83%	-11%	-11%	-11%
Biomass	-26%	15%	-24%	-24%	-24%
Biomass-CC	-115%	120%	-28%	-27%	-27%

Table 10: CO_2 emissions, energy consumption and cost reduction of different configurations compared to a natural gas-fired kiln – 2040

Case	CO_2 emissions	Energy consumption	Cost (ELEC)	Cost (CLEAN)	Cost (CENTR)
NG-CC	-69%	83%	-27%	-26%	-26%
NGOxy	-3%	-6%	6%	6%	6%
NGOxy-CC	-90%	16%	-41%	-40%	-40%
H2	-26%	23%	3%	1%	8%
H2-CC	-77%	84%	-16%	-18%	-10%
Plasma	-26%	-28%	-9%	-6%	-5%
Plasma-CC	-93%	-12%	-45%	-42%	-40%
Biogas	-26%	30%	-17%	-17%	-17%
Biogas-CC	-124%	147%	-41%	-40%	-40%
BioCH4	-13%	0%	-8%	-8%	-8%
BioCH4-CC	-82%	83%	-35%	-34%	-34%
Biomass	-26%	15%	-23%	-23%	-23%
Biomass-CC	-115%	120%	-49%	-49%	-49%

Table 11: CO_2 emissions, energy consumption and cost reduction of different configurations compared to a natural gas-fired kiln – 2050

Case	CO_2 emissions	Energy consumption	Cost (ELEC)	Cost (CLEAN)	Cost (CENTR)
NG-CC	-69%	83%	-37%	-36%	-36%
NGOxy	-3%	-6%	4%	4%	4%
NGOxy-CC	-90%	16%	-54%	-52%	-51%
H2	-26%	23%	-12%	-8%	-5%
H2-CC	-77%	84%	-38%	-34%	-30%
Plasma	-26%	-28%	-18%	-11%	-9%
Plasma-CC	-93%	-12%	-62%	-54%	-51%
Biogas	-26%	30%	-19%	-19%	-19%
Biogas-CC	-124%	147%	-54%	-54%	-53%
BioCH4	-13%	0%	-9%	-9%	-9%
BioCH4-CC	-82%	83%	-46%	-45%	-45%
Biomass	-26%	15%	-24%	-24%	-24%
Biomass-CC	-115%	120%	-61%	-60%	-60%

C Breakdown of the specific total cost

In the following tables, the relative shares of CAPEX, fuel (i.e., natural gas, hydrogen, biogas, biomethane, solid biomass), electricity, CO_2, cooling water, compressed air and limestone are listed for 2030, 2040 and 2050.

Table 12: Relative shares of CAPEX, fuel, electricity, CO_2, cooling water, compressed air and limestone – 2030

Case	CAPEX	Fuel	Electricity	CO_2	Cooling Water	Compressed Air	Limestone
NG	4%	21%	1%	59%	0%	0%	14%
NG-CC	20%	39%	5%	20%	0%	0%	15%
NGOxy	4%	16%	4%	52%	0%	9%	13%
NGOxy-CC	19%	22%	23%	7%	0%	12%	17%
H2	6%	47%	1%	35%	0%	0%	11%
H2-CC	16%	58%	3%	11%	0%	0%	12%
Plasma	3%	0%	42%	41%	0%	0%	14%
Plasma-CC	14%	0%	64%	5%	0%	0%	17%
Biogas	6%	30%	1%	47%	0%	0%	16%
Biogas-CC	23%	54%	7%	0%	1%	0%	15%
BioCH4	5%	25%	1%	54%	0%	0%	15%
BioCH4-CC	21%	45%	6%	12%	1%	0%	16%
Biomass	8%	14%	2%	58%	0%	0%	19%
Biomass-CC	29%	43%	8%	0%	1%	0%	20%

Table 13: Relative shares of CAPEX, fuel, electricity, CO_2, cooling water, compressed air and limestone – 2040

Case	CAPEX	Fuel	Electricity	CO_2	Cooling Water	Compressed Air	Limestone
NG	3%	13%	1%	72%	0%	0%	10%
NG-CC	18%	33%	4%	30%	0%	0%	14%
NGOxy	3%	11%	3%	66%	0%	7%	10%
NGOxy-CC	19%	20%	19%	12%	0%	13%	18%
H2	5%	33%	1%	51%	0%	0%	10%
H2-CC	16%	49%	3%	19%	0%	0%	12%
Plasma	3%	0%	29%	57%	0%	0%	11%
Plasma-CC	15%	0%	58%	9%	0%	0%	18%
Biogas	5%	18%	1%	64%	0%	0%	13%
Biogas-CC	26%	49%	7%	0%	1%	0%	18%
BioCH4	3%	16%	1%	68%	0%	0%	11%
BioCH4-CC	21%	39%	5%	19%	1%	0%	16%
Biomass	6%	10%	1%	69%	0%	0%	14%
Biomass-CC	30%	42%	7%	0%	1%	0%	21%

Table 14: Relative shares of CAPEX, fuel, electricity, CO_2, cooling water, compressed air and limestone – 2050

Case	CAPEX	Fuel	Electricity	CO_2	Cooling Water	Compressed Air	Limestone
NG	3%	10%	1%	78%	0%	0%	8%
NG-CC	17%	29%	3%	38%	0%	0%	13%
NGOxy	3%	9%	2%	73%	0%	6%	8%
NGOxy-CC	19%	19%	17%	16%	0%	12%	17%
H2	5%	23%	1%	63%	0%	0%	9%
H2-CC	17%	41%	3%	27%	0%	0%	12%
Plasma	2%	0%	22%	66%	0%	0%	9%
Plasma-CC	15%	0%	54%	13%	0%	0%	18%
Biogas	4%	14%	1%	71%	0%	0%	10%
Biogas-CC	26%	49%	6%	0%	1%	0%	18%
BioCH4	3%	13%	1%	75%	0%	0%	9%
BioCH4-CC	19%	36%	4%	25%	0%	0%	15%
Biomass	4%	8%	1%	76%	0%	0%	11%
Biomass-CC	30%	42%	7%	0%	1%	0%	21%

D TRL scale

Where a topic description refers to a TRL, the following definitions apply, unless otherwise specified [95]:

- TRL 1 – basic principles observed.
- TRL 2 – technology concept formulated.
- TRL 3 – experimental proof of concept.
- TRL 4 – technology validated in lab.
- TRL 5 – technology validated in relevant environment (industrially relevantenvironment in the case of key enabling technologies).
- TRL 6 – technology demonstrated in relevant environment (industrially relevant environment in the case of key enabling technologies).
- TRL 7 – system prototype demonstration in operational environment.
- TRL 8 – system complete and qualified.
- TRL 9 – actual system proven in operational environment (competitive manufacturing in the case of key enabling technologies, or in space).

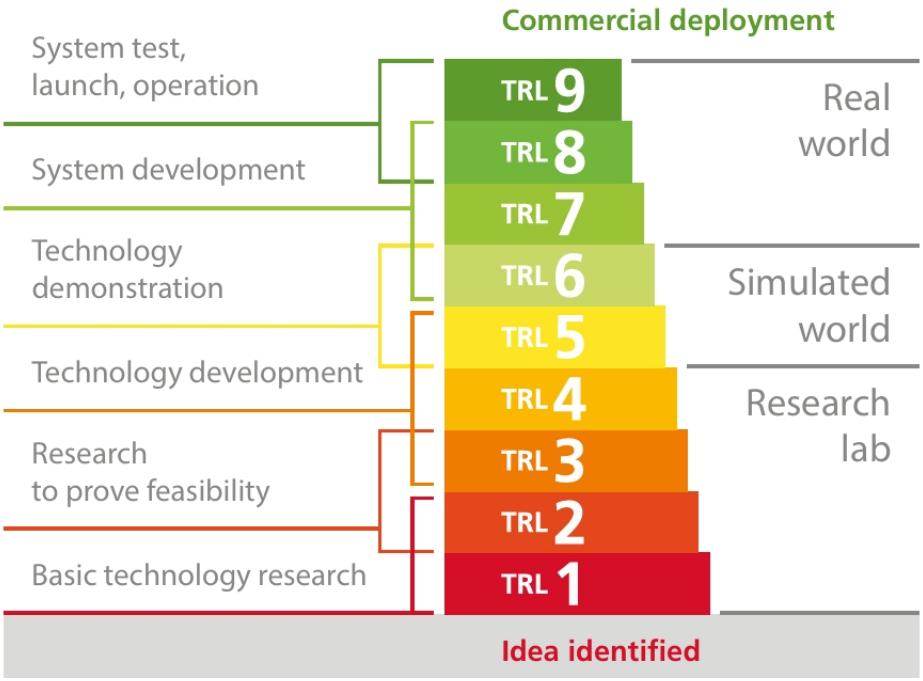

Figure 57: Technology Readiness Levels (From [3])